Technische Universität München

Fakultät Wissenschaftszentrum Weihenstephan für Ernährung, Landnutzung und Umwelt

Lehrstuhl für Systembiologie der Pflanzen

The contribution of the GATA transcription factors GNC and GNL in the greening of *Arabidopsis thaliana*

Emmanouil Bastakis

Vollständiger Abdruck der von der Fakultät Wissenschaftszentrum Weihenstephan für Ernährung, Landnutzung und Umwelt der Technischen Universität München zur Erlangung des akademischen Grades eines

Doktors der Naturwissenschaften

genehmigten Dissertation.

Vorsitzender:	Prof. Dr. W. Schwab
Prüfer der Dissertation:	1. Prof. Dr. C. Schwechheimer
	2. Prof. Dr. B. Poppenberger-Sieberer

Die Dissertation wurde am 31.05.2017 bei der Technischen Universität München eingereicht und durch die Fakultät Wissenschaftszentrum Weihenstephan für Ernährung, Landnutzung und Umwelt am 31.07.2017 angenommen.

Abstract

Photosynthesis helps the assimilation of the atmospheric CO_2, which is later used for the production of sugars and ATP in plants. The synthesis and accumulation of the chlorophylls, which eventually lead to the greening of the plants, is one of the first and maybe the most essential steps in photosynthesis. Therefore, greening is a process, which is tightly regulated at multiple levels. Studies of the chlorophyll biosynthesis pathway have as yet been mainly focused on the biochemical and functional characterization of its metabolic enzymes. However, very little is known about the regulation and fine-tuning of chlorophyll biosynthesis in the transcriptional level. The major goal of my thesis was to study the transcriptional regulation in the chlorophyll biosynthesis pathway by the LLM-domain B-GATAs transcription factors GNC and GNL. To this end, I analyzed pre-existing gene expression data and then combined the results from this analysis with newly produced RNA-seq and chromatin immunoprecipitation (ChIP) coupled with NGS data, to discover direct targets of LLM-domain B-GATAs with a role in greening. These efforts were combined with molecular, genetic and physiological studies, which led to the conclusion that the transcriptional control of greening by GNC and GNL occurred at multiple levels. Specifically, GNC and GNL are able to regulate the greening in Arabidopsis through the (1) control of genes encoding for enzymes in the chlorophyll pathway (*GUN5*, *GUN4*, *CHLI1*/*2*, *CHLD*, *DVR*), (2) regulation of the heme pathway (*GUN2*), (3) control of the expression *POR* genes, (4) transcriptional regulation of transcription factors with prominent roles in greening (*GLK1*, *GLK2*), (5) direct transcriptional control of *SIG* factors (*SIG2*, *SIG6*), which control transcription in the chloroplasts. Finally, they also function as positive regulators of the retrograde signaling pathway.

Zusammenfassung

Der Vorgang der Photosynthese hilft bei der Assimilierung des atmosphärischen CO_2, welches später wiederum für die Produktion von Zuckern und ATP in Pflanzen verwendet wird. Die Synthese und die folgende Akkumulierung der Chlorophylle, die letztendlich zum Ergrünen der Pflanzen führen, sind die ersten und womöglich die essentiellsten Schritte der Photosynthese, weshalb dieser Prozess auf etlichen Ebenen streng reguliert wird. Studien zur Chlorophyllbiosynthese haben sich bisher hauptsächlich auf die biochemische und funktionelle Charakterisierung der daran beteiligten metabolischen Enzyme fokussiert. Allerdings ist über die Regulierung und Feinjustierung der Chlorophyllbiosynthese auf transkriptioneller Ebene nur sehr wenig bekannt. Das Hauptziel meiner Dissertation war die Untersuchung der transkriptionellen Regulation der Chlorophyllbiosynthese durch die LLM-Domain B-GATA Transkriptionsfaktoren GNC und GNL. Zu diesem Zweck untersuchte ich schon vorhandene Genexpressionsdaten und kombinierte die Resultate dieser Analysen mit neu geschaffenen RNA-Seq und Chromatin-Immunpräzipitation (ChIP) Experimenten, welche mit NGS Daten gekoppelt wurden, um direkte Ziele der in der Ergrünung involvierten LLM-Domain B-GATAs zu entdecken. Diese Versuche wurden des Weiteren mit molekularen, genetischen und physiologischen Studien kombiniert, die zur Schlussfolgerung führten, dass die transkriptionelle Kontrolle der Ergrünung durch GNC und GNL auf multiplen Ebenen stattfindet. Im Speziellen sind GNC und GNL fähig, die Ergrünung in Arabidopsis zu regulieren (1) durch die Kontrolle der Gene, die für Enzyme im Chlorphyllbiosyntheseweg (*GUN5, GUN4, CHLI1/2, CHLD, DVR*) kodieren, (2) durch die Regulierung der Hämbiosynthese (*GUN2*), (3) durch Kontrolle der Expression der *POR*-Gene, (4) durch transkriptionelle Regulierung von Transkriptionsfaktoren mit wichtigen Rollen in der Ergrünung (*GLK1, GLK2*), (5) sowie durch direkte transkriptionelle Kontrolle der *SIG*-Faktoren (*SIG2, SIG6*), welche die Transkription in den Choroplasten kontrolliere. Schlussendlich funktionieren sie auch über die positive Regulierung des retrograden Signalwegs.

Acknowledgements

From this point, I would like to thank my supervisor Prof. Dr. Claus Schwechheimer, for all of his assistance and support through the journey of my PhD all these years. Many thanks to the groups, with which I collaborated in order to enhance and broad the perspective of my work for this thesis, specifically: the group of Prof. Dr. Klaus Mayer with Dr. Manuel Spannagl and Dr. Sapna Sharma, the group of Prof. Dr. Bernhard Grimm and Dr. Boris Hedtke, the group of Prof. Dr. Christoph Peterhänsel and Dr. Christian Blume and the group of Dr. Markus Schmid and Dr. David Posé. I am also thankful to the committee of my PhD, Prof. Dr. Brigitte Poppenberger and Prof. Dr. Wilfried Schwab.

I would also like to thank Rene for all of his help in the beginning of my PhD and my GA-colleagues Uli, Quirin and Carina for all the fruitful discussions and support through all of these years of my PhD. Many thanks to my colleges from the lab with which we were in different teams, but they were always very helpful and supportive, specifically: Melina, Ines, Benny, Björn, Anthi, Franzi, Maike, Erika, Stephan, Lilly, Angela and Pascal. Thanks to Valentin for his help with the translation of the abstract in Deutsch.

I also want to thank Jutta for her great technical assistance and Petra for her help regarding administrative stuff.

I would also like to convey my sincere thanks to my family in Greece, for all of their support and believe.

Finally, I would like to express my heartful thanks to my wife Evgenia, which was always there for me, to listen, to support and to encourage me, no matter what.

Manolis

To

Alkyoni and Evgenia

Table of contents

1. Introduction

Sunlight is the driving power of life on earth. In photosynthetic organisms, such as plants, chlorophyll molecules capture the energy from sunlight. Photosynthesis helps with the assimilation of the atmospheric CO2, which is used for the production of sugars, ATP and O2. The synthesis and accumulation of chlorophyll, which eventually leads to the greening of plants, is the most essential step of photosynthesis. The knowledge gained over the last decades has enriched our understanding of the biochemical aspects of photosynthesis as well as chlorophyll biosynthesis. However, as yet little is known about the transcriptional regulation of the genes, which encode for either enzymes or regulators involved in the chlorophyll biosynthesis pathway. Previous studies have shown that so-called LLM-domain B-GATA transcription factors can strongly promote the greening of plants (Behringer & Schwechheimer 2015).

1.1 B-GATA transcription factors

GATA transcription factors are present in many organisms such as fungi, echinoderms, nematodes, insects, vertebrates and plants. GATAs are zinc finger proteins, which carry one or more zinc ions (Lowry & Atchley 2000). The zinc finger family is divided into six classes with regard to the amino acid sequence of the zinc domain (Krishna et al. 2003). GATAs belong to the class IV of zinc finger proteins, and this class is further divided into the subclasses IVa and IVb. The difference between these two classes is the amino acid sequence of the zinc finger domain. Class IVa has the consensus sequence C-X2-C-X17-C-X2-C where C is cysteine and X any amino acid, and includes GATAs from fungi and animals but not from plants. Class IVb has the consensus sequence C-X2-C-X18-C-X2-C and is comprised of GATAs from plants and many fungi.

GATA factors recognize and bind to the conserved DNA motif W-G-A-T-A-R where W is a thymidine (T) or an adenosine (A) and R is a guanidine (G) or adenosine (A) (Reyes et al. 2004). GATA factor DNA-binding can cause the regulation of the transcription of genes located in proximity to this motif (Evans et al. 1988). The domain of the GATA proteins responsible for the interaction with the DNA is the type IV zinc-finger domain. Structurally, this domain consists of

one zinc ion surrounded by four cysteins, together with two anti-parallel β-sheets, one α-helix and one carboxyl-terminal tail (Omichinski et al. 1993). The interaction of the GATA-domain with the DNA takes place mostly between the thymines and the phosphate atoms of the DNA (Omichinski et al. 1993).

In Arabidopsis (*Arabidopsis thaliana*), the GATA family consists of 30 members, which can be further categorized into four distinct groups A, B, C and D (Behringer and Schwechheimer, 2015). Each of these groups preserve certain characteristics, for example, exon-intron structure, the position of the zinc finger domain, the presence or absence of CCT and acidic domain, and the number of residues of the zinc finger domain (Reyes et al. 2004). Additionally, the group of B-GATAs can be sub-divided into two sub-groups, B-GATAs with a HAN- (HANABA TARANU-) domain, and B-GATAs with an LLM- (leucine-leucine-methionine-) domain (Behringer and Schwechheimer 2015) (Figure 1).

Figure 1: Schematic illustration of B-GATAs with an LLM-domain or a HAN-domain. The part of the protein, which interacts with DNA is assigned as B-class GATA-domain. Modified figure based on (Behringer and Schwechheimer 2015).

GNC (GATA21) and *GNL (GATA22)* are paralogous LLM-domain B-GATA transcription factors, which regulate different aspects of plant life, such as germination, flower development, flowering time and greening (Behringer and Schwechheimer 2015; Kiba et al. 2005). *GNC* is induced by nitrate and can increase the expression of genes related to carbon metabolism. Therefore, *GNC* is designated as GATA, *NITRATE INDUCIBLE CARBON METABOLISM INVOLVED* (Bi et al. 2005). *GNL* (*GNC-LIKE*) expression is upregulated by light and cytokinin and the gene was therefore originally designated *CGA1* (*CYTOKININ INDUCED GATA1*) (Naito et al. 2007). *GNL* is more strongly

cytokinin-regulated and red light-induced than *GNC* (Naito et al. 2007; Ranftl et al. 2016).

1.2 The role of GNC and GNL in greening

Single mutants of *GNC* and *GNL* show reduced chlorophyll levels compared to the wt (wild type), and chlorophyll levels are further reduced in a *gnc gnl* double mutant compared to the single mutants (Bi et al. 2005; Richter et al. 2010). On the other side, plants that overexpress *GNC* or *GNL* show increased levels of chlorophyll compared to wt (Richter et al. 2010; Hudson et al. 2011). Currently, it is believed that GNC and GNL influence greening through the upregulation of the expression of genes encoding for enzymes in the chlorophyll biosynthesis pathway, such as *PORs* (*PROTOCHLOROPHYLLIDE OXIDOREDUCTASE*), *GUN4* (*GENOMES UNCOUPLED 4*) and *HEMA1/GLUTR* (*GLUTAMYL-tRNA REDUCTASE*) (Richter et al. 2010; Hudson et al. 2011).

GNC and GNL appear to not only affect chlorophyll biosynthesis but also chloroplast development. In particular, the number of chloroplasts is reduced in plants with reduced expression of *GNC* and *GNL* and increased in plants that overexpress *GNC* or *GNL* (Hudson et al. 2011). The influence of GNC and GNL on chloroplast number takes place downstream of cytokinin and can also occur ectopically in roots when *GNC* is overexpressed; this underlines the important role of B-GATAs in chloroplast development (Chiang et al. 2012). Moreover, the contribution of B-GATAs to chloroplast development is conserved in other plant species, such as rice (*Oryza sativa*) and poplar (*Populus tremula*) (Hudson et al. 2013; An et al. 2014).

The significance of GNC and GNL in greening is further shown by a micrografting experiment between wt and *GNC* overexpressing seedlings, which shows that greening is regulated in a cell autonomous manner by *GNC* (Figure 2) (Klermund et al. 2016). The role of B-GATAs in greening is not restricted to GNC and GNL but also the other Arabidopsis LLM-domain B-GATAs GATA16, GATA17, and GATA17L have a redundant function during greening of Arabidopsis.

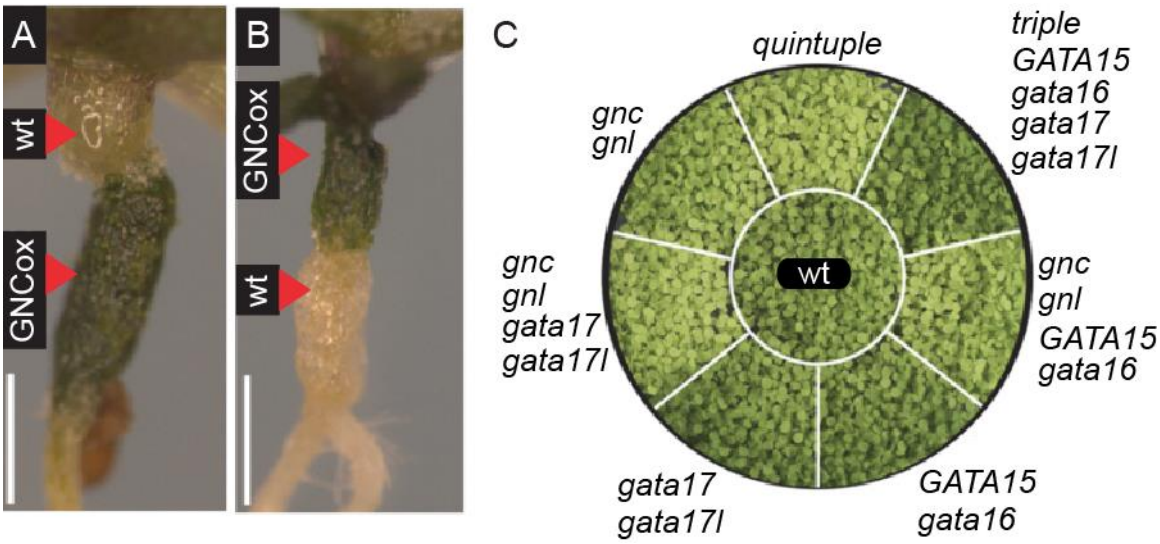

Figure 2: LLM-domain B-GATA are required for chlorophyll biosynthesis. (**A** and **B**) Photos of a micro-grafting experiment between GNCox and wt show that GNCox controls greening in Arabidopsis in a cell-autonomous manner; red arrowheads point to the part of seedlings from either wt GNCox; scale bar = 500 µm. Modified from (Klermund et al. 2016). (**C**) Photo of 14-d-old light-grown B-GATA mutant seedlings. Modified from (Ranftl et al. 2016).

A quintuple mutant, defective in *GNC*, *GNL*, *GATA16*, *GATA17* and *GATA17L*, accumulates less chlorophyll than any other mutant combination (Figure 2C) (Ranftl et al. 2016).

1.3 Greening and photosynthesis

Plants are autotrophic organisms that produce their food from inorganic matter. Atmospheric CO_2 is assimilated through the Calvin cycle into triose phosphate, which later gives rise to sucrose, a fundamental sugar used as a source of carbon and as an energy molecule. The assimilation of CO_2 takes place in the stroma of the chloroplasts and the energy required for this process is provided by light and photosynthesis. In particular, for each fixed molecule of CO2, nine molecules of adenosine triphosphate (ATP) and six molecules of nicotinamide adenine dinucleotide phosphate (NADPH) are required, which are provided by photosynthesis.

The synthesis and accumulation of chlorophyll a and b in the chloroplasts of the plant cells result in greening. Chlorophylls are derivatives from the tetrapyrrole biosynthesis pathway, which takes place in chloroplasts (Tanaka & Tanaka 2007).

Chlorophylls can interact with light harvesting proteins (LHPs) and carotenoids in order to form light harvesting complexes (LHC), which are embedded in the thylakoid membranes of the chloroplasts (Cheng & Fleming 2009). Many LHCs together form structures known as photosystems (PS), and all higher plants have two PS types, PSI and PSII (Nelson & Yocum 2006). Every PS is essentially divided into two parts, the antenna and the reaction center. Chlorophyll is distributed in the antenna as such; the inner part of the antenna is rich in chlorophyll a, which absorbs mostly low energy light with longer wavelengths, while the outer part is rich in chlorophyll b and absorbs mostly high energy light with shorter wavelengths (Hirashima et al. 2006). The reaction center of the PS is where the conversion of physical energy to chemical energy occurs and it consists predominantly of chlorophyll a. Photons from light excite chlorophyll molecules in the antenna creating energy, which is delivered via other chlorophyll molecules to the reaction center of the PS (Cheng & Fleming 2009). There, chlorophyll a can donate an electron to NADP+ and convert it to NADPH, a reducing agent, which is then released in the stroma and used in the reduction step of the Calvin cycle for CO_2 assimilation (Berry et al. 2013). PSII and PSI function in series and are connected to each other by the electron transport chain, electron protein carriers that are derived from chlorophyll oxidation (Nelson & Yocum 2006). Finally, a chlorophyll molecule in the PSI loses an electron and reduces one molecule of $NADP^+$ to NADPH.

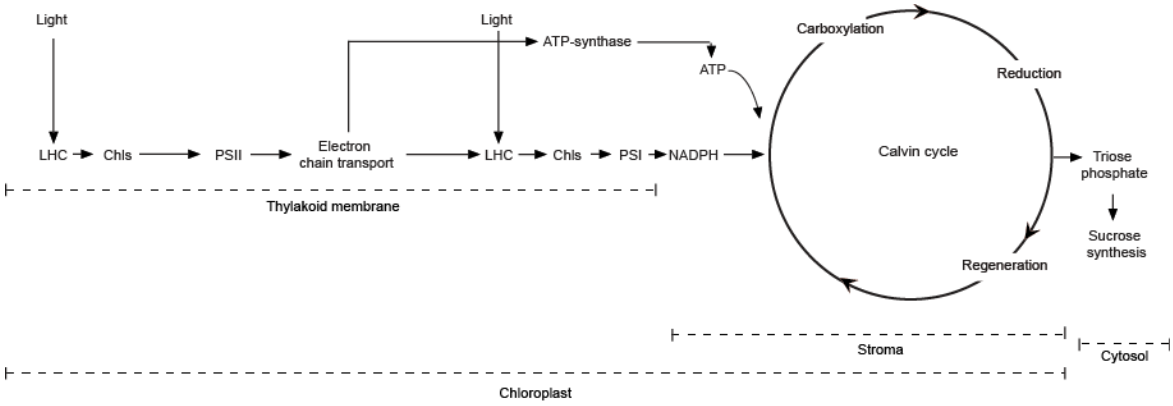

Figure 3: Schematic representation of the photosynthesis machinery.

The flow of electrons through the electron chain, from the PSII to the PSI, causes the import of protons from the stroma of the chloroplast to the lumen of the thylakoids. Therefore, the approximate pH inside thylakoids is 4 and outside about 8 (Jagendorf & Uribe 1966). The protons, which are imported from the stroma, can be exported outside of the thylakoids through the ATP-synthase complex. The flow of the protons through the channel of this complex, which is also embedded in the thylakoid membranes, starts the conversion of ADP to ATP (Eberhard et al. 2013).

Chlorophyll can absorb light in the range of 400 - 480 nm (blue light) and 550 - 700 nm (red light), but it cannot absorb mid-range visible light between 480 - 550 nm (green light). Green light is reflected by the plants and because of this, plants have the visible green color. Although it is well studied and understood how chlorophyll contributes to photosynthesis, it is not yet clear how chlorophyll synthesis is transcriptionally controlled. The goal of this thesis was to reveal the mode of chlorophyll biosynthesis regulation through the B-GATA transcription factors GNC and GNL.

1.4. The role of the tetrapyrrole biosynthesis pathway in greening

Chlorophyll biosynthesis, a branch of the tetrapyrrole biosynthesis pathway takes place in chloroplasts (Figure 4). This metabolic cascade starts with the adjunction of glutamyl-tRNA (Glu-tRNA) to 5-aminolevulinic acid (ALA) and eventually leads to the synthesis of three metabolic products, heme, siroheme and chlorophyll a and b. The enzymes, which contribute to the synthesis of the chlorophylls, are all well characterized. It is, however, not well understood how the chlorophyll pathway is regulated at the transcriptional level.

1.5 The chlorophyll biosynthesis branch

The first step in the chlorophyll pathway is the addition of an Mg^{2+} ion to the proto-IX (protoporphyrin-IX), which gives rise to Mg-proto-IX (Mg-protoporphyrin-IX). This particular reaction is catalyzed by the multi-subunit enzyme MgCh (Mg-chelatase) that consists of the subunits GUN5 (GENOMES UNCOUPLED 5), CHLD (CHELATASE D) and CHLI (CHELATASE I) (Tanaka & Tanaka 2007).

Additionally, GUN4 activates the complex and places it in its proper position in the chloroplast membranes. GUN4 and GUN5 also have a role in chloroplast to nucleus communication in a process referred to as retrograde signaling (Mochizuki et al. 2001; Larkin 2003). Since the communication between the chloroplast and nuclear genomes is disturbed in *gun2* (*gun2-1*), *gun4* (*gun4-1*), and *gun5* (*gun5-1*) mutants, the corresponding genes were designated as *GUN*

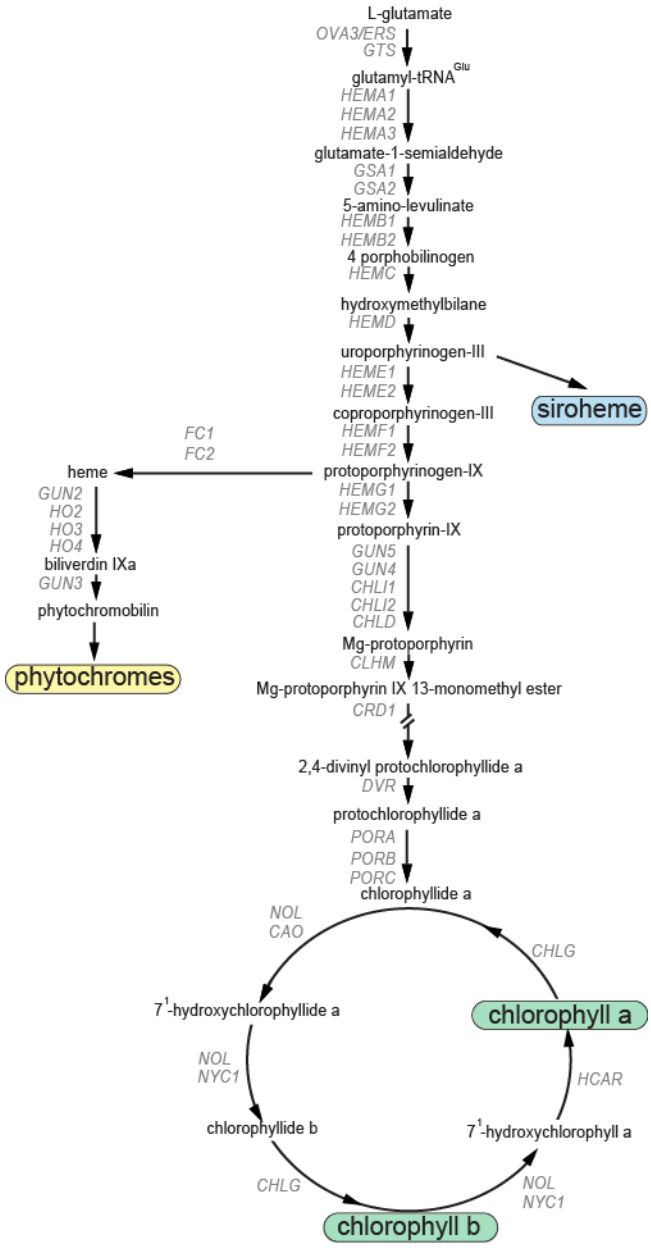

Figure 4: Schematic representation of the tetrapyrrole biosynthesis pathway. Arrows represent enzymatic steps; enzymatic products are indicated by black regular letters; proteins implicated in each step of the pathway are in grey color; colored frames mark the main 4 products of the tetrapyrrole pathway. (⇝): indicates presence of additional steps not presented in this figure.

(*GENOMES UNCOUPLED*) genes (Susek et al. 1993).

GUN5 catalyzes the insertion of Mg^{2+} into proto-IX. This process needs MgCh to be activated by ATP and is dependent on the concentration of free Mg*2*+ in the stroma of the chloroplast (Gibson et al. 1999; Tanaka & Tanaka 2007). Regarding greening, mutants of the *GUN5* gene (*gun5-1*; *cch1*, *conditional chlorina*; *rtl1*, *rapid transpiration in detached leaves 1*) and RNAi suppression lines of *GUN5* show impaired chlorophyll biosynthesis (Mochizuki et al. 2001; Tsuzuki et al. 2011).

In the Arabidopsis genome, the CHLI subunit of the MgCh complex is encoded by two homologous genes, *CHLI1* and *CHLI2*. The *CHLI1* is expressed at much higher levels than *CHLI2*, indicating that the CHLI1 protein has the major function in the MgCh complex. However, *CHLI2* expressed from the *CHLI1* promoter can rescue the pale green phenotype of the *chli1 chli2* double mutant (Huang & Li 2009). CHLI may interact with the CHLD subunit of MgCh and MgCh activity is dependent on CHLI (Rissler et al. 2002)(Huang & Li 2009). The most likely reason for this is that ATPase activity is necessary for the insertion of Mg^{2+} into the proto-IX substrate (Kobayashi et al. 2008). Additionally, *chli1 chli2* double mutant show a *gun* phenotype after the application of NF (norfluorazon) to young seedlings, which blocks retrograde signaling through inhibition of carotenoid biosynthesis. The *chli1 chli2* double mutant shows severe defects in chlorophyll biosynthesis but the *chli1* and *chli2* single mutants show only a very mild reduction in chlorophyll levels compared to the wt (Huang & Li 2009).

GUN4 is not an essential subunit of MgCh. Instead, it works as an assistant protein to the MgCh enzymatic complex. The role of GUN4 on the function of the MgCh complex is crucial for the proper placement of the complex on the chloroplast membranes and the enhancement of MgCh activity (Tanaka & Tanaka; Adhikari et al. 2009). GUN4 may function as a Mg^{2+}-dependent molecular

switch for the activation of MgCh. When the concentration of Mg^{2+} is at normal levels, the MgCh complex is activated by GUN4. Alternatively, when the concentration of Mg^{2+} is very low, GUN4 may inactivate the MgCh complex (Davison et al. 2005). Furthermore, GUN4 has a role in retrograde signaling (Larkin et al. 2003). *gun4-1* (*gun4*) seedlings subjected to NF treatment show disrupted communication between the chloroplasts and the nucleus (Mochizuki et al. 2001). Moreover, *gun4* mutant shows severe defects in greening with reduced chlorophyll levels (Mochizuki et al. 2001; Larkin et al. 2003). It has been proposed that GNC and GNL affect the expression of *GUN4*, although it is unclear whether this regulation is direct or indirect (Hudson et al. 2011). It is also unknown whether the expression of the three MgCh subunits is regulated by the GATAs. Elucidating the role of GNC and GNL in MgCh gene expression is a goal of the present thesis.

1.6 The heme pathway and chlorophyll biosynthesis

At the stage of proto-IX, the tetrapyrrole pathway bifurcates into two branches, the chlorophyll biosynthesis and the phytochromobilin or heme branch (Figure 4). The heme branch gives rise to phytochromobilin, the chromophore of the PHY (PHYTOCHROME) proteins, through which plants can perceive light (Parks & Quail 1991). *GUN2/HO1* encodes for a heme oxygenase in the heme branch where it catalyses the opening of the ring of protoheme (heme B or heme) to produce biliverdin IXa (Ishijima et al. 2003). Plants are able to synthesize other types of heme, such as heme A and C, but the ways through which these forms are produced have yet to be explored. The light-grown *gun2* mutant is pale green and shows defects in chlorophyll biosynthesis (Mochizuki, Brusslan, Larkin, A. Nagatani, et al. 2001). Moreover, when grown under normal light conditions, *gun2* displays an elongated hypocotyl compared to the wt. Presumably, both phenotypes are results of the reduced phytochrome function due to the reduction in phytochromobilin in *gun2*.

1.7 Transcriptional control of greening

As of now, only a small number of transcription factors has been associated with the regulation of greening in plants (Figure 5). Some known transcription factors such as PIFs (PHYTOCHROME INTERACTING FACTORS), GLKs (GOLDEN2-LIKES), HY5 (ELONGATED HYPOCOTYL5) and EIN3 (ETHYLENE INSENSITIVE 3), that are implicated in many different developmental processes and hormonal pathways, play also an important role in the transcriptional regulation of greening (Kobayashi & Masuda 2016). It can be postulated that there must be multiple levels of regulation and control for a complex pathway such as chlorophyll biosynthesis. Therefore, one goal of this thesis was to investigate the existence of potential interactions between B-GATAs with some of the known regulators of greening.

1.8 Phytochromes and PHYTOCHROME INTERACTING FACTORS

PIFs are transcription factors of the basic helix-loop-helix (bHLH) family (Bailey et al. 2003). PIFs promote skotomorphogenesis and they are degraded rapidly following light exposure after their phyA- and phyB-dependent phosphorylation (Al-Sady et al. 2006). PIFs are also implicated in other processes, such as the repression of seed germination, shade avoidance and high temperature responses (Leivar & Quail 2011). PIF1 and PIF3 repress chlorophyll biosynthesis and chloroplast development in the dark-grown seedlings (Huq et al. 2004; Liu et al. 2013). In particular, PIF1 reduces the levels of Pchlide (protochlorophyllide), an intermediate of the chlorophyll biosynthesis pathway, through the induction of *FeCHLII*, *PORA*, *PORB*, *PORC* and *HEMAC* expression (Moon et al. 2008). PORs convert Pchlide to Chlide (chlorophyllide). Overaccumulation of Pchlide in etiolated seedlings, followed by light exposure, leads to photooxidative damage in seedlings, which can be lethal when dark-grown seedlings are shifted to the light (Huq et al. 2004). Thus, PIF1 can differentially regulate the expression of chlorophyll biosynthesis genes, probably to increase the adaptation of young seedlings during the transition from skotomorphogenesis to photomorphogenesis (Moon et al. 2008). PIF3 is also implicated in the regulation of chlorophyll biosynthesis in dark-grown seedlings.

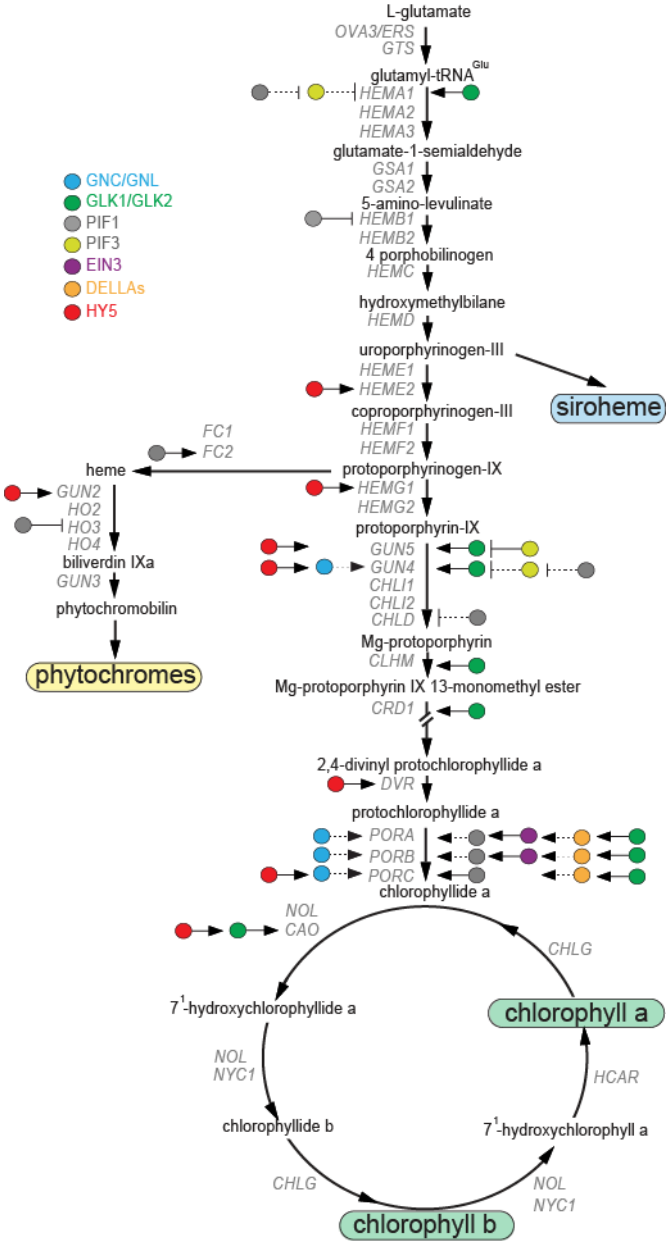

Figure 5: The tetrapyrrole biosynthesis pathway and its known transcriptional regulators. Schematic representation of the tetrapyrrole pathway from plants; (⇝): indicates presence of additional steps not presented in this figure; small colored circles represent known regulators of the pathway; horizontal arrows, linked with circles, depict a direct regulation supported by chromatin immunoprecipitation (ChIP); arrows with dashed lines represent transcriptional regulation not supported by ChIP. Horizontal arrows, which end with arrow-heads (⟶) imply activation of gene expression; horizontal arrows, which end in a vertical line (⟞), imply repression of gene expression; horizontal arrows.

Specifically, PIF3 binds to certain promoters of some chlorophyll biosynthesis genes, such as *GUN5* and *CHLD*, and then attracts the HDA15 (HISTONE DEACETYLASE15) enzyme. HDA15 reduces histone acetylation and thereby

represses gene expression (Liu et al. 2013). Following light exposure, PIF3 is degraded and the recruitment of HDA15 to gene promoters is lost (Liu et al. 2013). Due to the protective role, which PIF1 and PIF3 show agsinst the photooxidation of etiolated seedlings, by the downregulation of chlorophyll biosynthesis genes in the dark, It was hypothesized that GNC and GNL could also participate to this protective mechanism, to eventually promote the normal greening process of the plant after the light exposure.

1.9 GOLDEN2-LIKE (GLK) transcription factors

The G2 (GOLDEN2) transcription factor was initially discovered in maize (*Zea mays*) and characterized as a gene with a pivotal role in the development of the chloroplasts of photosynthetic tissues. The maize G2 mutant is very pale green when compared to the wt (Hall et al. 1998). Characterization of the G2 homologous *ZmGLK1* (*G2-LIKE1*) from maize or *OsGLK*1 and *OsGLK2* from rice revealed that also these genes play an important role in the development of chloroplast and photosynthesis (Rossini et al. 2001). *GLK* genes are expressed predominately in all photosynthetic tissues (rosette and cauline leaves and cotyledons) (Fitter et al. 2002), and they are able to function in a cell-autonomous manner (Waters et al. 2008). Two *GLK* genes have been identified in all higher plants such as maize, rice, tomato (*Solanum lycopersicum*) and Arabidopsis, where the *GLK* genes have been studied so far (Fitter et al. 2002).

Arabidopsis *GLK1* and *GLK2* have partially redundant functions and *glk1 glk2* double mutant is pale green (Waters et al. 2008; Waters et al. 2009). In Arabidopsis, GLK transcription factors can influence the expression of genes, with a role in the light harvesting complexes, the electron transport chain, and the chlorophyll biosynthesis pathway (Waters et al. 2009). Additionally, GLK2, together with HY5 (ELONGATED HYPOCOTYL5), can induce greening in Arabidopsis roots in a cytokinin-dependent manner (Kobayashi et al. 2012). This induction of greening in the root can be suppressed by the auxin hormone. This result underlines the important role of GLK2 in promoting chlorophyll biosynthesis, even in non-photosynthetic tissues such as the root.

The contribution of GLKs to greening is not restricted to basic photosynthetic plant tissues, such as the leaves, but it extends also to fruits. In tomato, overexpression of *SlGLK* leads to enhanced photosynthesis and subsequently elevated levels of carotenoids and carbohydrates of the tomato fruit, beneficial features for the overall fruit quality (Powell et al. 2012).

GLKs and B-GATAs play an important role in the greening of the plants. It has so far not been investigated to what extend these two classes of genes interact, whether they cross-regulate each other or co-regulate common target genes. Therefore, this thesis investigates a potential relationship between B-GATA GNC and GNL with GLK transcription factors in the control of greening.

1.10 Sigma factors (SIGs)

Chloroplasts maintain their own genome, and they have their own transcription apparatus. Chloroplasts have two types of RNA-polymerase enzymes, nucleus-encoded polymerase (NEP) and plastid-encoded polymerase (PEP) (Allison 2000). NEP is responsible mostly for the transcription of chloroplast housekeeping

Table 1: Tissue-specific expression pattern of the six Arabidopsis *SIG* genes.

	SIG1	*SIG2*	*SIG3*	*SIG4*	*SIG5*	*SIG6*
Seeds	No	No	Yes	No	No	No
Roots	No	No	No	No	Yes	No
Cotyledons	No	Yes	Yes	No	No	Yes
Leaves	Yes	Yes	Yes	Yes	Yes	Yes

genes, and only for few genes related to photosynthesis (Börner et al. 2015). PEP is responsible for the transcription of the majority of photosynthetic genes encoded by the chloroplast genome as well as for genes with a role in chloroplast development (Fujiwara et al. 2000; Börner et al. 2015). NEP is nucleus-encoded and a single subunit enzyme. PEP is a multi-subunit enzyme consisting of two parts, the core catalytic domain built entirely of plastid-encoded proteins (rpoA, rpoB, rpoC1 and rpoC2) and the nucleus-encoded sigma factor proteins (SIGs).

These factors incorporate into the core domain PEP and provide promoter specificity to the enzyme (Kanamaru & Tanaka 2004). The nucleus can control the expression of chloroplast-specific genes by controlling the expression of SIG factors (Allison 2000).

The Arabidopsis genome encodes for six SIG genes, *SIG1* - *SIG6* (Böner et al. 2015). The expression pattern of *SIG* genes is restricted predominantly to green-photosynthetic tissue (Table 1). Nevertheless, *SIG3* is also expressed in seeds and *SIG5* in the roots of young seedlings (Table 1) (Lysenko 2007). Furthermore, the expression of *SIG* genes is light-regulated (Allison 2000).

SIG2 and SIG6 contribute to chloroplast development and photosynthesis in seedlings and the *sig2* (*sig2-1*) and *sig6* (*sig6-2*) single mutants show severe defects in greening. Young *sig6* mutant seedlings have a pale green color, which is completely restored as the plants become older (Ishizaki et al. 2005). SIG2 seems to play a role in the formation of chloroplasts but has no role in etioplasts development. Additionally, the expression levels of chloroplast-encoded photosynthetic genes remain unchanged in the *sig2* mutant, as well as that of the nuclear encoded *CAB* (*CHLOROPHYLL A/B BINDING PROTEIN*) and *RBCS* (*RIBULOSE BISPHOSPHATE CARBOXYLASE*) photosynthetic genes. At the same time, the levels of proteins related to photosynthesis are markedly reduced in *sig2*.

SIG6 also plays a role in the greening of Arabidopsis but its role is restricted to the cotyledons early in development, and older plants appear to be normal with regard to greening. In contrast to *sig2* mutants, *sig6* mutants show changes in the transcript levels of genes, which are known to be regulated by the PEP (Ishizaki et al. 2005). The hypothesis is that SIG6 has overlapping function with another SIG factor or related proteins.

Until now, the promotion of greening through the induction of nuclear genes encoding for *SIG* factors has remained unexplored. Here, it is being examined how the B-GATAs GNC and GNL cross-talk with the *SIG* factors at the transcriptional and genetic level.

1.11 Aim of this thesis

Studies of the chlorophyll biosynthesis pathway have as yet been mainly focused on the biochemical and functional characterization of its metabolic enzymes. However, very little is known about the regulation and fine-tuning of chlorophyll biosynthesis at the transcriptional levels. The major aim of my thesis was to shed light on the regulation of chlorophyll biosynthesis by the LLM-domain B-GATAs transcription factors. Initially, I analyzed pre-existing gene expression data in combination with RNA-seq data and chromatin immunoprecipitation (ChIP) coupled with NGS (next generation sequencing) to identify direct targets of LLM-domain B-GATAs. This was combined with molecular, physiological and genetic studies, which showed that the transcriptional control of greening by GNC and GNL occurred at multiple levels. GNC and GNL were able to regulate the greening in Arabidopsis through the (1) control of genes encoding for enzymes in the chlorophyll pathway (*GUN5*, *GUN4*, *CHLI1*/2, *CHLD*, *DVR*), (2) transcriptional regulation of transcription factors with prominent roles in greening (*GLK1*, *GLK2*), (3) direct transcriptional control of SIG factors (*SIG2*, *SIG6*), (4) regulation of the heme pathway (*GUN2*) and, finally, (5) retrograde signaling.

2. Material and methods

2.1 Material

All the experiments presented in this thesis were conducted with the accession Columbia-0 (Col-0) of *Arabidopsis thaliana* as genetic background, except of the *sig2-1* (*abc1*) mutant, which had as background accession Wassilewskija. Nevertheless, the *sig2-1* mutant was chosen because of its strong phenotype regarding greening, compared to other mutants of *SIG2*.

Table 2: List of mutant lines used in this thesis.

Name	Locus	Reference
gnc (SALK_001778)	AT5G56860	Bi et al., 2005
gnl (SALK_003995)	AT4G26150	Richter et al., 2010
gun2-1	AT2G26670	Susek et al., 1993
gun4-1	AT3G59400	Larkin et al., 2003
gun5-1	AT5G13630	Mochizuki et al., 2001
cch1	AT5G13631	Mochizuki et al., 2001
cs	AT4G18480	Koncz et al., 1990
dvr/pcb2	AT5G18660	Nakanishi et al., 2005
sig2-1	AT1G08540	Shirano et al., 2000
sig6-2 (GABI_242G06)	AT2G36990	Loschelder et al., 2006
glk1-1 (dSpm insertion)	AT2G20570	Fitter et al., 2002
glk2-1 (dSpm insertion)	AT5G44190	Fitter et al., 2002
pif1-1 (SALK131872)	AT2G20180	Huq et al., 2004
pif3-3	AT1G09530	Monte et al., 2004
pif1345 (pifq)	AT2G20180	Leivar et al., 2008
	AT1G09530	
	AT2G43010	
	AT3G59060	

Table 3: List of transgenic lines.

Genotype	Reference
pGNL:GNL:HA gnc gnl	Transgenic lines and genetic crosses generated for this study
35S:GNC:YFP:HA:GR gnc gnl	
35S:GNL:YFP:HA:GR gnc gnl	
gnc gnl gun2-1	
gnc gnl 35S:GUN2	
35S:GUN2 Col-0	
gun2-1 35S:YFP:GNL	
gun4-1 gnc gnl	
gnc gnl 35S:GUN4	
35S:GUN4 Col-0	
gun4-1 35S:YFP:GNL	
gun5-1 gnc gnl	
cch1 gnc gnl	
gnc gnl 35S:GUN5	
35S:GUN5 Col-0	
gun5-1 35S:YFP:GNL	
cch1 35S:YFP:GNL	
gnc gnl 35S:SIG2	
sig2-1 35S:YFP:GNL	
35S:SIG2 Col-0	
sig6-2 gnc gnl	
gnc gnl 35S:SIG6	
35S:SIG6 Col-0	
sig6-2 35S:YFP:GNL	
cs gnc gnl	
cs 35S:YFP:GNL	
gnc gnl glk1-1 glk2-1	
glk1-1 glk2-1 35S:YFP:GNL	
pif1-1 gnc gnl	
pif1-1 35S:YFP:GNL	
pi3-3 gnc gnl	
pif3-3 35S:YFP:GNL	
pifq 35S:YFP:GNL	René Richter (unpublished)
35S:YFP:GNL Col-0	René Richter et al., 2010
35S:GNC:GFP Col-0	René Richter et al., 2010

Table 4: List of primers used for cloning.

Name	Sequence 5' - 3'	Construct
pGNL:GNL:HA attB1 Fw	GGGGACAAGTTTGTACAAAAAAGCAGGCTC ATAAAAATTTGAACATGTGGT	*pGNL:GNL: HA*
pGNL:GNL:HA attB2 Rv	GGGGACCACTTTGTACAAGAAAGCTGGGTT ACACCCGTGAACCATTCCGT	
GR Fw	AAAAGGCGCGCCATACGACCCAACCGATGC CCTTGGAATTGAC	*35S:GNC:Y FP:HA:GR*
GR Rv	AAAAGGCGCGCCTCATTTTTGATGAAACAGA AGCTTTTTG	
pEarleyGate 101 mutation PCR to introduce *GR*	GATTACGCTTATGGCGCGCCATTAAGACCC GGG	
35S:GUN2 attB1 Fw	GGGGACAAGTTTGTACAAAAAAGCAGGCTC AATGGCGTATTTAGCTCCGATT	*35S:GUN2*
35S:GUN2 attB2 Rv	GGGGACCACTTTGTACAAGAAAGCTGGGTC TCAGGACAATATGAGACGAAGTATC	
35S:GUN4 attB1 Fw	GGGGACAAGTTTGTACAAAAAAGCAGGCTC AATGGCGACCACAAACTCT	*35S:GUN4*
35S:GUN4 attB2 Rv	GGGGACCACTTTGTACAAGAAAGCTGGGTC TCAGAAGCTGTAATTTGTTTTAAAC	
35S:GUN5 attB1 Fw	GGGGACAAGTTTGTACAAAAAAGCAGGCTC AATGGCTTCGCTTGTGTATTCTC	*35S:GUN5*
35S:GUN5 attB2 Rv	GGGGACCACTTTGTACAAGAAAGCTGGGTC TTATCGATCGATCCCTTCGATC	
35S:SIG2 attB1 Fw	GGGGACAAGTTTGTACAAAAAAGCAGGCTC AATGTCTTCTTGTCTTCTTCCTCAGT	*35S:SIG2*
35S:SIG2 attB2 Rv	GGGGACCACTTTGTACAAGAAAGCTGGGTC TTATGATTGTGCAACCAAGTATTG	
35S:SIG6 attB1 Fw	GGGGACAAGTTTGTACAAAAAAGCAGGCTC AATGGAAGCTACGAGGAACTTGGT	*35S:SIG6*
35S:SIG6 attB2 Rv	GGGGACCACTTTGTACAAGAAAGCTGGGTC CTAGACAAGCAAATCAGCATAAGCA	
35S:DVR attB1 Fw	GGGGACAAGTTTGTACAAAAAAGCAGGCTC AATGTCACTTTGCTCTTCCTTCAA	*35S:DVR*
35S:DVR attB2 Rv	GGGGACCACTTTGTACAAGAAAGCTGGGTC CTAGAAGAACTGTTCACCGAGTTCT	

Table 5: List of primers used for genotyping.

Name	Sequence 5' - 3'	T-DNA	Allele
LBb1.3	ATTTTGCCGATTTCGGAAC		SALK
GABI (08409)	ATATTGACCATCATACTCATTGC		GABI
gnc LP	TTTGATCTTGCACTTTTTGGC		*gnc*
gnc RP	GCCAAGATGTTTGTGGCTAAC	LBb1.3	
gnl LP	TATCTGATGGTGGTTCATCATCAAG		*gnl*
gnl RP	ATGCTAGATCATCGAAATAGATATTG	LBb1.3	
gun2-1 dCAPS Fw	CGAGATTCCAGAACCAACAG		*gun2-1*
gun2-1 dCAPS Rv	GATGTTGTAGAAGTGACAAATGAATGCTC		
gun4-1 Fw	ACTCTCTCCACCACCACCAC		*gun4-1*
gun4-1 Rv	AGATCTTCGGGGGAGATTGT		
gun5-1 Fw	ACCAACCGGTAAAAACATGCATG		*gun5-1*
gun5-1 Rv	CTCACACCAATCATCCAAAGAAC		
cch-1 Fw	GAGGCTGCTTTTCTCCAAGTCAGCAAGTCTTC		*cch-1*
cch-1 Rv	CAAAATGAAGAACAGC		
cs Fw	ACCGAGCAGGACAAGC		*cs*
cs Rv	GTCTATGATTTGAAGTTTG		
sig6-2 Fw	TGTCACATGCGTTAAGAGACG		*sig6-2*
sig6-2 Rv	CTTATCCCCATAGCTTCAGCC	GABI	
glk1-1 wt Fw	GAAGAAAGAGACTTAC		*glk1-1*
glk1-1 wt Rv	GCTCTGGTGTCCAATC		
glk1-1 mutant Fw	CGGGATCCGACACTCTTTAATTAACTGACACTC		
glk1-1 mutant Rv	AACTGCAGGTTACTGATCCGATTGTTCTT		
glk2-1 wt Fw	CGATTACTACGACGATC		*glk2-1*
glk2-1 wt Rv	CGTGGCATGTCTCCGG		
glk2-1 mutant Fw	GTTTTGGCCGACACTCCTTACC		
glk2-1 mutant Rv	TCCGATGTGACCTATATTTC		
pif1-1 LP	CTCTTTTGGATCTTTCTGGGG		*pif1-1*
pif1-1 RP	GACTTGCGCACGATAGCTAAC	LBb1.3	
pif3-3 wt Fw	AGAAGCAATTTGGTCACCATGCTC		*pif3-3*
pif3-3 wt Rv	TGCATACAAATAGTCGATCGTATG		
pif3-3 del Fw	GGTGTGTATGTGAGAAGGTACATCCATCG		
pif3-3 del Rv	AAGCTTAGCTTTGGTGAGCCTGAAAAGCTC		

Table 6: List of primers used for qRT-PCR.

Name	Sequence 5' - 3'
qRT *GNC* Fw	GCGTGATTAGGGTTTGTTCG
qRT *GNC* Rv	CTTTGCCGTATACCACATGC
qRT *GNL* Fw	CCATATCTCCCAACCTCTCG
qRT *GNL* Rv	TGGGCACCATTTGATCACT
qRT *GUN2* Fw	TCCTGGAGAATCAAAGGGTTT
qRT *GUN2* Rv	GTGTTCTTGAACTCGGCAT
qRT *GUN4* Fw	ACTTCTCTTTCCCTCAAACAACC
qRT *GUN4* Rv	GCTGTATCCGAATCTACCATCAC
qRT *GUN5* Fw	CAACCAAACCAGCCAAATCT
qRT *GUN5* Rv	AGAGATTGCACGGCTTCACT
qRT *CHLI1* Fw	CCGGCGAGGTTTATCT
qRT *CHLI1* Rv	TTTGTAAGTGTCACGGAAAT
qRT *CHLI2* Fw	TCTTGACCTGCCCTCG
qRT *CHLI2* Rv	GCAGCAAACGGATAAACA
qRT *CHLD* Fw	CTATGGCCGACAGTTTTTCC
qRT *CHLD* Rv	GCGCCAAGTAAAAGAGCAGT
qRT *GLK1* Fw	CCGGTAGACTTACATCCGTCA
qRT *GLK1* Rv	CATGGCCTCGTCAATACATCT
qRT *GLK2* Fw	AACGTTGCTAGCCATCTTCAG
qRT *GLK2* Rv	CTCCTACTCCGGGCACTG
qRT *DVR* Fw	AGCAGCGTTTATAGCGGATT
qRT *DVR* Rv	CTCCTTGCTCTAATGGCGTT
qRT *SIG2* Fw	CGATGGTCCTTCCACTGAG
qRT *SIG2* Rv	CTGCTTCATCGCTTGTGAGA
qRT *SIG6* Fw	AATCGTGGACTCAACTTTCAGG
qRT *SIG6* Rv	ACTTTTCATTAGCCCCATGC
qRT *PIF1* Fw	AGAAGCCACCACTACTGATGA
qRT *PIF1* Rv	TGAAGGAAGGAGGAGGAATAG
qRT *PIF3* Fw	GACGACTATGGTGGACGAGAT
qRT *PIF3* Rv	CGTAGCAGAAGCAACAGACTC
qRT *CAO* Fw	AACTCAAGAACTCTGCAGCTGAT
qRT *CAO* Rv	CAAGCTTCTCACGCATCTCA
qRT *CRD1* Fw	AACTCAAGAACTCTGCAGCTGAT
qRT *CRD1* Rv	CAAGCTTCTCACGCATCTCA
qRT *HEMA1* Fw	AACTCAAGAACTCTGCAGCTGAT
qRT *HEMA1* Rv	CAAGCTTCTCACGCATCTCA
qRT *LHCB1.3* Fw	ATGGCCGCCTCAACAATGG
qRT *LHCB1.3* Rv	CGGTAAGGTAGCTGGGTGAC
qRT *25R1* Fw	GAACTTTGAAGGCCGAAGAG
qRT *25R1* Rv	ATCGACTAACCCATGTGCAA

qRT *ACT8* Fw	GCAGCATGAAGATTAAGGTCGTG
qRT *ACT8* Rv	TGTGGACAATGCCTGGACCTGCT

Table 7: List of primers used for ChIP qRT-PCRs.

Name	**Sequence 5' - 3'**
ChIP *GNC* N17 Fw	GGGTTGTTGTTCGTGATGGTTTT
ChIP *GNC* N18 Rv	TTGGACTCTTTTTGCCGTCT
ChIP *GNL* N43 Fw	ACTTGTGTTTTGGGGTCGTC
ChIP *GNL* N44 Rv	CCTTGTCAAACTGTGGAGGA
ChIP *GUN2* set-1 Fw	TTCATTCACCCTCTCATCGTT
ChIP *GUN2* set-1 Rv	GCAATGTAGTTTTAGTTGGCTTGA
ChIP *GUN2* set-2 Fw	GCAACACTCAACGCACTGTC
ChIP *GUN2* set-2 Rv	TTGAATTTTTAAATAGGCGAAAA
ChIP *GUN4* set-1 Fw	CCTGAGCCATAAGTGACCAA
ChIP *GUN4* set-1 Rv	GTGGTGGTGGTGGAGAGAGT
ChIP *GUN4* set-2 Fw	GGGCCTATTTATACGCCAATG
ChIP *GUN4* set-2 Rv	CGTCATTTCTCTCGTTATCGTT
ChIP *GUN4* set-3 Fw	CGATAACGAGAGAAATGACGTAGA
ChIP *GUN4* set-3 Rv	TGGCTCAGGTTTGATTTTCTC
ChIP *GUN4* set-3 Fw	CGATAACGAGAGAAATGACGTAGA
ChIP *GUN4* set-3 Rv	TGGCTCAGGTTTGATTTTCTC
ChIP *GUN5* set-1 Fw	ATGGGATGCAGACCAAGTGT
ChIP *GUN5* set-1 Rv	TGGTTTTGCTCTTGTTGGTG
ChIP *GUN5* set-3 Fw	CATCTCATTGTCCCAAGC
ChIP *GUN5* set-3 Rv	ACTCCAAGCCTTCATCTGGA
ChIP *GUN5* set-6 Fw	CTCCCACTTGGAGCTCAAAAAGT
ChIP *GUN5* set-6 Rv	CGGAGGAAAGAATGTTTGGT
ChIP *GUN5* set-7 Fw	TTGAAACATGATAAGTTTTTACATCCA
ChIP *GUN5* set-7 Rv	TTTTGGTTCAGCTAGGTCTGG
ChIP *CHLD* set-2 Fw	TGTGGATAGTGCTGCAATCA
ChIP *CHLD* set-2 Rv	CGAAAGAGTCTGCAGGTTGA
ChIP *GLK1* set-4 Fw	GGGTACACCCGCCTCAATAG
ChIP *GLK1* set-4 Rv	TAACATCGATCAATCTTCACTT
ChIP *GLK1* set-5 Fw	CGACAAGAGATGGTTGCGACG
ChIP *GLK1* set-5 Rv	TCGTTGAAGAAGCGTTCATG
ChIP *GLK2* set-1 Fw	CATGTCAGTATCCACCAACACA
ChIP *GLK2* set-1 Rv	ATGAGTACTGGAGCCGGAGA
ChIP *SIG2* set-1 Fw	AGGCCCAAAAGAAGTGGAAA
ChIP *SIG2* set-1 Rv	GCGGATGATGAAGACGAAGA
ChIP *SIG2* set-2 Fw	AGCCATTTTAAGATGTACAACAGCA
ChIP *SIG2* set-2 Rv	TTTGCAAAGTCAACCCATATGTAA

ChIP *SIG6* set-1 Fw	GGAGGGAGAAGAAGATGATTCG
ChIP *SIG6* set-1 Rv	GTGGATCATGTTGGGCCTTA
ChIP *SIG6* set-2 Fw	TTCCATGGCAACAAACAAGT
ChIP *SIG6* set-2 Rv	TGACGAACAGATAAGGCGACA
ChIP *DVR* set-2 Fw	CGCCGTACATCTGTTCGTTA
ChIP *DVR* set-2 Rv	GGTGAAATTCGGTGGGAGTT
ChIP *DVR* set-3 Fw	CGGTACAGGTTTTTGTCTTCTT
ChIP *DVR* set-3 Rv	CCCCAATACTTTATCAATGGTG
ChIP *GATA17* set-2 Fw	CTGTTGCTACTAACCGC
ChIP *GATA17* set-2 Rv	CGCTGCTACTGCAGTTCTCG

2.2 Methods

2.2.1 Seed sterilization and growth conditions

For all experiments presented in this thesis, the sterilization of the seeds was performed by rotating the seeds for 12 min in 1 ml solution of calcium hypochloride followed by four washes with autoclaved H_2O. Sterilized seeds were placed on GM plates (growth medium plates) consisting of 4.3 g/l Murashige and Skoog Medium, 10 g/l Saccharose, 0.5 g/l MES, 5.5 g/l Plant-agar, pH 5.8). Seeds were stratified for 3-d in the dark and at 4°C. Young seedlings and adult plants were grown under constant white light (120 µmol m^{-2} s^{-1}), unless stated otherwise.

2.2.2 Transformation of Arabidopsis plants

To introduce transgenes to Arabidopsis, *Agrobacterium tumefaciens* was used with the floral dip method as described (Clough and Bent, 1998).

2.2.3 DNA extraction from Arabidopsis tissues

Plant tissue was isolated and ground in extraction buffer (250 mM NaCl, 200 mM Tris/HCl [pH 7.5], 25 mM EDTA [pH 8.0], 0.5% SDS). Then the homogenized material was incubated for 25 min at 65°C and subsequently mixed with 300 µl phenol/chloroform (1:1) and centrifuged at 16,000 *g* for 10 min at 21°C in order to separate hydrophobic and hydrophilic phases. Approximately 350 µl from the upper phase was taken, mixed with 700 µl isopropanol, and centrifuged at 16,000 *g* for 10 min at 4°C. Next, the supernatant was discarded and the nucleic acid

pellet mixed with 500 µl 70% ethanol and centrifuged at 16,000 *g* for 5 min at 4°C. After that, the supernatant was discarded and the nucleic acid pellet dried in a speed-vac at 30°C for 10 min. Finally, the pellet was dissolved in ultrapure autoclaved water.

2.2.4 Genotyping PCR

The identification of mutant lines was performed by PCR using specific primers as listed in Table 5. The PCR mix used for the genotyping consisted of 2.5 µl 10xPCR reaction buffer (200mM Tris/HCl [pH 8.4], 25mM MgCl2 and 500mM KCl), 2.5 µl mix of dNTPs (100mM dATP, 100mM dTTP, 100mM dGTP and 100mM dCTP), 1.0 µl mix of forward and reverse primer (final concentration 10 µM each), 0.2 µl DNA Taq-polymerase, 16.8 µl ultrapure autoclaved water, and 2.0 µl genomic DNA. The conditions used in the thermo cycler for the genotyping PCR were: Step 1: 94°C for 4 min, Step 2: 94°C for 1 min, Step 3: 58°C for 0:30 min, Step 4: 72°C for 1 min/1000 bp PCR product, repeat step 2 to 4 for 32 times, Step 5: 72°C for 6 min. The PCR products were visualized afterwards in agarose gels using staining by ethidium bromide.

2.2.5 RNA extraction

For RNA extraction from Arabidopsis tissue, the NucleiSpin RNA kit (Macherey-Nagel, Düren, Germany) was used. The extraction was performed as indicated in the manual of the kit, with a minor modification at the elution step: Instead of 60 µl RNAase-free H_2O, RNA was eluted with 25 µl RNAse-free H_2O. Subsequently, the concentration of each sample was measured with the Nanodrop spectrophotometer (ThermoScientific, Waltham, MA). 2 µg RNA was reverse-transcribed using 0.5 µl oligo-dT-primer (20 µM, sequence: TTTTTTTTTTTTTTTTTTTTVN), 4 µl RT-buffer, 2 µl mix of dNTPs (100 mM dATP, 100 mM dTTP, 100 mM dGTP and 100 mM dCTP), 2 µl (40 U) M-MuLV reverse transcriptase (ThermoScientific, Waltham, MA) and filled up to 20 µl with ultrapure autoclaved water. The conditions used in the thermo cycler for the cDNA synthesis were: Step 1: 37°C for 60 min and 10 min, Step 2: 70°C for 10 min.

2.2.6 Real time qRT-PCR

The quantification, either of transcript abundance or of DNA bound in the ChIP experiments was performed by quantitative real time PCR (qRT-PCR) in a CFX96 thermocycler (BioRad, Freiburg, Germany). The total volume of the reaction was 10 µl and all gradients were used according to the protocol of the SsoAdvanced™ Universal SYBR® Green Supermix (BioRad, Freiburg, Germany). The conditions for the qRT-PCR for gene expression were: step 1: 50°C for 2:00 min, step 2: 95°C for 3:00 min, step 3: 95°C for 0:15 min, step 4: 60°C for 0:40 min. Steps 3 to 4 were repeated 32 times followed by 95°C for 0:10 min. The expression of all genes tested in this thesis was normalized to *ACT8* except the experiment with norflurazon treated seedlings, where *25R1* was used for the normalization. The conditions for the qRT-PCR to quantify ChIP binding events were: (1) 50°C for 2:00 min, (2) 95°C for 3:00 min, (3) 95°C for 0:15 min, (4) 60°C for 1 min. Steps 3 to 4 were repeated 35 to 40 times followed by 95°C for 0:10 min. The primers used for the Real time qRT-PCR are listed in Table 6.

2.2.7 Cloning of *pGNL:GNL:HA gnc gnl*

To generate *pGNL:GNL:HA*, a 2.3 kb *GNL* promoter fragment, and the *GNL* genomic sequence was amplified as one fragment by PCR. Subsequently, the PCR product was inserted in pDONR207 with a BP reaction, followed by an LR reaction using the destination vector pEarleyGate-301 (Earley et al. 2006). The final clone was transformed into the *Agrobacterium tumefaciens* strain GV3101 pMP90 and subsequently transformed to the *gnc gnl* double mutant plants using the floral dip method (Clough and Bent, 1998). The primers used for this cloning are listed in Table 4.

2.2.8 Cloning of overexpression lines of *GUN2*, *GUN4*, *GUN5*, *DVR*, *SIG2*, *SIG6*, *GLK1*

For the cloning of the overexpression lines, the corresponding gene fragments were amplified with PCR using cDNA as template. Next, they were cloned by a BP-reaction to the pDONR201 vector and subsequently via LR-reaction to the pAligator-N2 destination vector (Bensmihen et al. 2004). The final destination

clone was transformed to *Agrobacterium tumefaciens* strain GV3101 pMP90 and, using the floral dip method, into the *gnc gnl* double mutant and wt plants (Clough and Bent, 1998). The primers used for this cloning are listed in Table 4.

2.2.9 Cloning of *35S:GNC:YFP:HA:GR* and *35S:GNL:YFP:HA:GR*

To obtain *35S:GNC:YFP:HA:GR* and *35S:GNL:YFP:HA:GR*, an *AscI* restriction site was introduced after the *HA* sequence of the vectors *35S:GNC:YFP:HA* and *35S:GNL:YFP:HA*. *AscI* is a non-cutter enzyme for these particular vectors. Next, the ligand binding domain of the *GR* (*GLUCOCORTICOID RECEPTOR*) was amplified from the vector pTA7002 (Aoyama and Chua 1997) using primers including the *AscI* restriction site. The *GR* fragment was then introduced as an *AscI* site into the modified *35S:GNC:YFP* and *35S:GNL:YFP:HA* vectors to obtain *35S:GNC:YFP:HA:GR* and *35S:GNL:YFP:HA:GR*. The final vector was transformed to *Agrobacterium tumefaciens* strain GV3101 pMP90 followed by transformation into the *gnc gnl* double mutant with the floral dip method (Clough and Bent, 1998). The primers used for this cloning are listed in Table 4.

2.2.10 Chromatin immunoprecipitation (ChIP)

For ChIP experiments with *pGNL:GNL:HA gnc gnl*, seedlings were grown on GM plates for 10-d under long-day conditions (16 h light (120 µmol m^{-2} s^{-1}) / 8 h dark). Subsequently, plant tissue from *pGNL:GNL:HA gnc gnl* and *gnc gnl* seedlings was fixed in 1% formaldehyde for 20 min. The rest of the ChIP experiment was performed as previously described (Kaufmann et al., 2010). A ChIP-grade anti-HA tag (Abcam, Cambridge, UK) was used for the immunoprecipitation of chromatin. Three independent biological replicates were used for the *pGNL:GNL:HA gnc gnl* seedlings and two independent biological replicates were used for the *gnc gnl* double mutant seedlings (negative controls). Each biological replicate consisted of approximately 2 g seedling tissue.

The ChIP experiment with *35S:GNL:YFP:HA:GR gnc gnl* seedlings was conducted with 10-d-old seedlings, grown on GM plates under constant white light. At day 10, a 4 h treatment with 10 µM Dex (dexamethasone) and mock was applied, followed by fixation in 1% formaldehyde for 20 min. The rest of the ChIP

experiment was performed as previously described (Kaufmann et al., 2010). A GFP-TRAP®A (Chromotek, Planegg-Martinsried, Germany) antibody conjugated to agarose beads was used for ChIP. Three independent biological replicates were used for the Dex-treated and the mock (negative control) samples. Each biological replicate consisted of 2 g seedlings. The primers used for the ChIP qRT-PCR are listed in Table 7.

2.2.11 Next generation sequencing library preparation

The DNA derived from the pGNL:GNL:HA gnc gnl and *35S:GNL:YFP:HA:GR gnc gnl* ChIP samples was used to produce libraries compatible with the Illumina GAIIx and MiSeq (San Diego, CA) platform, respectively. The standard Illumina protocol was followed for that purpose. The preparation of the library for the *pGNL:GNL:HA gnc gnl* ChIP was performed in the Department of Molecular Biology at the Max Planck Institute for Developmental Biology, Tübingen, Germany by Dr. David Posé from the group of Dr. Markus Schmid.

2.2.12 ChIP-seq analysis

The reads derived from each of the ChIP experiments were mapped to Arabidopsis genome (TAIR10) using SOAPv1 with the settings: 3 mismatches, mapping to unique positions only, no gaps allowed and iterative trimming set from 41 to 50 (Li et al. 2008). The further downstream analysis of peak identification was conducted with CSAR, which calculates the false discovery rate (FDR) threshold for the read-enriched regions (Muiño et al. 2011). Only those with FDR < 0.05 and score > 7 were retained as statistically significant peaks. Association of the peaks to the gene models was performed by using the function ‘genesWithPeaks’ of the CSAR software. For the *de novo* motif discovery, a *de novo* regulatory motif search was used based on a Gibbs sampling method from 1000 bp upstream and downstream regions from the genes (Thijs et al. 2001; Thijs et al. 2002). This method identifies over-represented motifs. The motifs were sampled to the Arabidopsis background model, which was created from the input set of sequences from the *Arabidopsis thaliana* genome. The sampler was set to

run over 100 iterations using default settings for all other parameters (Claeys et al. 2012). The motifs were ranked using the consensus score [2+plog(p)].

The total number of statistically significant annotated peaks (n = 3615) was used as an input for the *de novo* motif detection. To this end, sequences around the summit of each peak were extracted and subsequently grouped according to the annotations of the summit of the peak (e.g., 5'-UTR, exon, intron, 3'-UTR and intragenic regions). The total number of sequences which were used in this analysis, according to their annotation category were 172 (5'-UTR), 99 (3'-UTR), 409 (exon), 263 (intron) and 1519 (intragenic). Next, the identified motifs were sorted according to their log likelihood (L.L) and subsequently for each annotated category (genetic element). Finally, the top 10 overrepresented motifs were selected (Table 8). All of these selected motifs were used as a query to search for closely related motifs in the JASPAR database for transcription factor binding sites (Table 8).

2.2.13 Dex (Dexamethasone) and CHX (cycloheximide) treatments for RNA-seq experiments

Seedlings were grown under constant white light on GM plates for 10-d. On day 10, half of them were transferred to liquid GM with 10 µM CHX (mock) and the other half to liquid GM with 10 µM Dex and 10 µM CHX. The treatments were continued for three more hours and then the samples were frozen in liquid nitrogen and subsequently ground with a TissueLyser II (Qiagen, Hilden, Germany). Total RNA extraction was performed using the NucleoSpin RNA-kit (Macherey-Nagel, Düren, Germany). Three independent biological replicates were used for each of the experimental groups. Next, the samples from both groups were further used in order to create libraries for the sequencing followed the standard Illumina protocol for the Illumina HiSeq 1000 sequencing platform at the Kompetenzzentrum Fluoreszente Bioanalytik, Regensburg, Germany by Dr. Thomas Stempfl.

2.2.14 RNA-seq analysis

The reads produced from the sequencing were mapped to the Arabidopsis genome (TAIR10) using the Genomic Workbench software (CLC bioinformatics) with allowance of two miss-matches for the reads during the mapping. The differentially expressed genes were identified using the same software with the thresholds for the differentially expressed genes set to FDR < 0.01 and fold changes ≥ 1.2 for the *35S:GNL:YFP:HA:GR gnc gnl* experiment and FDR < 0.01 and fold changes ≥ 2.45 for the *35S:GNC:YFP:HA:GR gnc gnl* experiment and ≥ 1.5 for the *35S:GNL:YFP:HA:GR gnc gnl* experiment. The reason for using different thresholds for the two RNA-seq experiments was that the experiment with *35S:GNL:YFP:HA:GR* showed large variation among the different biological replicates of each group. This led to the increased p-values and subsequently fewer differentially expressed genes.

2.2.15 HPLC for tetrapyrroles and carotenoids

Tetrapyrroles and carotenoids were extracted from approximately 60 mg aerial part of 10-d-old light-grown seedlings. The frozen tissue was homogenized in a Retsch mill using steal beads and porphyrins were extracted with acetone:0.2M NH4OH (9:1, v/v) at −20°C for 1 h. It followed centrifugation (16,000 *g* for 10 min at 4°C) and subsequently the supernatant was used to determine tetrapyrroles and carotenoids. Heme was extracted from the pellet using acetone:HCl:dimethyl sulfoxide (10:0.5:2, v/v/v). The HPLC analysis for the tetrapyrroles and the carotenoids was performed as described in Schlicke et al. 2014 and Kim et al. 2013.

2.2.16 Chlorophyll quantification

Chlorophyll measurements were conducted as described previously by using 7-d-old seedlings grown under constant white light, unless stated otherwise (Moran 1982).

2.2.17 Dipyridyl treatment

Seedlings were grown under constant white light for 6-d and then placed in liquid GM with 1 mM DP (dipyridyl) (Sigma-Aldrich, Taufkirchen, Germany), which inhibits the first step of the heme pathway. The relative transcript levels of *GNC* and *GNL* were quantified 24 h after the treatment with DP. RNA extraction, cDNA synthesis, and qRT-PCR were performed as described above.

2.2.18 Cytokinin treatment

Seedlings were grown on GM plates for 10-d under constant white light. At day 10, half of the seedlings were transferred to liquid GM with 10 μM 6-BA and the other half to liquid GM (mock). Seedlings were frozen in liquid nitrogen and ground with a TissueLyser II (Qiagen, Hilden, Germany). RNA extraction, cDNA synthesis, and qRT-PCR were performed as described above.

2.2.19 Photobleaching experiment

To assess the greening rate of seedlings growing for various days in the dark, prior to 2-d exposure to constant white light, seedlings were initially grown in the dark for 0, 5 and 7-d and each of these groups was then exposed to constant white light for 2-d. The greening rate was determined as the fraction of seedlings with green cotyledons after the 2-d period growing under the light.

2.2.20 Quantification of protochlorophyllide

Germination of the seeds was promoted by exposure to light for 6 h and seedlings were then left growing on GM plates for 6 more days in the dark. Extraction of the pigments was performed from frozen tissue ground with the TissueLyser II (Qiagen, Hilden, Germany). The powder was dissolved in 1 ml ice-cold 80% acetone followed by agitation for 1 h at 4°C in the dark. Following centrifugation at 14,000 g for 10 min, fluorescence emission spectra were measured with a fluorescence spectrophotometer (TECAN-infinite 200 PRO, Crailsheim, Germany) after excitation at 440 nm and 5 nm band width between 600 nm and 800 nm.

2.2.21 Norflurazon treatment

Seedlings were grown for 7-d on GM medium with 5 µM NF (Norflurazon) (Sigma-Aldrich, Taufkirchen, Germany) and mock, under constant white light (300 µmol m^{-2} s^{-1}). RNA extraction, cDNA synthesis and qRT-PCR were performed as described above.

2.2.22 Quantification of the assimilation of CO_2

Plants were grown under long day conditions (16 h light / 8 h dark) for 7 weeks. Then, the assimilation of CO_2 was measured by the LiCor 6400XT under the conditions of 500 µE light intensity, 22°C and 400 ppm CO_2 or 100 ppm CO_2, respectively. Plants were allowed to adapt to the conditions, before the measurement was started.

2.2.23 Chlorophyll fluorescence measurements in the Imaging-PAM

Seedlings were grown for 7-d under long day conditions (8h/16h). Measurements were made in an Imaging PAM M-series Maxi version, (Walz, Effeltrich, Germany), at each seedling, two distinct parts of the hypocotyls were measured, the first one right below the cotyledons (apical), the second one right above the root-hypocotyl junction (distal). Intensity of chlorophyll fluorescence of the lower hypocotyl part was often below the detection limit. The effective photochemical quantum yield of photosystem II (Y(II)) was determined after adaptation to 150 µE, which was reached after 7 min.

3. Results - Systems biology approaches for the identification of GNC and GNL targets

3.1 Identification of the direct target genes of GNC and GNL with an important role in greening

3.1.1 Expression analysis of existing microarray datasets suggests the implication of B-GATAs in chlorophyll biosynthesis and chloroplast development

To have a look at the genes, which play an important role in chlorophyll biosynthesis and chloroplast development that may be regulated by the B-GATAs, a gene expression analysis was performed with existing microarray data of GNCox (*35S:GNC:GFP*) and GNLox (*35S:YFP:GNL*) Arabidopsis seedlings, all compared to the Col-0 (wild-type) (Richter et al. 2010).

In regard to the tetrapyrrole pathway, 25 genes were found to be differentially regulated in GNCox seedlings (22 upregulated, 3 downregulated) and 26 genes in GNLox (23 upregulated, 3 downregulated) (Figure 6A). Specifically, in the chlorophyll biosynthesis branch of the tetrapyrrole pathway, 9 genes were differentially expressed in GNCox seedlings (8 upregulated, 1 downregulated), and 8 in GNLox all upregulated (Figure 6A). Then the expression of genes was examined encoding for proteins of the chloroplast protein import machinery. 19 genes in GNCox as well as 19 genes in GNLox were found to be upregulated (Figure 6B). Genes with a role in chloroplast division were also upregulated in the overexpression lines of GNC (6 genes) and GNL (7 genes) (Figure 6C). In conclusion, the overexpression of the B-GATAs *GNC* and *GNL* affected the expression of genes with roles in the tetrapyrrole and specifically the chlorophyll pathway, the protein import machinery of the chloroplasts and the mechanism of the chloroplast division.

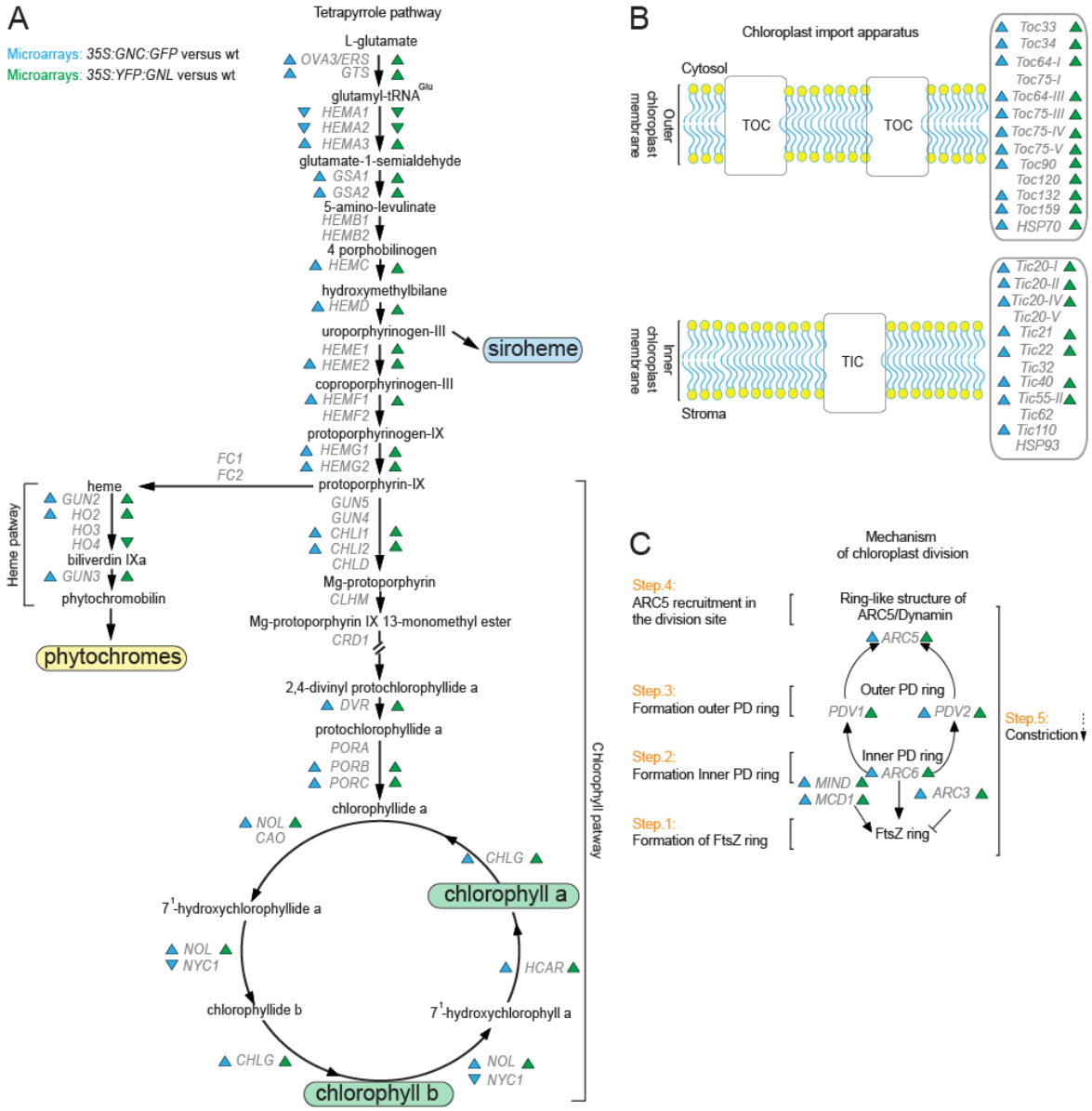

Figure 6: Transcriptome analysis with existing microarray data of GNCox (*35S:GNC:GFP* versus wt) and GNLox (*35S:YFP:GNL* versus wt). (**A**) Model of the tetrapyrrole pathway. (**B**) Model of the chloroplast import apparatus. (**C**) Model of the chloroplast division mechanism. Genes with a role in each step of each pathway are depicted with italics and grey letters. Blue arrowheads show genes differentially expressed in the GNCox microarrays, green arrowheads show genes differentially expressed in the GNLox microarrays; upregulation of a gene is depicted by an upward pointing arrowhead, while an arrowhead facing downward depicts downregulation of a gene. Fold change expression values are presented in Appendix Table 9.

3.1.2 The B-GATAs GNC and GNL are essential for the synthesis of chlorophyll intermediates

To better understand if the transcriptional regulation of chlorophyll biosynthesis pathway genes has an effect on the synthesis of chlorophyll intermediates, a high-performance liquid chromatography (HPLC) was performed with 10-d-old light-grown wt and *gnc gnl* double mutant seedlings by Dr. Boris Hedtke from the lab of Prof. Dr. Bernhard Grimm. The chlorophyll intermediates quantified by HPLC were Mg-protoIX (Mg-protoporphyrin IX), MME (Mg-protoporphyrin IX 13-monomethyl ester), Pchlide (protochlorophyllide) and Chlide (chlorophyllide), Chl a (chlorophyll a) and Chl b (chlorophyll b). All of the measured chlorophyll intermediates were reduced in *gnc gnl* double mutant compared to wt (Figure 7). These results showed that B-GATAs GNC and GNL strongly contributed to the production of the proper levels of some chlorophyll intermediates.

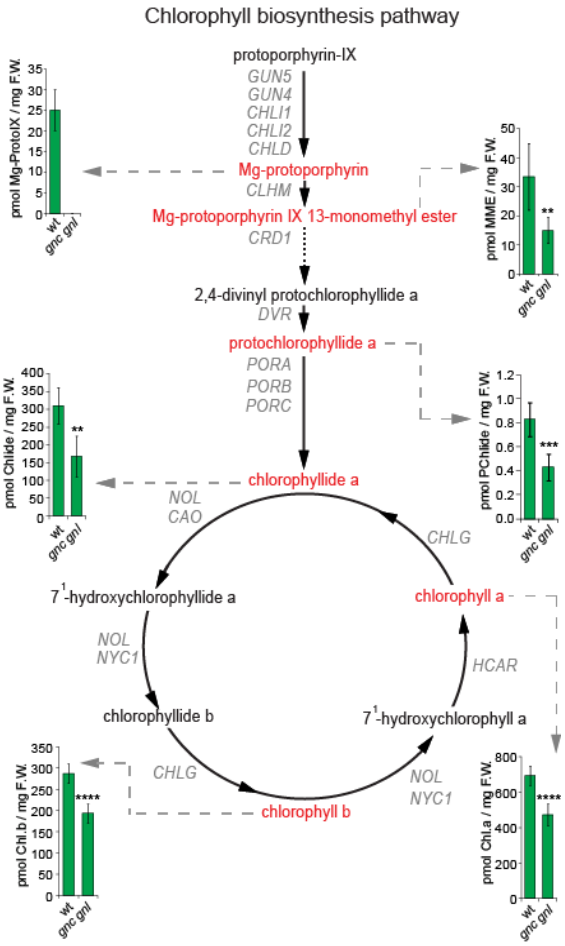

Figure 7: The levels of chlorophyll intermediates are reduced in the *gnc gnl* double mutant as determined by HPLC. Schematic representation of the chlorophyll biosynthesis pathway. Intermediates with red color were quantified by HPLC analysis in 10-d-old light-grown seedlings. Bar diagrams display the levels of chlorophyll intermediates. Genes with a role in each step of the pathway are depicted with italics and grey letters. Student's *t*-test: *P< 0.05, **P < 0.01, ***P < 0.001; n.s., not significant.

3.1.3 Identification of the GNC and GNL target genes with a role in greening

The current results suggested a role of GNC and GNL in the greening of Arabidopsis and in chloroplast development and function. However, in which way these two B-GATAs control the greening still remained unknown. To uncover the direct targets of GNC and GNL, two different kinds of NGS experiments were designed. The first being a chromatin immunoprecipitation coupled with NGS (ChIP-seq), which provided evidence for the direct binding of GNL to promoters of such genes. The second, an RNA-seq experiment, revealed greening related genes, which their transcription controlled by GNC and GNL.

3.1.4 ChIP-seq with *pGNL:GNL:HA gnc gnl* from light-grown seedlings

For the ChIP-seq experiment, transgenic of *pGNL:GNL:HA gnc gnl* plants were generated expressing *GNL* from a *GNL* promoter fragment to come as close as possible to the native status of *GNL* expression. The *pGNL:GNL:HA gnc gnl* seedlings were grown under long-day conditions and were able to rescue the pale green phenotype of *gnc gnl* double mutant (Figure 8A and B). Next, the immunoprecipitation of the GNL:HA protein from nuclear extracts was established (Figure 8C) and subsequently, a ChIP experiment was performed to confirm the ability of GNL:HA to bind to certain positions on the genome. Data produced by

NGS of the ChIP samples were aligned to the Arabidopsis genome. Reads that aligned unambiguously to a unique position of the genome were kept and

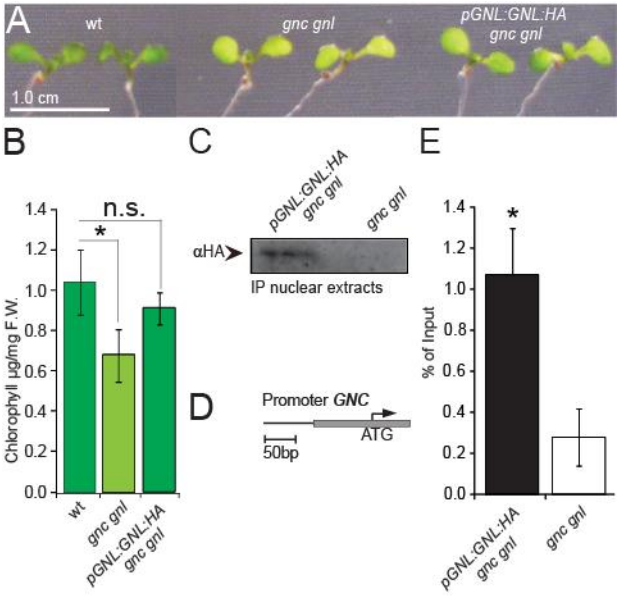

Figure 8: Establishing a *pGNL:GNL:HA gnc gnl* line for ChIP-seq. (A) Representative photo of 10-d-old light-grown seedlings. (B) Quantification of chlorophyll content in *gnc gnl* and *pGNL:GNL:HA gnc gnl* 10-d-old light-grown seedlings in comparison with wt. (C) Immunoblot with αHA antibody after immunoprecipitation (IP) of GNL:HA from nuclear extracts. (D) Schematic representation of the promoter of *GNC*, which GNL can bind. Grey-box shows the amplicon ChIP-qRT-PCR, ATG is the translation start codon and black line represents part of the *GNC* promoter. (E) ChIP-qRT-PCR shows binding of GNL close to the ATG in the 5´-UTR of *GNC*. Grey-box shows the amplicon for ChIP-qRT-PCR. Student's *t*-test: *P < 0.05; n.s., not significant.

subjected to further analysis.

Subsequently, regions with a statistically significant accumulation of reads obtained with *pGNL:GNL:HA gnc gnl* compared to *gnc gnl* were identified. In total, 3598 peaks with different annotations were found ($p < 0.005$ and FDR < 0.05). The total number of unique peaks was 1969 (this number referred to peaks with no annotation assigned to them), derived from all different sets of analysis (6 sets in total).

3.1.5 GNL binds not only to promoters but also to exonic and intronic regions of genes

To investigate the preferred binding sites of GNL in regard to the corresponding gene models, the distribution of the strong peaks was further examined. This particular part of the ChIP-seq analysis was performed by Dr. Manuel Spannagl in collaboration with the group of Prof. Dr. Klaus Mayer using a custom-made Java script.

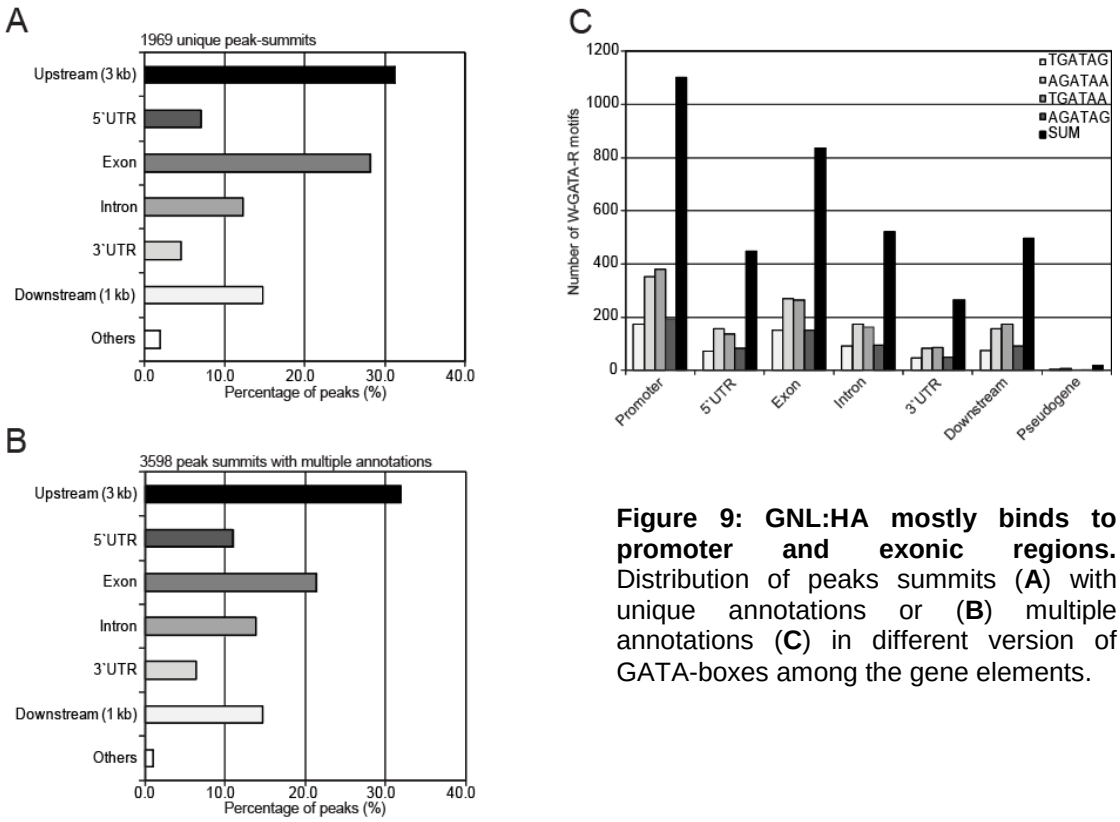

Figure 9: GNL:HA mostly binds to promoter and exonic regions. Distribution of peaks summits (**A**) with unique annotations or (**B**) multiple annotations (**C**) in different version of GATA-boxes among the gene elements.

Since GNL is a GATA transcription factor, a subsequent step in the ChIP-seq analysis was the quantification of GATA-boxes (W-GATA-R with W as A/T and R as A/G) in the different genetic elements. For all 1969 unique peak-summits, a sequence equal to the length of the peaks was extracted and analyzed for W-GATA-R motifs. Among all of the examined GATA boxes, the prevailing GATA-boxes were A-GATA-A and T-GATA-A. These GATA-boxes were strongly overrepresented in the promoter regions, found moderately in exons, introns and downstream regions and less frequently in 5´-UTRs and 3´-UTRs (Figure 9). In summary, this analysis revealed that GNL has a strong preference for binding mostly to promoter and exonic regions of genes. Furthermore, the typical GATA-boxes were found to be overrepresented in these regions.

3.1.6 *De novo* motif discovery supports the previous finding of the preference of GNL to bind to GATA-boxes

To further investigate the binding preference of GNL to certain motifs, a de-novo motif discovery was conducted with the data from the ChIP-seq experiment. Analysis was done with the web-based-tools MEME (http://meme-suite.org/tools/meme-chip) and RSAT (http://floresta.eead.csic. es/rsat/). Unfortunately, these efforts did not yield any reasonable result, probably due to the overrepresentation of GATA-motifs in the Arabidopsis genome. To solve this problem, a different method was performed by Dr. Manuel Spannagl and Dr. Sapna Sharma from the group of Prof. Dr. Klaus Mayer using a custom-made analysis pipeline as described in Materials and Methods section. Derivatives of the GATA-boxes belonging to the family of GATA proteins, of either *Saccharomyces cerevisiae* or *Mus musculus*, in the intronic, exonic and intragenic regions showed some of the most highly ranked over-represented motifs. Additionally, some versions of binding motifs of Arabidopsis MADS, MYB and LEAFY transcription factors were among the top ranked overrepresented motifs (Table 8).

From the results of the *de novo* motif discovery, two basic conclusions could be derived. First, no hints of the family of GATA proteins were seen, neither from

Table 8: *De novo* motif discovery for the ChIP-seq of GNL:HA.

	Consensus	Sequences	Instances	LL	Name	Class	Family	Score	Organism
5'-UTR	nnmATG	166	335	1597.16	LEC2	EcoRII fold	ABI3VP1	11.477	*Arabidopsis thaliana*
	ATGnnn	160	319	1569.08	ABI3	EcoRII fold	ABI3VP1	11.2218	*Arabidopsis thaliana*
	nATGGn	162	322	1560.31	YY1	Zinc-coordinating	BetaBetaAlpha-zinc finger	11.5029	*Homo sapiens*
	nATGnn	154	310	1547.58	LEC2	EcoRII fold	ABI3VP1	11.1982	*Arabidopsis thaliana*
	nnATGn	155	308	1539.76	Pou5f1::Sox2	Helix-Turn-Helix	Homeo	11.2814	*Mus musculus*
	ATGGnr	166	330	1517.24	RFX2	Winged Helix-Turn-Helix	RFX	11.6376	*Homo sapiens*
	nATGnn	155	307	1471.28	LEC2	EcoRII fold	ABI3VP1	11.1982	*Arabidopsis thaliana*
	wGmrG	163	321	1401.16	AtMYB84	Helix-Turn-Helix	Myb	10.7602	*Arabidopsis thaliana*
	AAywwG	163	316	1395.04	AG	Other Alpha-Helix	MADS	10.9725	*Arabidopsis thaliana*
	rwnATG	154	303	1391.15	BATF::JUN	Zipper-Type	Leucine-Zipper	11.5962	*Homo sapiens*
Exon	CGnAnC	390	786	3246.57	ASH1	Zinc-coordinating	GATA	10.7972	*Saccharomyces cerevisiae*
	yCmCG	348	761	3232.51	LFY	Helix-Turn-Helix	LEAFY	11.1908	*Homo sapiens*
	yGnnnC	361	722	3209.81	TAL1::GATA1	Zipper-Type	Helix-Loop-Helix	11.027	*Drosophyla melanogaster*
	CGwnnC	365	721	3184.59	h	Zipper-type	Helix-Loop-Helix	10.936	*Drosophyla melanogaster*
	nCsnCG	337	730	3170.33	LFY	Helix-Turn-Helix	LEAFY	10.7242	*Arabidopsis thaliana*
	AnCGnC	347	705	3149.61	LFY	Helix-Turn-Helix	LEAFY	10.8161	*Arabidopsis thaliana*
	CmAnC	368	716	3058.64	ASH1	Zinc-coordinating	GATA	10.9772	*Saccharomyces cerevisiae*
	TnwCCr	351	692	3020.89	LFY	Helix-Turn-Helix	LEAFY	11.1767	*Arabidopsis thaliana*
	CmCGn	332	703	3010.1	Mad	Zinc-coordinating	MH1	11.0767	*Drosophyla melanogaster*
	wmnCGT	357	686	2985.78	AtSPL3	Zinc-coordinating	SBP	11.314	*Arabidopsis thaliana*
Intron	GAsrGA	245	516	2307.12	Gata4	Zinc-coordinating	GATA	10.3599	*Mus musculus*
	CAmGA	241	497	2302.29	EcR::usp	Zinc-coordinating	Hormone-nuclear Receptor	11.1712	*Drosophyla melanogaster*
	sArAGA	241	495	2289.03	Gata4	Zinc-coordinating	GATA	10.3599	*Mus musculus*
	sAnnGA	234	488	2248.56	AtMYB77	Helix-Turn-Helix	Myb	11.1586	*Arabidopsis thaliana*
	sAnnrA	243	500	2239.28	RXR::RAR_DR5	Zinc-coordinating	Hormone-nuclear Receptor	11.2675	*Homo sapiens*
	sAsnnA	242	515	2213.06	EOR-1	Zinc-coordinating	BetaBetaAlpha-zinc finger	11.1993	*Caenorhabditis elegans*
	GAnrGA	236	481	2206.73	EOR-1	Zinc-coordinating	BetaBetaAlpha-zinc finger	11.1564	*Caenorhabditis elegans*
	rrsAGA	237	495	2167.56	Gata4	Zinc-coordinating	GATA	11.6024	*Mus musculus*
	nArrGA	229	462	2128.71	Spi1	Winged Helix-Turn-Helix	Ets	11.1181	*Mus musculus*
	nGAnnr	228	462	2103.68	ABF1	Zinc-coordinating	BetaBetaAlpha-zinc finger	11.2891	*Saccharomyces cerevisiae*
3'-UTR	AACAnA	90	192	851.92	RAV1	Beta-Hairpin-Ribbon	AP2 MBD-like	11.5	*Arabidopsis thaliana*
	Amsnmn	94	192	851.89	Su(H)	Other	LAG1	11.5	*Drosophyla melanogaster*
	ACAmmr	96	193	848.69	FOXP1	Winged Helix-Turn-Helix	Forkhead	11.5252	*Homo sapiens*
	Amskmr	94	180	825.09	Su(H)	Other	LAG1	11.4	*Drosophyla melanogaster*
	sATrsn	92	178	824.34	LEC2	EcoRII fold	ABI3VP1	10.9169	*Arabidopsis thaliana*
	AnrACA	92	189	824.04	D	Other Alpha-Helix	High Mobility Group box (HMG)	11.5479	*Drosophyla melanogaster*
	AmyCAm	93	172	810.42	RREB1	Zinc-coordinating	BetaBetaAlpha-zinc finger	11.4917	*Homo sapiens*
	mACnsm	91	181	804.64	Gamyb	Helix-Turn-Helix	Myb	11.0508	*Hordeum vulgare*
	mmTyAA	91	175	804.56	C15	Helix-Turn-Helix	Homeo	11.1399	*Drosophyla melanogaster*
	nACmsm	90	180	794.8	NR3C1	Zinc-coordinating	Hormone-nuclear Receptor	11.1909	*Mus musculus*
Intergenic	CTyTCT	299	545	2079.94	FLC	Other Alpha-Helix	MADS	10.6984	*Arabidopsis thaliana*
	GArAGA	323	540	2120.57	FLC	Other Alpha-Helix	MADS	10.6383	*Arabidopsis thaliana*
	rGAGAG	331	594	2134.98	Trl	Zinc-coordinating	BetaBetaAlpha-zinc finger	11.5928	
	rAGAGA	320	642	1847.78	Gata4	Zinc-coordinating	GATA	10.7044	*Mus musculus*
	CAssnG	242	569	inf	RAV1 (var.2)	EcoRII fold	ABI3VP1	10.8886	
	TTTGTT	408	512	2579.85	FKH1	Winged Helix-Turn-Helix	Forkhead	11.8086	*Saccharomyces cerevisiae*
	TTCTTT	388	492	2496.96	AZF1	Zinc-coordinating	BetaBetaAlpha-zinc finger	11.722	*Saccharomyces cerevisiae*
	AAGAAA	418	571	2667.64	AZF1	Zinc-coordinating	BetaBetaAlpha-zinc finger	11.722	*Saccharomyces cerevisiae*
	TTTTCT	364	459	2330.48	PI	Other Alpha-Helix	MADS	10.8926	*Arabidopsis thaliana*
	ACAAAA	390	508	2428.45	NDT80	Ig-fold	NDT80/PhoG	11.8477	*Saccharomyces cerevisiae*

Arabidopsis nor from the plant kingdom in general. This was probably because of the lack of the respective data (e.g., from ChIP-seq experiments) with this particular protein family in the JASPAR database. Second, the discovery of binding boxes for MADS, MYB and LEAFY transcription factors, which may be an indication that GNL can potentially interact with transcription factors from these families to co-regulate gene expression.

3.1.7 Cross-regulation between the B-GATAs GNC, GNL and GATA17

Some of the strongest peaks identified by ChIP-seq were linked to the *GNC*, *GNL* and *GATA17* genes (Figure 10). It was noticeable that there were also strong peaks not only on the promoters of these genes but also in the regions inside the genes. The fact that these binding events were true binding positions and not a result of a putative DNA contamination were supported by the fact that: there were no reads mapped to the corresponding regions of the negative control sample *gnc gnl* (Figure 10) and a varying number of GATA-box (W-GATA-R) motifs was found in almost all of these peaks (Figure 10).

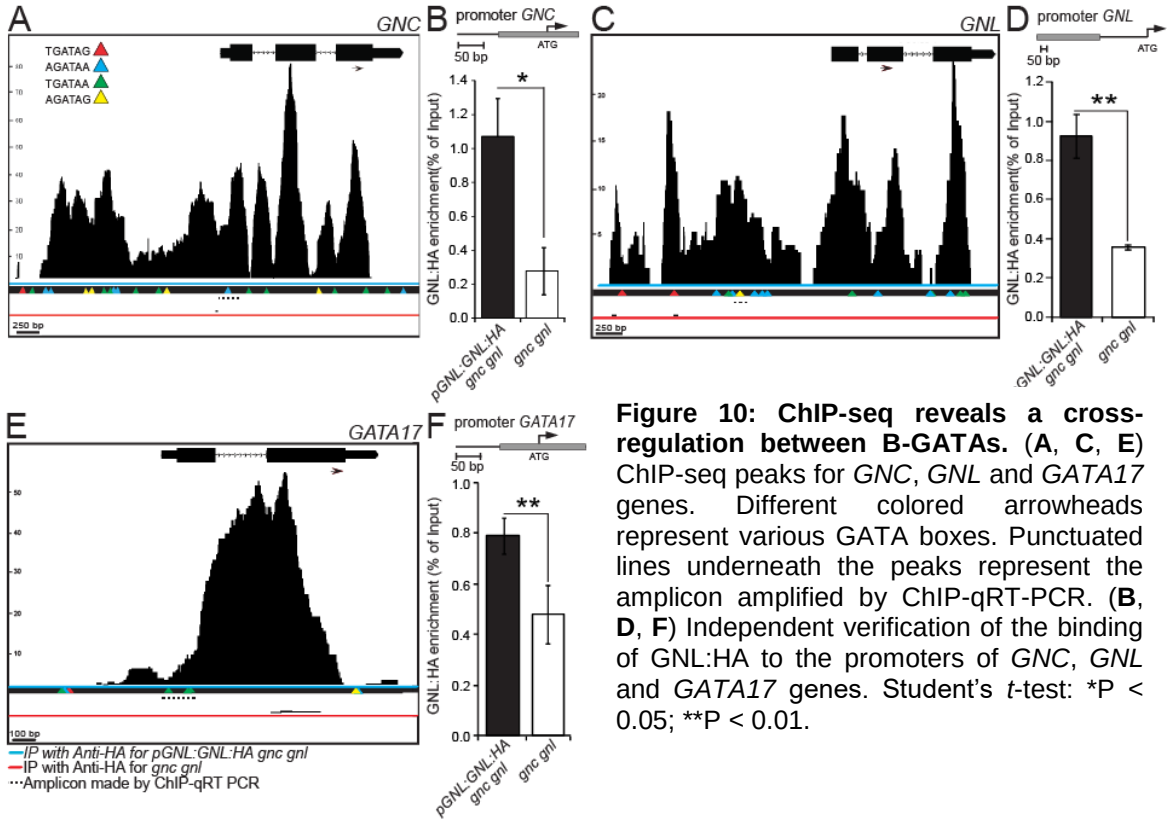

Figure 10: ChIP-seq reveals a cross-regulation between B-GATAs. (**A**, **C**, **E**) ChIP-seq peaks for *GNC*, *GNL* and *GATA17* genes. Different colored arrowheads represent various GATA boxes. Punctuated lines underneath the peaks represent the amplicon amplified by ChIP-qRT-PCR. (**B**, **D**, **F**) Independent verification of the binding of GNL:HA to the promoters of *GNC*, *GNL* and *GATA17* genes. Student's *t*-test: *P < 0.05; **P < 0.01.

To further verify the authenticity of these peaks from the ChIP-seq, independent ChIP experiments were conducted. For all three genes, GNL:HA was shown to bind to their promoters, particularly to regions in close proximity to the transcription start site (TSS) (Figure 10). In conclusion, the ChIP-seq experiment and additional independent ChIPs showed that GNL was not only able to directly bind its own promoter but also to the promoters of the two other B-GATAs *GNC*

and *GATA17*. Peak-binding positions of GNL were also detected inside the *GNL*, *GNC* and *GATA17* genes. These peaks would need to be further verified by independent ChIPs, but this was not one of the goals of this thesis.

3.1.8 Generation of inducible translational fusion variants of GNC and GNL for RNA-seq experiments

The ChIP-seq gave a good overview of the binding sites of GNL:HA in the genome of Arabidopsis. The binding of a transcription factor to a certain position in a gene can lead to at least three different scenarios: (1) direct regulation of the nearby gene, (2) regulation of the gene only in the presence of additional partner-protein(s), and (3) no transcriptional regulation at all. To find out, which of the binding events of GNL:HA (found in the ChIP-seq) led to direct differential expression of genes, RNA-seq experiments were performed.

To this end, transgenic plants of *35S:GNC:YFP:HA:GR gnc gnl* and *35S:GNL:YFP:HA:GR gnc gnl* were generated and used for the RNA-seq experiment (Figure 11). The advantage of using the glucocorticoid receptor-domain (GR) fused with GNC and GNL proteins was that the GR-fused proteins could be sent to the nucleus in a controllable manner after Dex application (Huq et al. 2003).

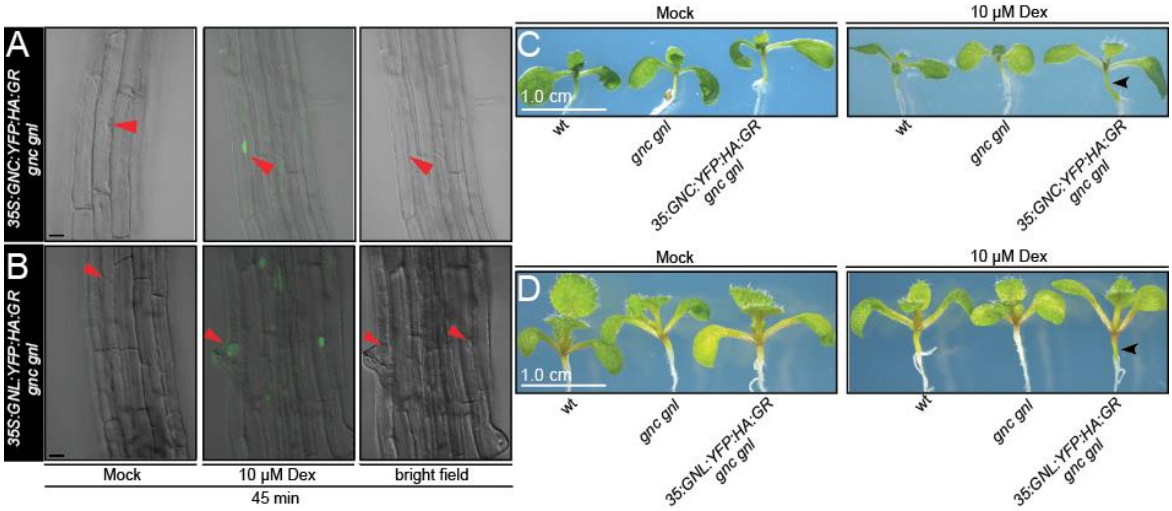

Figure 11*: 35S:GNC:YFP:HA:GR gnc gnl* and *35S:GNL:YFP:HA:GR gnc gnl* lines for RNA-seq. (**A**-**B**) Representative confocal microscopy images of the root of *35S:GNC:YFP:HA:GR gnc gnl* and *35S:GNL:YFP:HA:GR gnc gnl* 7-d-old light-grown seedlings localizing the GNC:YFP:HA:GR and the GNL:YFP:HA:GR proteins to the nucleus after a 45 min application of Dex. Red arrowheads indicate the position of a single nucleus. (**C**-**D**) Representative photos of 10-d-old light-grown seedlings growing on Dex and mock medium. Black arrowheads show greening of the hypocotyl in Dex-treated seedlings.

To test the functionality of these Dex-inducible transgenic lines, 7-d-old light-grown seedlings were treated with Dex for 45 min. After but not before the Dex application, YFP signal was detected in the nucleus (Figure 11A and B). In line with this, 7-d-old *35:GNC:HA:YFP:GR gnc gnl* and *35S:GNL:HA:YFP:GR gnc gnl* seedlings grown on 10 µM Dex medium showed enhanced greening of the hypocotyl, which is an established phenotype for GNCox and GNLox lines (Figure 11C and D). Taken together, these results showed that the transgenic plants successfully translocated the GR translational fusion to the nucleus and that the movement of the proteins was able to induce one of the known GNCox and GNLox phenotypes, rendering these plants suitable for the subsequent RNA-seq experiments.

3.1.9 Identification of the differentially expressed genes after induction of Dex and CHX of *35S:GNC:YFP:HA:GR gnc gnl* and *35S:GNL:YFP:HA:GR gnc gnl* seedlings.

Since the transgenic *35:GNC:YFP:HA:GR gnc gnl* and *35:GNL:YFP:HA:GR gnc gnl* plants were functional, RNA-seq experiments were performed in order to initially identify the differentially expressed genes. For the purpose of the RNA-seq, in addition to Dex, CHX (cycloheximide) was also used. CHX is an inhibitor of protein synthesis and the simultaneous application with Dex should result in the identification of direct targets of the GATAs, without the interference of newly synthesized proteins. Therefore, 10-d-old light-grown *35:GNC:YFP:HA:GR gnc gnl* and *35:GNL:YFP:HA:GR gnc gnl* seedlings were treated at the end of day 10 for 3 h with 10 µM Dex and 10 µM CHX, followed by RNA extraction and NGS

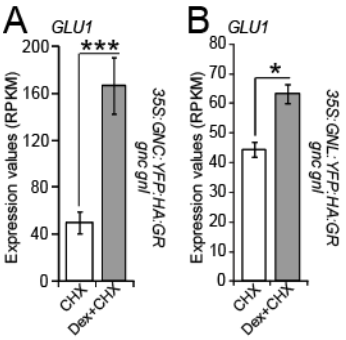

Figure 12: *GLU1*, a known target of B-GATAs, is upregulated in the RNA-seq experiments with GNC and GNL. Expression values in RPKM (reads per kilobase of transcript per million mapped reads) for *GLU1* from the RNA-seq of GNC (**A**) and GNL (**B**) after 3 h treatment with Dex and CHX. Student's *t*-test: *P < 0.05, **P < 0.01, ***P < 0.001.

sequencing and analysis of the samples. The RNA-seq analysis showed that

4323 genes (3288 upregulated and 1035 downregulated) were differentially expressed for the experiment with *35:GNC:YFP:HA:GR gnc gnl* (data were filtered using 2.45 fold change threshold and false discovery rate < 0.01), and only 60 genes (38 upregulated and 22 downregulated) were found for the experiment with *35S:GNL:YFP:HA:GR gnc gnl* (data were filtered using 1.2 fold change threshold and false discovery rate < 0.1). In both experiments, the *GLU1* (*GLUTAMATE SYNTHASE 1*) gene was upregulated (Figure 12). This was a good indication that both experiments were successful since *GLU1* had been reported to be directly regulated by GNC and GNL in a previous study (Hudson et al. 2011).

Since, GNC and GNL have redundant functions, observing a discrepancy in the total number of differentially expressed genes was unexpected.

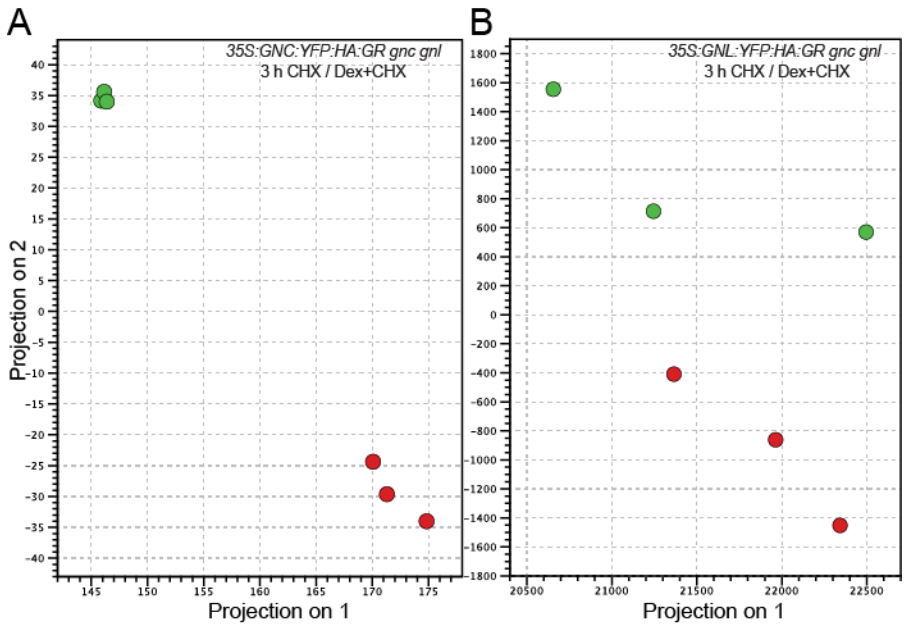

Figure 13: PCA (principal component analysis) between the different biological replicates of the RNA-seq experiments with *35S:GNC:YFP:HA:GR gnc gnl* (A) and *35S:GNL:YFP:HA:GR gnc gnl* (B).

To understand this, a PCA (principal component analysis) was performed for both RNA-seq experiments. In the case of *35S:GNC:YFP:HA:GR gnc gnl*, the different biological replicates between the two different experimental groups (dots with green and red color) clustered well together (Figure 13A), indicating very low variance between each one of these groups. In the case of *35S:GNL:YFP:HA:GR*

gnc gnl, the different biological replicates for the two different experimental groups clustered together, but not in a uniform way (Figure 13B). In conclusion, on the one hand, the RNA-seq for *35S:GNC:YFP:HA:GR gnc gnl* seedlings revealed that GNC was able to directly control the transcription of 4323 genes. On the other hand, the RNA-seq for *35S:GNL:YFP:HA:GR gnc gnl* showed that the variation among the different biological replicates was very high. This made the expression values for the majority of the genes to have p-values and false discovery rate values above acceptable thresholds (false discovery rate < 0.1) and, therefore, only 60 genes were found to be differentially expressed in the experiment with *35S:GNL:YFP:HA:GR gnc gnl* under the acceptable thresholds.

3.1.10 Genes related to chlorophyll biosynthesis, regulation of greening, chloroplast import machinery, photosynthesis and the chloroplast division apparatus are strongly upregulated in the RNA-seq experiments

To shed more light on the influence of B-GATAs GNC and GNL on greening, the rest of the RNA-seq analysis focused particularly on genes related to greening and chloroplast biology (Figure 14A). Four genes of the tetrapyrrole pathway were found to be differentially regulated by GNC (3 upregulated and 1 downregulated) but none after GNL induction (Figure 14A). In the chlorophyll biosynthesis pathway, 13 genes were differentially expressed (all upregulated) after GNC and only one, *GUN5*, was upregulated by GNL (Figure 14A). Two genes were found to be differentially expressed after the GNC induction in heme branch, *FC2* and *GUN2* but none after GNL induction (Figure 14A). Genes encoding for known regulators of the chlorophyll biosynthesis pathway such as *GLK2*, *SIG2*, *SIG6*, *PIF1* and *PIF3* were also strongly induced by GNC (Figure 14B). The mechanism controlling the import of proteins from the cytosol to the chloroplast was found to be transcriptionally controlled by GNC. In particular, nine genes encoding for proteins of this mechanism were differentially expressed in GNC after the treatment with Dex and CHX (8 upregulated and 1 downregulated) but not by GNL (Figure 14C). It was also investigated how genes related to the chloroplast division machinery were affected transcriptionally by GNC and GNL after treatment with Dex and CHX.

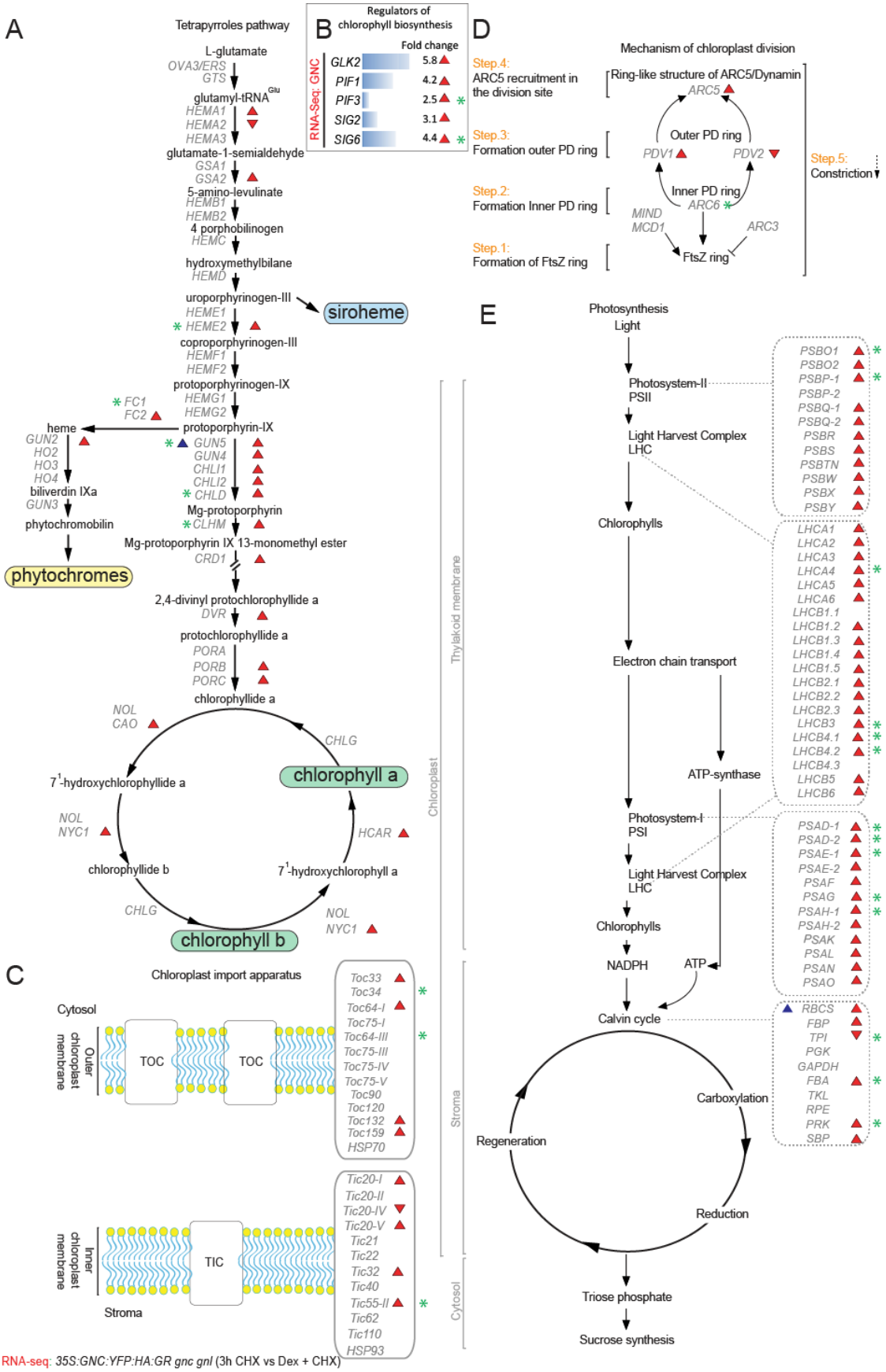
A
Tetrapyrroles pathway
L-glutamate
OVA3/ERS
GTS
glutamyl-tRNA Glu
HEMA1
HEMA2
HEMA3
glutamate-1-semialdehyde
GSA1
GSA2
5-amino-levulinate
HEMB1
HEMB2
4 porphobilinogen
HEMC
hydroxymethylbilane
HEMD
uroporphyrinogen-III
siroheme
HEME1
HEME2
coproporphyrinogen-III
HEMF1
HEMF2
protoporphyrinogen-IX
HEMG1
HEMG2
FC1
FC2
heme
protoporphyrin-IX
GUN2
HO2
HO3
HO4
biliverdin IXa
GUN3
phytochromobilin
phytochromes
GUN5
GUN4
CHLI1
CHLI2
CHLD
Mg-protoporphyrin
CLHM
Mg-protoporphyrin IX 13-monomethyl ester
CRD1
2,4-divinyl protochlorophyllide a
DVR
protochlorophyllide a
PORA
PORB
PORC
chlorophyllide a
NOL
CAO
CHLG
chlorophyll a
7[1]-hydroxychlorophyllide a
NOL
NYC1
HCAR
chlorophyllide b
7[1]-hydroxychlorophyll a
CHLG
NOL
NYC1
chlorophyll b
B
Regulators of chlorophyll biosynthesis
Fold change
RNA-Seq: GNC
GLK2
5.8
PIF1
4.2
PIF3
2.5
SIG2
3.1
SIG6
4.4
C
Chloroplast import apparatus
Cytosol
Outer chloroplast membrane
TOC
TOC
Toc33
Toc34
Toc64-I
Toc75-I
Toc64-III
Toc75-III
Toc75-IV
Toc75-V
Toc90
Toc120
Toc132
Toc159
HSP70
Inner chloroplast membrane
TIC
Stroma
Tic20-I
Tic20-II
Tic20-IV
Tic20-V
Tic21
Tic22
Tic32
Tic40
Tic55-II
Tic62
Tic110
HSP93
Thylakoid membrane
Chloroplast
Stroma
Cytosol
D
Mechanism of chloroplast division
Step.4:
ARC5 recruitment in the division site
Ring-like structure of ARC5/Dynamin
ARC5
Step.3:
Formation outer PD ring
Outer PD ring
PDV1
PDV2
Step.5:
Constriction
Step.2:
Formation Inner PD ring
Inner PD ring
ARC6
MIND
MCD1
ARC3
Step.1:
Formation of FtsZ ring
FtsZ ring
E
Photosynthesis
Light
Photosystem-II
PSII
Light Harvest Complex
LHC
Chlorophylls
Electron chain transport
ATP-synthase
Photosystem-I
PSI
Light Harvest Complex
LHC
Chlorophylls
NADPH
ATP
Calvin cycle
Carboxylation
Reduction
Regeneration
Triose phosphate
Sucrose synthesis
PSBO1
PSBO2
PSBP-1
PSBP-2
PSBQ-1
PSBQ-2
PSBR
PSBS
PSBTN
PSBW
PSBX
PSBY
LHCA1
LHCA2
LHCA3
LHCA4
LHCA5
LHCA6
LHCB1.1
LHCB1.2
LHCB1.3
LHCB1.4
LHCB1.5
LHCB2.1
LHCB2.2
LHCB2.3
LHCB3
LHCB4.1
LHCB4.2
LHCB4.3
LHCB5
LHCB6
PSAD-1
PSAD-2
PSAE-1
PSAE-2
PSAF
PSAG
PSAH-1
PSAH-2
PSAK
PSAL
PSAN
PSAO
RBCS
FBP
TPI
PGK
GAPDH
FBA
TKL
RPE
PRK
SBP
RNA-seq: 35S:GNC:YFP:HA:GR gnc gnl (3h CHX vs Dex + CHX)
RNA-seq: 35S:GNL:YFP:HA:GR gnc gnl (3h CHX vs Dex + CHX)
: ChIP-seq pGNL:GNL:HA gnc gnl

Figure 14: Contribution of the B-GATAs GNC and GNL to the transcriptional regulation of genes related to the tetrapyrrole pathway, greening regulators, chloroplast import apparatus, chloroplast division machinery and photosynthesis. Combined results from the RNA-seq and ChIP-seq analysis. (**A**) Schematic representation of the tetrapyrrole pathway. (**B**) Greening regulators. (**C**) Schematic representation of the chloroplast protein import apparatus. (**D**) Schematic representation of the chloroplast division machinery. (**E**) Schematic representation of the photosynthesis machinery. Red arrowheads show genes differentially expressed in the RNA-seq with the *35S:GNC:YFP:HA:GR gnc gnl*, blue arrowheads show genes differentially expressed in the RNA-seq with the *35S:GNL:YFP:HA:GR gnc gnl*. Upregulation is depicted by upward pointing arrowheads, arrowheads facing downward depict downregulation. Green asterisks depict genes that were found in the ChIP-seq with *pGNL:GNL:HA gnc gnl*. Fold change expression values are presented in Appendix Table 9.

Three genes were found to be differentially regulated by GNC (2 upregulated and 1 downregulated) and none by GNL (Figure 14D). Lastly, focusing on the genes with a role in photosynthesis, 47 were found to be differentially expressed (46 upregulated and 1 downregulated) by GNC, and just one by GNL (Figure 14E). The 47 genes controlled by GNC contributed to different compound of the photosynthetic mechanism such as photosystems, the electron chain and the Calvin cycle, and were not restricted preferentially to one or the other compartment (Figure 14E). Taken together, these findings suggested that the B-GATAs GNC and GNL were able to promote greening at many different levels such as chlorophyll biosynthesis, chloroplast development and photosynthesis. It was very striking that the transcriptional regulation of chlorophyll biosynthesis enzymes was strongly linked to GNC. From a total of 16 genes, encoding for chlorophyll biosynthesis enzymes, 13 were strongly induced by GNC (Figure 14A).

3.1.11 The overlap between ChIP-seq and RNA-seq shows that GNC and GNL directly regulate the expression of genes with a prominent role in greening

On the one hand, the ChIP-seq experiment provided information about genes that GNL can bind. On the other hand, the RNA-seq experiment showed, which genes can be regulated directly by GNC and GNL. To examine if the ChIP-seq and the RNA-seq experiments have genes in common, the list of the 3615 peaks (from the ChIP-seq) was compared to the list of differential expressed genes from the RNA-seq experiments. From 4323 GNC- dependent differentially expressed genes, 674 were at the same time targets of GNL in the ChIP-seq

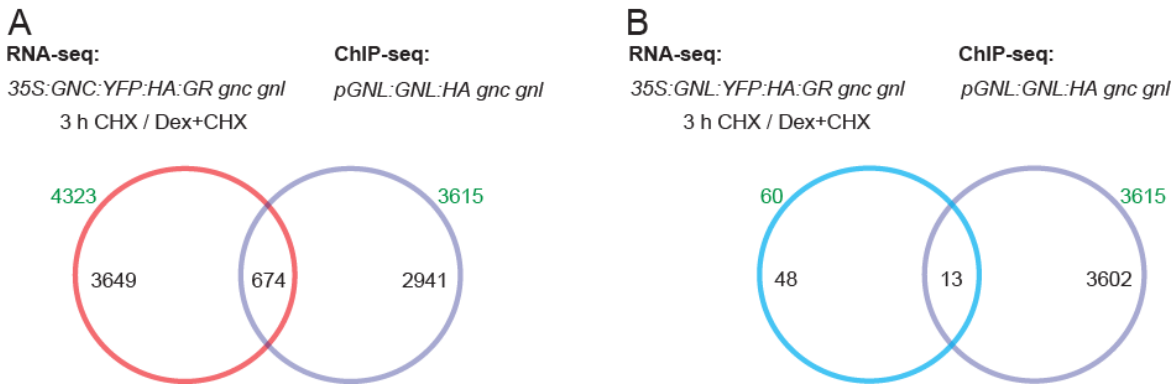

Figure 15: Overlaps between the ChIP-seq with *pGNL:GNL:HA gnc gnl* and the RNA-seq with (A) *35S:GNC:YFP:HA gnc gnl* and (B) *35S:GNL:YFP:HA gnc gnl* reveal putative target genes of GNL:HA, which at the same time are differentially expressed by the B-GATAs GNC and GNL.

(Figure 15A and Appendix Table 10). Similarly, 13 out of the 61 differentially expressed GNL-dependent genes were at the same time targets of GNL in ChIP-seq (Figure 15B and Appendix Table 11).

The next question was how many genes, from the previous comparisons, were related to greening. The overlap of the RNA-seq for GNC with ChIP-seq for GNL showed six genes, which were directly related to greening (Appendix Table 12). Additionally, the overlap of the RNA-seq for GNL with ChIP-seq for GNL, showed that only one gene, *GUN5*, was in common (Appendix Table 13).

In summary, the overlap between the ChIP-seq and the RNA-seq revealed direct targets of the B-GATAs GNC and GNL. Some of these genes were related to greening. Noteworthy to mention is the fact that *GUN5* appeared as a common gene in both overlaps of GNC and GNL. *GUN5* potentially one out of many common targets, which GNC and GNL can regulate in order to promote greening.

3.1.12 The combination of the results from the high-throughput experiments points to five major and distinct areas where later research for the role of B-GATAs in greening should be focus on

The analysis of the pre-existing microarray data sets of GNCox and GNLox, together with the recent NGS experiments, ChIP-seq and RNA-seq, showed that B-GATAs GNC and GNL had pivotal roles in the greening of Arabidopsis. Taken

into account the overall results, it was decided and planned to further investigate the contribution of B-GATAs in greening into five different levels: (1) the chlorophyll biosynthesis pathway, (2) the heme pathway, (3) transcription factors known to control greening, (4) regulators of transcription in the chloroplasts and (5) retrograde signaling. To better understand the ways, in which the B-GATAs control greening through these five different levels, additional experimental approaches were needed. For this reason, were designed and performed genetic, physiological and molecular experiments.

4. Results - Physiological and genetic studies for the validation of GNC and GNL targets

4.1 GNL and GNC promote chlorophyll biosynthesis through the upregulation of Mg-chelatase subunits

GNC and GNL seem to control the chlorophyll pathway in a redundant manner. MgCh (Mg-chelatase) is a multi-complex enzyme, which plays a role in the first step of chlorophyll biosynthesis. It consists of three different subunits, GUN5/CHLH, CHLD and CHLI and each one of these plays a specific role in the insertion of Mg2+ into the Proto-IX substrate (Tanaka & Tanaka 2007). To understand the relationship between B-GATAs and MgCh, experiments with genes encoding for each subunit of the MgCh complex were conducted.

4.1.1 *GUN5/CHLH* expression is regulated by B-GATAs

GUN5 is the catalytic subunit of the MgCh, which adjuncts Mg^{2+} to Proto-IX (protoporphyrin–IX) (Adhikari et al. 2009). In the NGS experiments, *GUN5* was found to be a target of GNL in the ChIP-seq and was upregulated in the RNA-seq (Figure 16A and Appendix Table 9). To test if GNL was able to bind to *GUN5*, independent ChIP experiments were performed with light-grown seedlings of *pGNL:GNL:HA gnc gnl*. It verified not only that GNL binds in the position identified by ChIP-seq (Figure16A, B and F) but also that there were at least two additional binding sites for GNL in the *GUN5* promoter (Figure 16C and E). Since the binding site of GNL, as predicted by ChIP-seq, was located in the first exon of *GUN5*, further tests were performed to determine if this was a true binding. Thus,

an additional ChIP with light-grown *35S:GNL:YFP:HA:GR gnc gnl* seedlings after 4 h Dex treatment was conducted. The results of this experiment verified the binding of GNL to the particular position in the first exon of *GUN5* (Figure 16G).

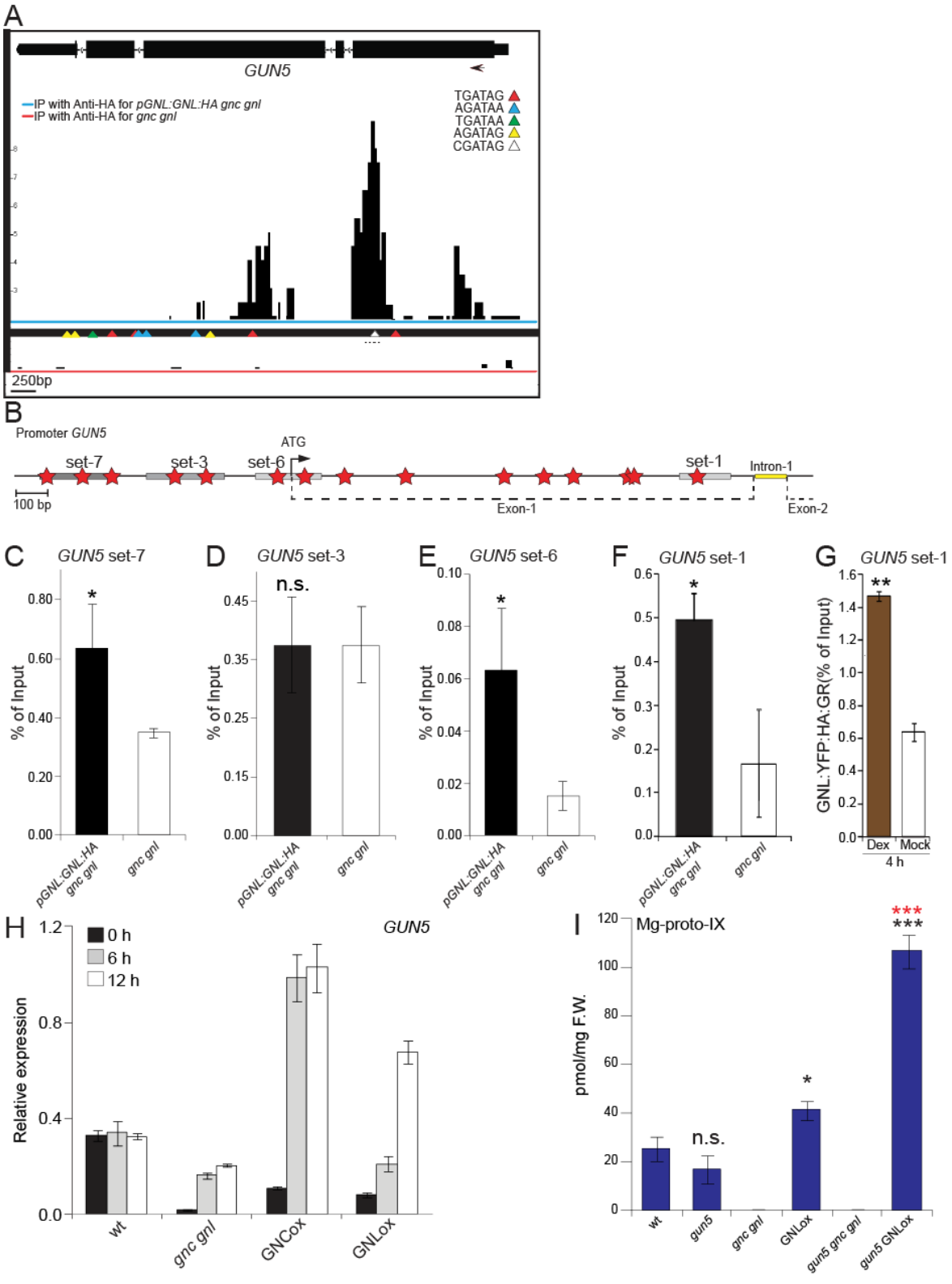

Figure 16: The expression of *GUN5* is directly regulated by the B-GATAs GNC and GNL. (**A**) Identified peaks from the ChIP-seq with *the pGNL:GNL:HA gnc gnl* transgenic line and *gnc gnl* double mutant associated with the *GUN5* gene. The blue line corresponds to the ChIP of GNL:HA, and the red line corresponds to the ChIP of the *gnc gnl* double mutant. Colored arrowheads depict different variants of GATA motifs where GNL:HA potentially can bind. (**B**) Gene model of *GUN5*. Red stars show locations of GATA boxes; grey boxes represent regions tested by qRT-PCR through independent ChIP experiments, testing the binding of the GNL:HA. Yellow boxes depict the first intron of the *GUN5* gene and punctuated lines mark the first and the second exon of *GUN5*. (**C**-**F**) Results from the ChIP-qRT-PCRs of independent ChIP experiment with the *pGNL:GNL:HA gnc gnl* transgenic line and *gnc gnl* double mutant. The amplicons of each qRT-PCR correspond to the regions on the *GUN5* gene designated as set 1, 3, 6 and 7. (**G**) Results from the ChIP-qRT-PCRs of the independent ChIP experiment with the *35S:GNL:YFP:HA:GR gnc gnl* transgenic line with Dex treatment. The amplicon amplified by the qRT-PCR corresponds to the region on the *GUN5*, designated as set-1. (**H**) Relative transcript levels of the *GUN5* gene in 6-d-old dark-grown seedlings, followed by light exposures for 0, 6 and 12 h. The data shown are the averages and standard errors of one biological replicate with three technical replicates. (**I**) Results from Mg-proto-IX HPLC analysis of 10-d-old light-grown seedlings. The black asterisks represent a statistically significant difference between wt, *gun5*, GNLox and *gun5* GNLox seedlings; red asterisks represent a statistically significant difference between the *gun5* and *gun5* GNLox seedlings. Mg-proto-IX levels of *gnc gnl* and *gun5 gnc gnl* seedlings were not detectable. Student's *t*-test: *P < 0.05, **P < 0.01, ***P < 0.001; n.s., not significant.

The direct binding of GNL to *GUN5* should lead to the transcriptional regulation of *GUN5*. This was tested next with independent qRT-PCR experiments. Since *GNC*, *GNL* and *GUN5* are light-regulated genes, it was decided to grow seedlings in the dark for 6-d and then expose them to light for 6 and 12 h. In the *gnc gnl* double mutant, the expression of *GUN5* was reduced compared to the wt (Figure 16H). In the GNCox seedlings, a strong upregulation of *GUN5* was observed after 6 and 12 h of light exposure (Figure 16H). The GNLox seedlings showed a strong increase in *GUN5* expression only after 12 h of light exposure (Figure 16H).

To further investigate the impact of the transcriptional regulation of *GUN5* by GNL and GNC, an HPLC experiment was performed to assess the levels of the Mg-proto-IX, the product of the MgCh enzymatic activity, by Dr. Boris Hedtke from the laboratory of Prof. Dr. Bernhard Grimm. Mg-proto-IX was severely reduced in the *gnc gnl* and *gun5 gnc gnl* seedlings compared to wt, but was increased in GNLox and even further in *gun5* GNLox seedlings (Figure 16I).

To examine the genetic relationship between *GNL* and *GUN5*, several genetic crosses were performed. The triple mutant of *gun5 gnc gnl* did not show any difference in greening compared to *gnc gnl* (Fig. 17A and D). On the other side, *gun5* GNLox seedlings displayed a significant increase in chlorophyll compared to

the *gun5* mutant (Figure 17B and D). Further, overexpression of *GUN5* in the *gnc gnl* background was not able to increase chlorophyll (Figure 17C and 17E).

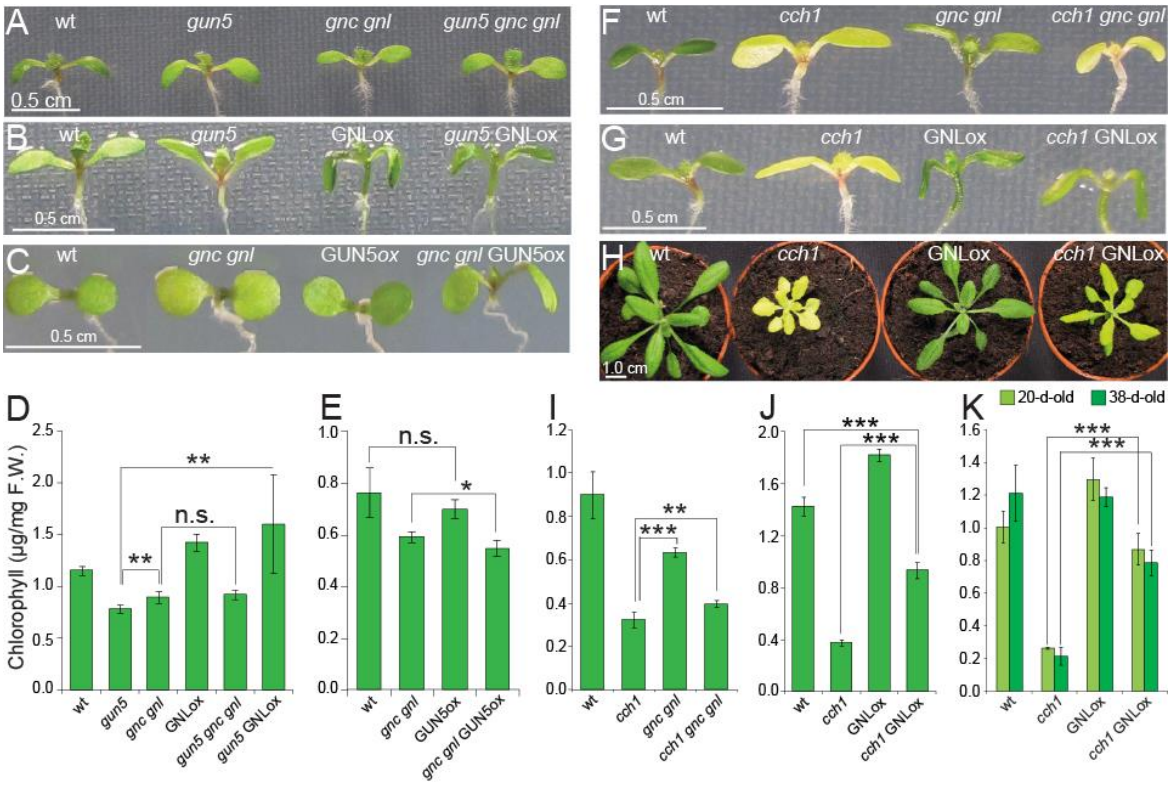

Figure 17: GNL is able to at least partially induce greening in the *gun5* mutant. (**A**-**C**, **F**-**G**) Representative photographs of 7-d-old light-grown seedlings. (**D**-**E**, **I**-**J**) Chlorophyll quantification in 7-d-old light-grown seedlings. (**H**) Representative photographs of 20-d-old adult plants. (**K**) Chlorophyll quantification of adult plants. Student's *t*-test: *P < 0.05, **P < 0.01, ***P < 0.001; n.s., not significant.

gun5 is a weak allele of *GUN5*. Therefore, the experiments were repeated with *cch1*, which is a stronger allele regarding the greening phenotype. *cch1* is paler than the *gnc gnl* double mutant and the triple mutant of *cch1 gnc gnl* had far less chlorophyll than the *gnc gnl* mutant, but slightly higher levels than *cch1* (Figure 17F and I). The *cch1* GNLox seedlings showed an increase in chlorophyll levels compared to the *cch1* mutant, but they were not equal to the levels detected in GNLox seedlings (Figure 17G and J).

To investigate if the chlorophyll levels changed as the plants became older, chlorophyll levels from rosette leaves of 20-d-old and 38-d-old adult plants were quantified. *cch1* GNLox adult plants showed rescue of the greening phenotype of the *cch1* mutant (Figure 17H and K). That meant that the pattern shown in 7-d-old

seedlings was maintained also in adult plants. Taken together, these findings suggested that the results from the NGS experiments were, indeed, true. GNL binds to the promoter of *GUN5* and can regulate its expression. Additionally, genetic experiments showed that GNLox was able to compensate, at least partially, the chlorophyll reduction, which was caused by the *cch1* mutation in the GUN5 protein. This could mean that the upregulation of the mutant *GUN5* gene, which carries a proline to leuchine substitution mutation, may suppress the greening defect in the *cch1* GNLox seedlings.

4.1.2 *CHLD* expression is regulated by B-GATAs

CHLD subunit together with the CHLI subunit facilitate the ATP-dependent metalation of the Proto-IX substrate (Adhikari et al. 2009). *CHLD* was found to be targeted by GNL in the ChIP-seq experiment (Figure 18A) but *CHLD* was not differentially regulated in the RNA-seq, neither of *35S:GNC:YFP:HA:GR gnc gnl* nor of *35S:GNL:YFP:HA:GR gnc gnl* (Figure 14 and Appendix Table 9). An independent ChIP with *pGNL:GNL:HA gnc gnl* seedlings verified the results from the ChIP-seq (Figure 18B and C). A qRT-PCR experiment with 6-d-old dark-grown seedlings showed that *CHLD* was less strongly induced after light treatment in *gnc gnl* compared to the wt (Figure 18D). Additionally, GNCox and GNLox showed stronger induction following illumination (Figure 18D).

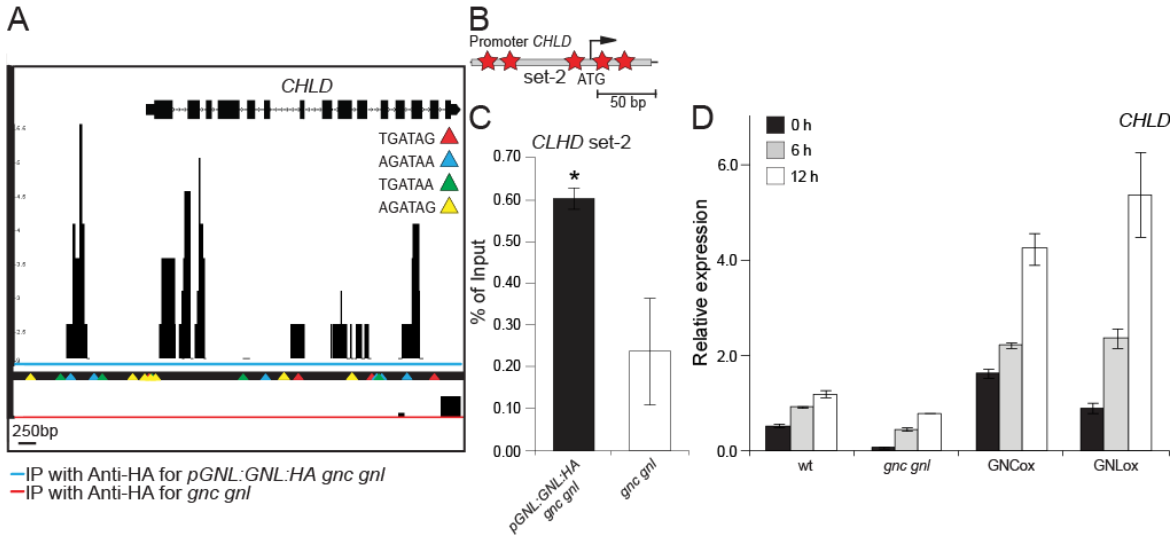

Figure 18: *CHLD* expression is regulated by GNL. (**A**) Identified peaks from the ChIP-seq with the *pGNL:GNL:HA gnc gnl* transgenic line and *gnc gnl* double mutant associated in the *CHLD* gene. The blue line corresponds to the ChIP of GNL:HA and the red line corresponds to the ChIP

of the *gnc gnl* double mutant. Colored arrowheads depict different variants of GATA motifs where GNL:HA can potentially bind. (**B**) Schematic representation of the *CHLD* promoter. Red stars show locations of GATA boxes; grey boxes represent regions tested by qRT-PCR through ChIP. (**C**) Results from the ChIP-qRT-PCR analysis of the ChIP experiment with the *pGNL:GNL:HA gnc gnl* transgenic line and the *gnc gnl* double mutant. The amplicons of each ChIP-qRT-PCR correspond to the regions with the grey boxes on the *CHLD* promoter designated as set-1, -2, -3. (**D**) Relative transcript levels of the *CHLD* gene in 6-d-old dark-grown seedlings, followed by light exposure for 0, 6 and 12 h. The data shown are the averages and standard errors one biological replicate with three technical replicates. Student's *t*-test: *P < 0.05.

No viable mutants for the *CHLD* gene were available when this research was performed. Thus, it was not possible to plan and conduct any kind of genetic experiments with *CHLD*. In conclusion, *CHLD*, may be directly transcriptionally regulated by the B-GATAs GNC and GNL.

4.1.3 *CHLI* expression is regulated by B-GATAs

CHLI, has an AAA-type ATPase activity and catalyzes the ATP-dependent hydrolysis, which is required for the insertion of Mg^{2+} into Proto-IX (Kobayashi et al. 2008). In Arabidopsis, CHLI is encoded by two isoforms, *CHLI1* and *CHLI2*, which share similar ATPase activity and expression profiles but CHLI1 protein seems to have a more prominent role in the MgCh complex (Kobayashi et al. 2008). The ChIP-seq with GNL did not reveal any binding to the promoter of *CHLI1* or *CHLI2*. Though, the RNA-seq of GNC showed that both isoforms were strongly upregulated after GATA induction (Figure 14 and Appendix Table 9). An additional qRT-PCR experiment showed that *CHLI1* and *CHLI2* were strongly upregulated after the exposure to light in GNCox and GNLox seedlings, although the induction of these genes was not compromised in the *gnc gnl* mutant (Figure 19A and B). Crosses were made to further study the genetic interaction between a mutant of *CHLI1* (*cs* or *ch-42*) with B-GATAs. The triple mutant of *cs gnc gnl* showed chlorophyll levels similar to *cs* (Figure 19C and F). Several efforts were made to generate *cs* GNLox, but the respective crosses did not succeed. Instead, *cs* GNCox was successfully obtained and revealed increased chlorophyll levels compared to *cs* supporting the notion that the GATAs may regulate *CHLI1*, through upregulation of the mutated *CHLI1* gene in the *cs* T-DNA insertion mutant, or, more likely, through the compensatory upregulation of *CHLI2* (Figure 19G).

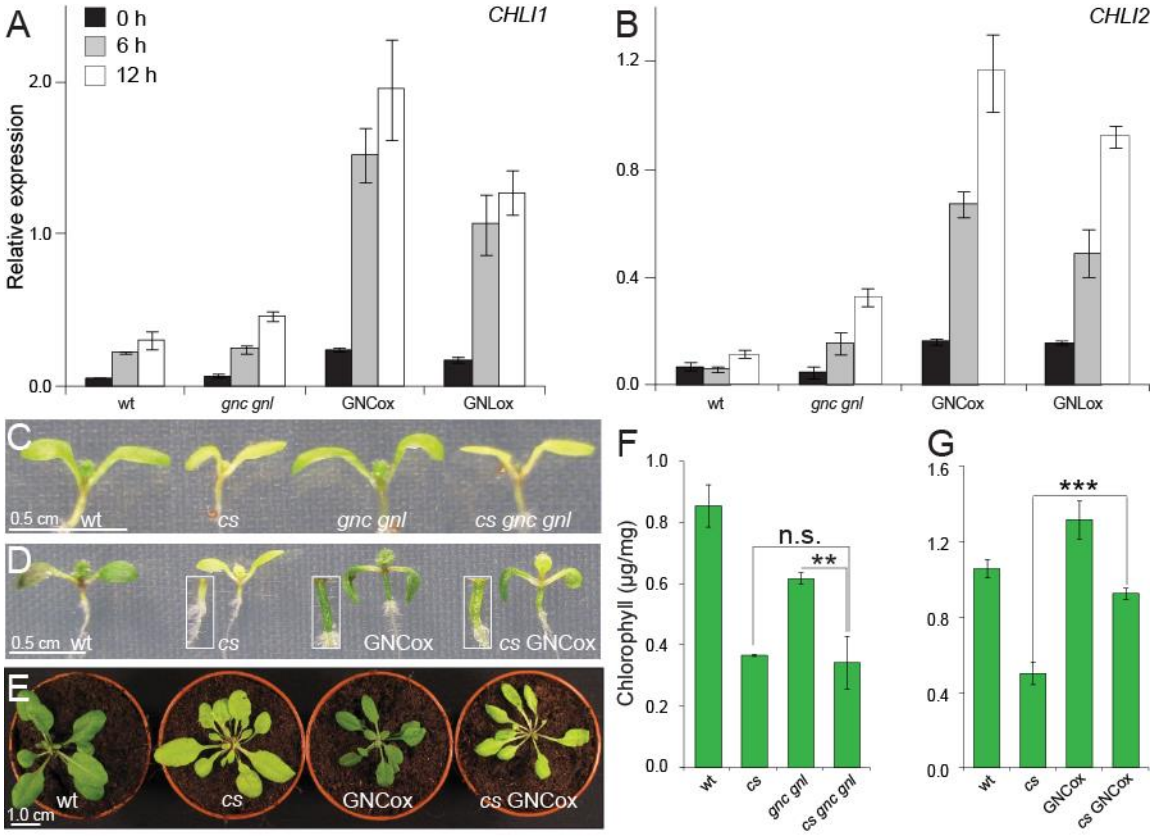

Figure 19: GNC and GNL induce the expression of *CHLI1* and *CHLI2* and promote greening partially independently from *CHLI*. (**A**-**B**) Relative transcript levels of *CHLI1* and *CHLI2* in 6-d-old dark-grown seedlings following light exposures for 6 and 12 h. The data shown are the averages and standard errors of two ≥ biological replicates each one with four technical replicates. (**C**-**D**) Representative photographs of 7-d-old light-grown seedlings. (**E**) Representative photos of 20-d-old adult plants. (**F**-**G**) Results of the quantification of chlorophyll a and b of 7-d-old seedlings. Student's *t*-test: **P < 0.01, ***P < 0.001; n.s., not significant.

4.1.4 *GUN4* is transcriptionally controlled by GNC and GNL

GUN4 does not belong to the enzymatic complex of MgCh but plays a role in the association of the enzymatic complex to the chloroplast membranes (Adhikari et al. 2011). Additionally, GUN4 can activate MgCh by its interaction with the GUN5/CHLH subunit (Larkin et al. 2003). *GUN4* was found to be strongly upregulated in the RNA-seq with GNC (Figure 14 and Appendix 9). Nevertheless, no binding by GNL to the *GUN4* promoter was observed by ChIP-seq. A qRT-PCR experiment with dark-grown seedlings after light exposure verified the results from the RNA-seq, where *GUN4* was shown to be markedly upregulated following illumination (Figure 20A). This particular induction of *GUN4* in GNLox and GNCox seedlings led to further investigations with an independent ChIP

experiment in order to determine if GNL had any binding sites in the *GUN4* promoter. Indeed, GNL bound to the *GUN4* promoter at a position close to the ATG start codon (Figure 20B and D). To further examine the relationship between *GNL* and *GUN4*, crosses and overexpression lines of *GUN4* in the wt and the *gnc gnl* background were generated. The *gun4 gnc gnl* triple mutant showed chlorophyll levels equal to the *gun4* mutant, which had lower levels of chlorophyll compared to the *gnc gnl* double mutant (Figure 21A and E). GNLox in the *gun4* background slightly decreased chlorophyll levels compared to *gun4* (Figure 21B, D and F). Lastly, though *gnc gnl* GUN4ox showed similar chlorophyll levels compared to the wt, chlorophyll levels were reduced in *gnc gnl* GUN4ox when compared to GUN4ox in the wt background (Figure 21C and G).

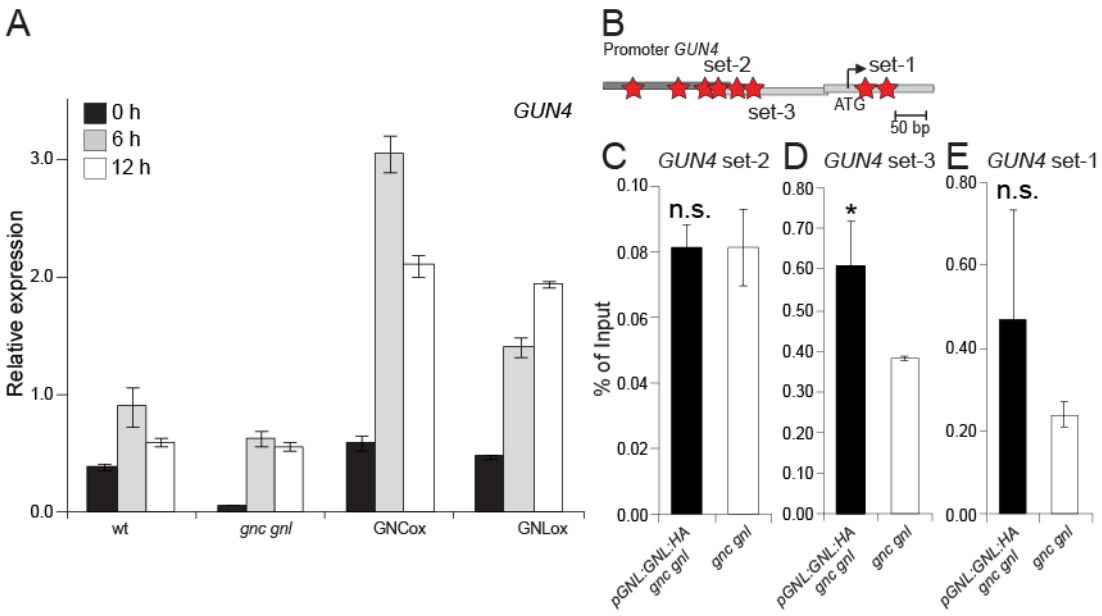

Figure 20: GNL and GNC induce the expression of *GUN4*. (**A**) Relative transcript levels of *GUN4* in 6-d-old dark-grown seedlings followed by light exposure for 0, 6 and 12 h. The data shown are the averages and standard errors one biological replicate with four technical replicates. (**B**) Schematic representation of the *GUN4* promoter. The red stars show locations of GATA boxes; the grey boxes represent regions tested by qRT-PCR through a ChIP experiment to determine binding sites of the GNL:HA protein. (**C**-**E**) Results from the qRT-PCR analysis following a ChIP experiment with the *pGNL:GNL:HA gnc gnl* transgenic line and the *gnc gnl* double mutant. The amplicons of each ChIP-qRT-PCR correspond to the regions with the grey boxes on the *GUN4* promoter, designated as set-1, -2, -3. Student's *t*-test: *P < 0.05; n.s., not significant.

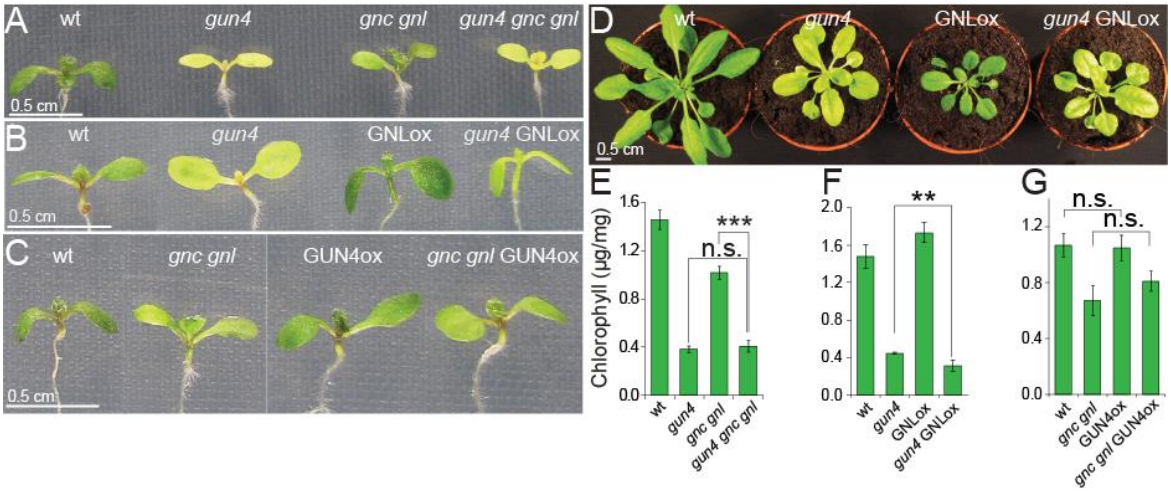

Figure 21: GNL functions upstream in the same pathway with *GUN4*. (**A**-**C**) Representative photographs of 7-d-old light-grown seedlings. (**D**) Representative photographs of 20-d-old adult plants. (**E**-**G**) Results of the quantification of chlorophyll a and b from 7-d-old seedlings. Student's *t*-test: **P < 0.01, ***P < 0.001; n.s., not significant.

In conclusion, *GUN4* expression is controlled by GNL, and GNL can directly bind to the *GUN4* promoter. Moreover, GNL is not even partially able to induce the greening of seedlings in the absence of GUN4. This underlines the essential role of GUN4 in the activation and further function of the MgCh enzymatic complex and moreover places *GUN4* downstream from *GNC* and *GNL* regarding greening.

4.1.5 *DVR* is a downstream target of B-GATAs in the chlorophyll biosynthesis pathway

DVR reduces divinyl protochlorophyllide *a* or divinyl chlorophyllide to monovinyl protochlorophyllide *a or* monovinyl chlorophyllide, upstream of the PORs (PROTOCHLOROPHYLLIDE OXIDOREDUCTASES) (Figure 4) (Nagata et al. 2005). No binding of GNL to the promoter of *DVR* was detected by ChIP-seq. The RNA-seq with GNC revealed that *DVR* expression was strongly upregulated after GATA induction (Figure 14 and Appendix Table 9). Moreover, an independent ChIP experiment with *pGNL:GNL:HA gnc gnl* seedlings revealed binding of GNL to two different positions in the *DVR* promoter (Figure 22A - C). To test if these binding events correlated with *DVR* gene regulation, a qRT-PCR was performed. There, *DVR* induction, after light exposure, was compromised in *gnc gnl* seedlings and enhanced in overexpression lines, at least in GNCox (Figure 22D).

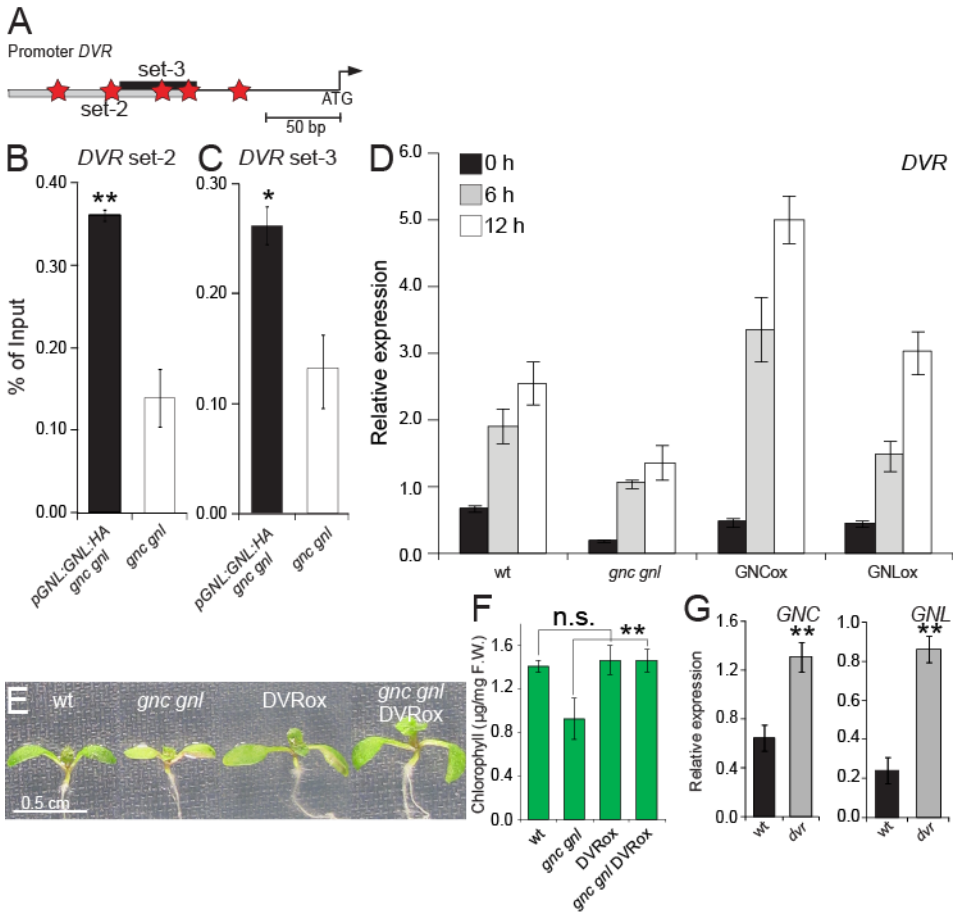

Figure 22: *DVR* is a target downstream from GNC and GNL in the chlorophyll biosynthesis pathway. (**A**) Model of the *DVR* promoter. The red stars show locations of GATA boxes; the grey boxes represent regions tested by qRT-PCR after a ChIP experiment to determine binding sites of the GNL:HA protein. (**B**-**C**) Results from the qRT-PCR analysis of a ChIP experiment with the *pGNL:GNL:HA gnc gnl* transgenic line and the *gnc gnl* double mutant. The amplicons of each ChIP-qRT-PCR correspond to the regions with grey boxes on the promoter of the *DVR* gene, designated as set-1, -2, -3. (**D**) Relative *DVR* transcript levels in 6-d-old dark-grown seedlings followed by light exposure for 6 and 12 h. Data shown are the averages and standard errors of one biological replicate with four technical replicates. (**E**) Representative photographs of 7-d-old light-grown seedlings. (**F**) Results of the quantification of chlorophyll a and b of 7-d-old seedlings. (**G**) Relative transcript levels of *GNL* and *GNC* in 14-d-old light-grown wt and *dvr* mutant seedlings. Data shown are the averages and standard errors of 2 ≥ biological replicates. Student's *t*-test: *P < 0.05, **P < 0.01; n.s., not significant.

To examine the genetic interaction between *DVR* with B-GATAs, it was repeatedly but unsuccessfully attempted to perform genetic crosses between *dvr* and *gnc gnl* or GNLox. In turn, a *DVR* overexpression transgene (DVRox) was introduced in the wt and in the *gnc gnl* background. The overexpression of *DVR* in wt seedlings displayed the same levels of chlorophyll as the wt (Figure 22E and F). However, when *DVR* was overexpressed in the *gnc gnl* background, the chlorophyll biosynthesis defect of the mutant was suppressed (Figure 22E and F).

These results showed that *GNC* and *GNL* function upstream of *DVR* in the chlorophyll biosynthesis pathway and are able to control *DVR* expression and bind to its promoter. Lastly, it was hypothesized that DVR can also potentially influence the expression of *GNC* and *GNL*. A qRT-PCR experiment with *dvr* mutant seedlings showed that the expression of *GNC* and *GNL* was markedly elevated in the *dvr* mutant (Figure 22G). This could mean that DVR, possibly indirectly, represses the expression of *GNC* and *GNL* as part of a negative feedback loop, which controls the proper production of chlorophyll intermediates.

4.2 Control of the heme pathway

4.2.1 The heme pathway

When the tetrapyrrole pathway reaches the point of Proto-IX, it diverges to the chlorophyll and to the heme biosynthesis branch (Figure 4). The heme branch eventually leads to the synthesis of phytochromobilin, which together with the PHY apoproteins, PHYA-PHYE in Arabidopsis, form the functional holo-phytochromes. These phytochrome photoreceptors move to the nucleus after light perception where they mediate the downstream light signal transduction through the interaction with other nuclear localized proteins such as PIFs (Kohchi et al. 2001).

4.2.2 *GUN2/HO1* is transcriptionally controlled mostly by B-GATAs

The synthesis of biliverdin-IXa through the oxidization of protoheme (heme) is the second step in the heme pathway and catalyzed by the heme oxygenase GUN2/HO1 (GENOMES UNCOUPLED 2/HEME OXYGENASE1) (Tanaka & Tanaka 2007). Light-grown *gun2* mutant seedlings have low levels of chlorophyll and much longer hypocotyls compared to wt (Figure 24A and L). The ChIP-seq with *pGNL:GNL:HA gnc gnl* seedlings did not reveal any binding of GNL to the promoter of *GUN2*, but the RNA-seq for GNC showed strong induction of *GUN2* after GATA induction (Figure 14 and Appendix Table 9). To determine if GNL is able to bind to the *GUN2* promoter, additional ChIP experiments were performed.

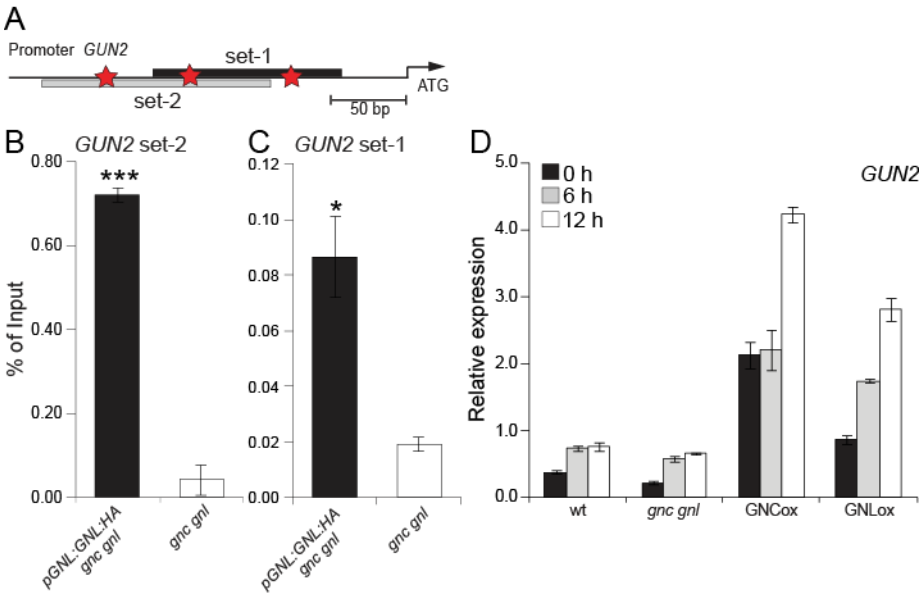

Figure 23: GNC and GNL strongly upregulate the expression of *GUN2*. (**A**) A model of the *GUN2* promoter. The red stars show locations of GATA boxes; the grey boxes represent regions tested by qRT-PCR after ChIP, for the binding of GNL:HA. (**B**-**C**) Results from qRT-PCR analysis of the ChIP experiment with a *pGNL:GNL:HA gnc gnl* transgenic line and the *gnc gnl* double mutant. The amplicons of each ChIP-qRT-PCR correspond to the regions with grey boxes on the promoter of the *GUN2* gene, designated as set-1, -2, -3. (**D**) Relative transcript levels of *GUN2* in 6-d-old dark-grown seedlings exposed to the white light for 0, 6 and 12 h. Data shown are averages and standard errors of one biological replicate with three technical replicates. Student's *t*-test: *P < 0.05, ***P < 0.001; n.s., not significant.

The ChIP with *pGNL::GNL:HA gnc gnl* seedlings showed that GNL was able to bind to 2 different positions, in close proximity to the start codon in the *GUN2* promoter (Figure 23A - C). A qRT-PCR with 6-d-old dark-grown seedlings exposed for 0, 6 and 12 h to light, showed that *GUN2* expression was slightly lower in the *gnc gnl* seedlings but markedly higher in GNCox and GNLox seedlings (Figure 23D).

To examine the genetic relationship between *GUN2* and the B-GATAs, genetic crosses were performed. The *gun2 gnc gnl* triple mutant showed slightly lower levels of chlorophyll compared to the *gun2* mutant (Figure 24A and E), indicating that *GUN2* and B-GATAs are in the same pathway with regard to chlorophyll biosynthesis. Since this slight decrease in chlorophyll levels was seen in the triple mutant, the possibility that B-GATAs can also affect the chlorophyll biosynthesis independently from *GUN2* cannot be excluded. To test this hypothesis, a genetic cross between *gun2* and GNLox was performed. The *gun2* GNLox seedlings showed a small but statistically significant increase in the chlorophyll content, and

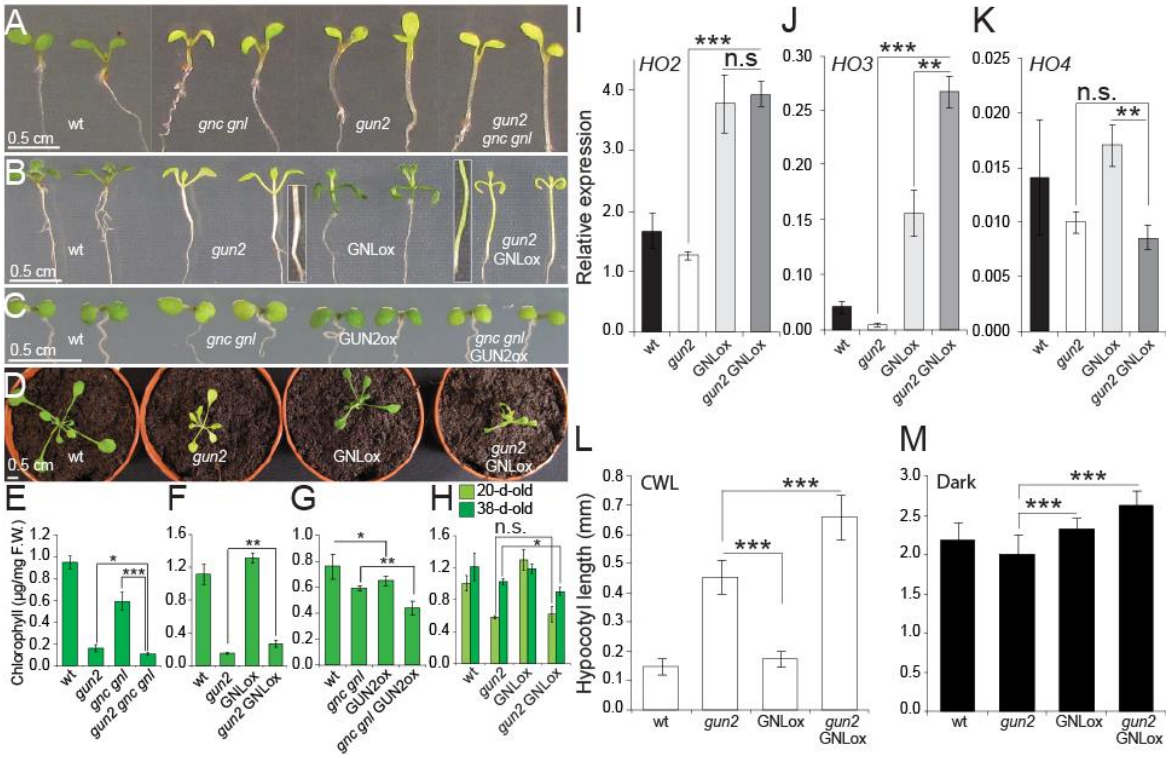

Figure 24: *GNL* functions upstream in the same pathway with *GUN2*. (**A**-**C**) Representative photographs of 7-d-old light-grown seedlings. (**D**) Representative photographs of 20-d-old adult plants. (**E**-**G**) Results of the quantification of chlorophyll a and b in 7-d-old seedlings. (**H**) Results of the quantification of chlorophyll a and b in 20-d-old and 38-d-old adult plants. (**I**-**K**) Relative transcript levels of *HO2*, *HO3* and *HO4* in 7-d-old light grown seedlings. Data shown are averages and standard errors of ≥2 biological replicates. (**L**-**M**) Hypocotyl length in 7-d-old seedlings grown under constant white light (CWL) and under the dark. Student's *t*-test: *P < 0.05, **P < 0.01, ***P < 0.001; n.s., not significant.

displayed prominent greening of their long hypocotyls, a feature completely absents in the *gun2* mutant (Figure 24B and F). That led to the hypothesis that either GNL can induce greening through the heme pathway, by upregulating the expression of other heme oxygenases (HO2, HO3 and HO4) participating in the same step as GUN2 or the rescue of greening is actually the result of the induction, which is caused by GNL in the chlorophyll branch. To test this, the expression of *HO2*, *HO3* and *HO4* was measured in the *gun2* GNLox seedlings. The mRNAs levels of *HO2* and *HO3*, but not *HO4* were found strongly increased in *gun2* GNLox seedlings (Figure 24I-K), which can be interpreted as the cause of the partially suppression of the greening defects of *gun2*. However, when hypocotyl measurements were performed with *gun2* GNLox light and dark grown seedlings, the long hypocotyl phenotype of *gun2* was not suppressed, as it would

be expected if GNL was able to induce the phytochrome pathway by the upregulation of the heme oxygenases HO2 and HO3 (Figure 24L-M). In fact, the hypocotyl length of the *gun2* GNLox was longer compared to *gun2* mutant, which underlines further that the induction of greening in *gun2* GNLox seedlings caused by GNLox in phytochrome-independent manner. From these results was concluded that the partial suppression of the greening defect in the *gun2* GNLox seedlings is because of the upregulation of chlorophyll pathway solely, which is induced by GNLox.

When chlorophyll from adult plants was quantified, it was found that 20-d-old *gun2* GNLox plants had chlorophyll levels identical to those of the *gun2* mutant (Figure 24D and H). In even older plants, 38-d-old, chlorophyll levels were slightly reduced compared to *gun2* mutants (Figure 24D and H). Therefore, these results suggested that *GNL* and *GUN2* function in the same pathway regarding greening. GNL is also able to promote greening in a *GUN2*-independent manner, particularly in the hypocotyl.

To investigate further the genetic relationship between *GUN2* and B-GATAs, transgenic plants were generated overexpressing *GUN2* in the wt and the *gnc gnl* background. GUN2ox in the wt background showed chlorophyll levels slightly higher than *gnc gnl*, but lower than wt (Figure 24G). GUN2ox in the *gnc gnl* background showed chlorophyll content lower than the *gnc gnl* double mutant (Figure 24G). In summary, it can be concluded that metabolites from the chlorophyll branch can be diverted from the chlorophyll to heme branch when GUN2 is in access, therefore reduce the overall chlorophyll levels.

4.2.3 Heme pathway can influence the expression of *GNC* and *GNL*

The heme pathway and its end product phytochromobilin are essential for the proper function of phytochromes, which can affect the expression of many light-regulated genes, including chlorophyll biosynthesis genes. GUN2ox in the *gnc gnl* background displayed lower chlorophyll levels compared to *gnc gnl* (Figure 24C and G). It was thus hypothesized that GUN2 might induce the expression of the B-GATAs *GNC* and *GNL* and by doing so, promotes greening in the wt. To test this, a qRT-PCR was performed with 7-d-old light-grown gun2 seedlings.

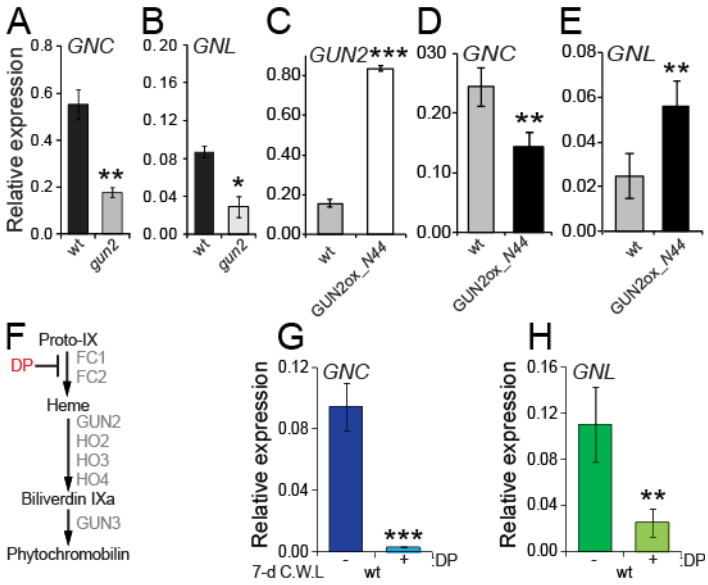

Figure 25: Heme pathway can influence the expression of B-GATAs *GNC* and *GNL*. (**A**-**B**) Relative transcript levels of *GNC* and *GNL* in 10-d-old light-grown seedlings. (**C**) Relative transcript levels of the *GUN2* in GUN2ox transgenic line. (**D**-**E**) Relative transcript levels of *GNC* and *GNL* in 10-d-old light-grown seedlings. (**F**) Schematic representation of the heme pathway; the grey letters depict the enzymes in each step of the heme pathway. The DP (dipyridyl) is an inhibitor of the first step of the heme pathway. (**G**-**H**) Relative transcript levels of *GNC* and *GNL* in 7-d-old light-grown seedlings after a 24 h treatment with DP. For all qRT experiments, the data shown are the averages and standard errors of 2 ≥ biological replicates. Student's *t*-test: *P < 0.05, **P < 0.01, ***P < 0.001; n.s., not significant.

GNC and *GNL* expression were found to be downregulated in *gun2* mutant seedlings (Figure 25A-B). To further verify these results, the expression of *GNC* and *GNL* was measured in 10-d-old light-grown GUN2ox seedlings. It was found that *GNL* but not *GNC* was significantly upregulated in GUN2ox seedlings (Figure 25C-E).

Furthermore, since GUN2 plays a role in the beginning of the heme pathway (Figure 25F), it was hypothesized that any of the intermediates of this pathway (heme, biliverdin IXa and phytochromobilin,) may affect the expression of *GNC* and *GNL*. To this end, the expression of *GNC* and *GNL* was examined after a treatment with DP (dipyridyl), an inhibitor of the first step of the heme pathway (Figure 25F). A qRT-PCR was performed with 7-d-old seedlings, treated for 24 h with DP. Both, *GNC* and *GNL* expression was found to be strongly reduced after DP treatment (Figure 25G and H). These findings suggested that either one of the heme intermediates indeed affected the expression of *GNC* and *GNL* or that any change in the synthesis of functional phytochrome, which heme pathway

contributes, affects the expression of B-GATAs, which is light-regulated and therefore depended from the phytochromes function.

4.3 PHYTOCHROME INTERACTING FACTORS (PIFs)

Apart from the essential role of PIFs in skotomorphogenesis, they also have a role in the control of greening. The basic role of PIFs in chlorophyll biosynthesis is to repress genes related to the chlorophyll branch in the dark (Liu et al. 2013). In this way PIFs help plants to avoid the deleterious effects of photobleaching, which are caused by the overaccumulation of chlorophyll intermediates in etiolated seedlings followed by light exposure. Among the seven members of the PIF protein family, only PIF1 and PIF3 have a direct role in chlorophyll biosynthesis regulation (Moon et al. 2008; Monte et al. 2004; Huq et al. 2004).

4.3.1 B-GATAs GNC and GNL induce the expression of PIF1 and PIF3

To investigate the molecular relationship between B-GATAs and PIFs, the expression of *PIFs* was initially examined in the RNA-seq experiments. Both *PIF1* and *PIF3* were strongly upregulated in the RNA-seq experiment for GNC after the 3 h treatment with Dex and CHX (Figure 14B and Appendix Table 9). To further confirm this transcriptional regulation, additional qRT-PCR experiments were performed. Because PIFs are light-unstable and mainly function in the dark, their expression was initially tested in etiolated seedlings. GNCox but not GNLox was found to induce the expression of *PIF1* and *PIF3* in dark-grown seedlings (Figure 26A). Though, the *gnc gnl* double mutant showed strong downregulation of *PIF3* (Figure 26A). When seedlings were grown under constant white light, GNCox was able to strongly induce the expression of *PIF1* and *PIF3* and GNLox slightly increased the expression of *PIF3* (Figure 26B). Moreover, *gnc gnl* seedlings showed reduced expression levels of *PIF3*, compared to wt (Figure 26B). It was thus concluded that B-GATAs are able to control the expression of *PIF1* and *PIF3* in dark-grown as well as in light-grown seedlings.

4.3.2 GNL regulates greening downstream of PIFs

The next step was to check the genetic relationship between *GNL* and *PIFs*. Therefore, genetic crosses between *pif1* (*pif1-1*), *pif3* (*pif3-1*) and GNLox, were performed. To further test the hypothesis that other *PIF* members, also function

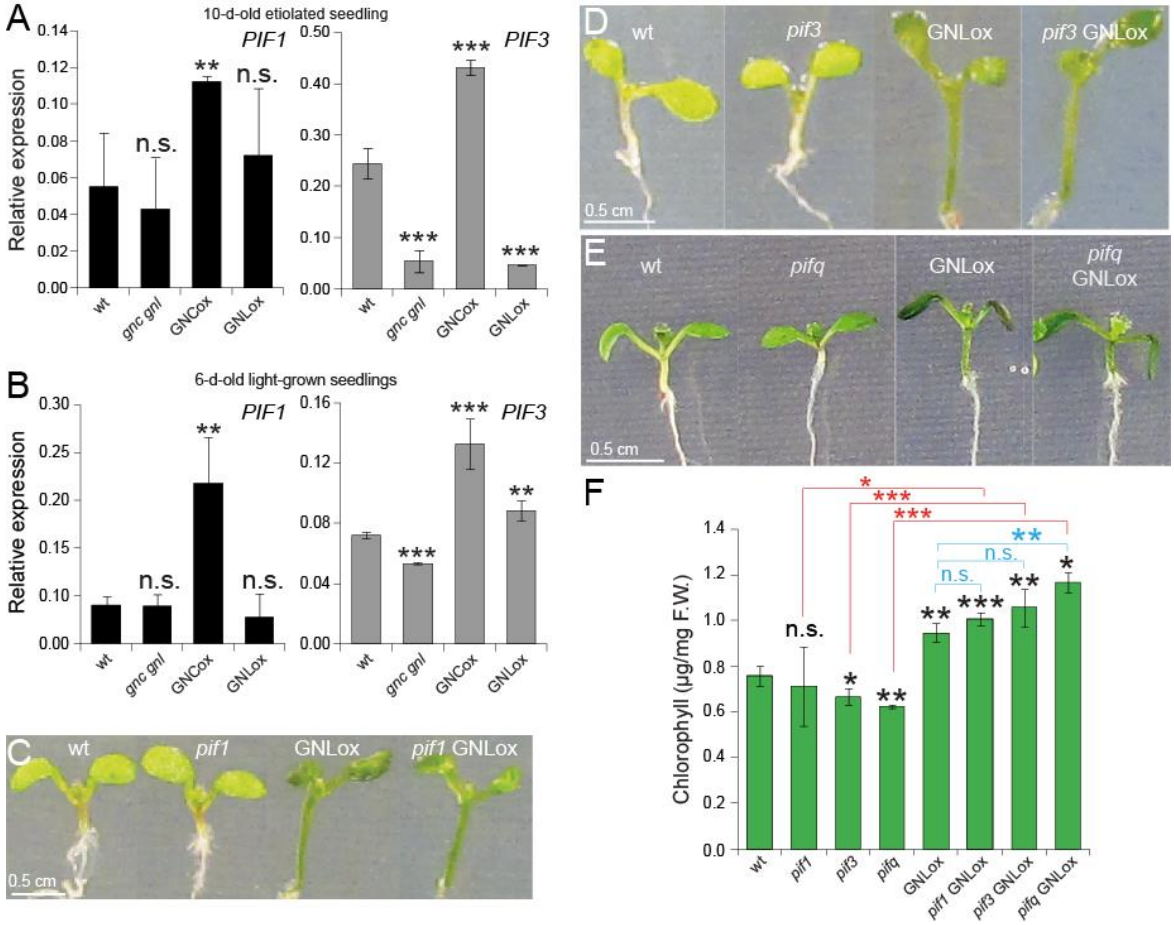

Figure 26: GNC and GNL control the expression of *PIF1* and *PIF3* and function downstream of *PIFs* in the control of greening. (**A**) Relative transcript levels of *PIF1* and *PIF3* in 10-d-old etiolated seedlings. Data shown are averages and standard errors of ≥ three biological replicates with each one ≥ three technical replicates. (**B**) Relative transcript levels of *PIF1* and *PIF3* genes in 10-d-old light-grown seedlings. Data shown are averages and standard errors of ≥ three biological replicates with each one ≥ three technical replicates. (**C**-**E**) Representative photographs of 7-d-old light-grown seedlings. (**F**) Results of the quantification of chlorophyll a and b of 7-d-old seedlings; The black asterisks depict statistically significant differences between wt and the rest of the genotypes. The red asterisks depict statistically significant differences between mutants and corresponding genetic combinations. The blue asterisks depict statistically significant differences between GNLox and the other GNLox genotypes. Student's *t*-test: *P < 0.05, **P < 0.01, ***P < 0.001; n.s., not significant.

downstream of *GNL* in the greening pathway, the chlorophyll levels of *pifq* (*pif1 pif3 pif4 pif5*) GNLox seedlings were quantified. This specific genotype had been generated in our lab by Dr. Rene Richter for the needs of a previous study

(Klermund et al. 2016). Importantly, GNLox was able to strongly induce greening in *pif1*, *pif3* and *pifq* mutant backgrounds (Figure 26C-F). These results proposed that GNL is able to regulate greening downstream of *PIFs*.

4.3.3 The B-GATA GNL protects etiolated seedlings from the photooxidative effects of the light exposure by decreasing the levels of protochlorophyllide

In the dark, PIFs attenuate the expression of genes encoding for enzymes of the chlorophyll biosynthesis pathway. Hence, after light exposure, the seedlings are able to overcome the photobleaching effect, associated with the over-accumulation of chlorophyll intermediates. To assess if B-GATAs contribute to the survival of etiolated seedlings after light exposure, seedlings were grown in the dark for 5 and 7-d and then exposed to light for an additional 2-d. When wt seedlings were grown in the dark for 5 and 7-d, ~60% of them were bleached after exposure to light (Figure 27A). Seedlings of *pifq* mutant bleached at 100%, already after 5-d in the dark and following light exposure, as previously reported (Huq et. al., 2004) (Figure 27A). The *gnc gnl* and wt seedlings showed a similar percentage of bleaching after 5-d in the dark, but after 7-d in the dark, *gnc gnl* they displayed ~90% bleaching compared to ~60% in the wt (Figure 27A). In contrast, GNLox seedlings grown either for 5-d or for 7-d in the dark followed by light exposure, were bleached in only ~10% and 20% of the cases, respectively (Figure 27A). However, *pifq* GNLox bleached at 100% to the same extent as *pifq* mutant after 5-d in the dark following illumination (Figure 27A). Taken together, these findings suggested that GNL contributes to the protection of seedlings against the photooxidative effects, which are caused by prolonged growth in the dark followed by light exposure. Furthermore, this positive regulation of the photooxidative effect most likely relies on the transcriptional regulation of *PIFs* by the B-GATAs since *pifq* GNLox seedlings completely failed to survive photooxidative stress.

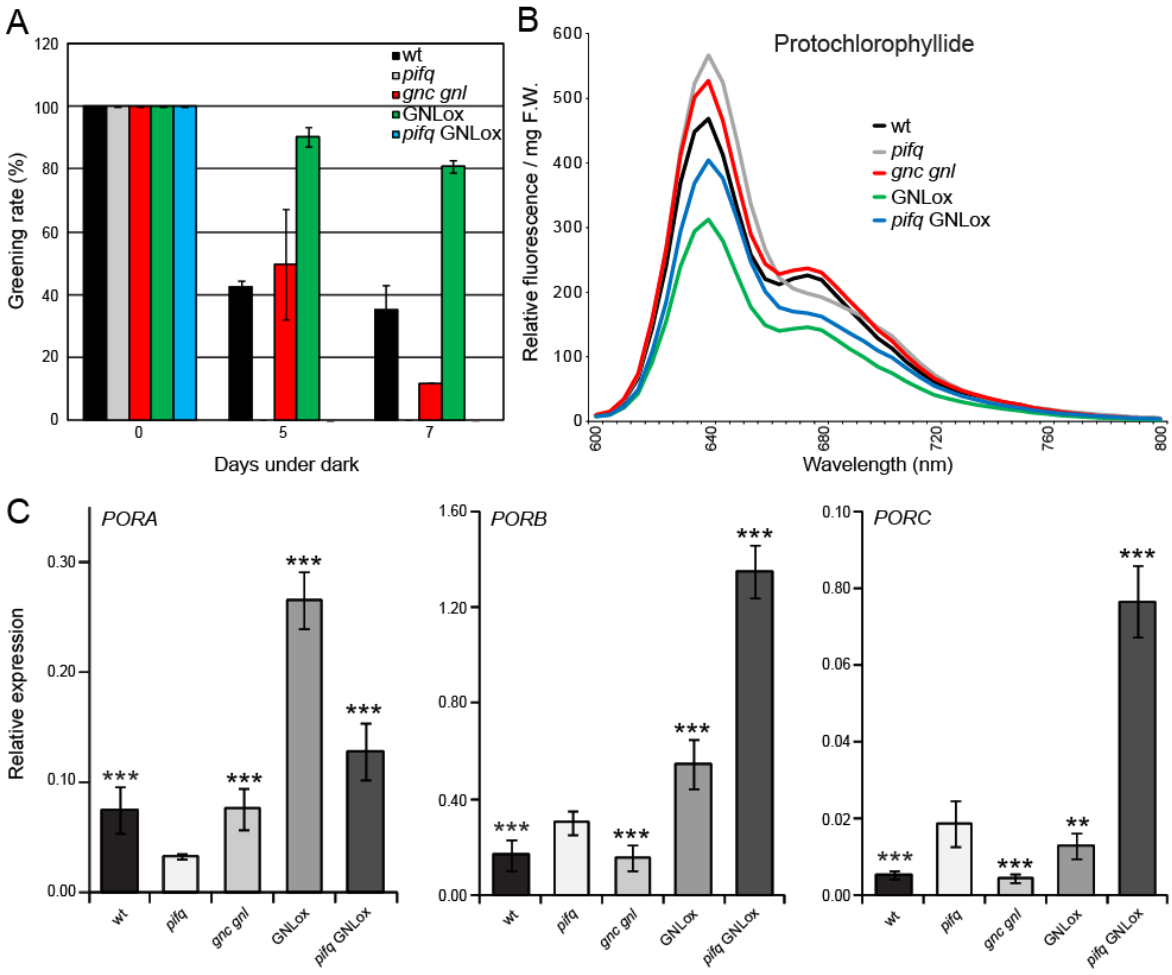

Figure 27: GNL increases the resistance of de-etiolated seedlings to photooxidative stress. (**A**) Greening rate (% of green seedlings) of seedlings grown in the dark for 0, 5 and 7-d following additional exposure to light for 2-d additionally. The data represents the average with standard errors of two independent experiments. (**B**) Accumulation of protochlorophyllide in 7-d-old dark-grown seedlings. The data represents the average with standard errors of three biological replicates. (**C**) Relative transcript levels of *PORA*, *PORB* and *PORC* genes in 10-d-old etiolated seedlings. The data shown are the averages and standard errors of ≥ two biological replicates with each one ≥ three technical replicates. Student's *t*-test: **P < 0.01, ***P < 0.001; n.s., not significant.

Next, it was hypothesized that GNLox seedlings are able to cope better with photooxidative stress because they are able to accumulate fewer chlorophyll intermediates during the etiolated period. To test this, the levels of Pchlide were quantified in 7-d-old etiolated seedlings. The *pifq* seedlings showed the highest levels of Pchlide, which was in line with the previous results of 100% bleached *pifq* seedlings after photooxidation (Figure 27A and B). Similarly, high levels of Pchlide of *pifq* were displayed in the *gnc gnl* mutant, which also agrees with the high percentage of bleached 7-d-old etiolated seedlings after illumination (Figure

27A and B). In contrast, GNLox seedlings showed the lowest levels of Pchlide, indicating that the reduced levels of this particular chlorophyll intermediate made GNLox seedlings to have a better chance against the deleterious effect of photooxidation than the others genotypes (Figure 27A and B). Finally, the *pifq* GNLox seedlings had intermediate levels of Pchlide, between *pifq* and GNLox (Figure 27A and B). In summary, these data suggested that GNL reduces the overaccumulation of Pchlide in the dark and thus helps the etiolated seedlings to overcome the lethal effects of photooxidation after light exposure. However, there must be compounds other than Pchlide, whose reduction in the dark is also dependent on the function of PIFs and GNL.

4.3.4 The B-GATAs may reduce protochlorophyllide by the transcriptional control of the *POR* genes

Angiosperms can reduce Pchlide to Chlide (chlorophyllide) through the POR proteins (PORA, PORB and PORC), which are light-dependent enzymes (Frick et al. 2003). It was therefore hypothesized that GNL may reduce the levels of Pchlide through the upregulation of *POR* genes. To this end, the expression of the POR genes in 10-d-old etiolated seedlings was examined. The expression of *PORA*, *PORB* and *PORC* was found to be decreased in the *gnc gnl* seedlings (Figure 27C). On the contrary, GNLox seedlings showed upregulation of the expression of *PORA* and *PORB*, but not for the *PORC* gene that was downregulated when compared to *pifq* mutant (Figure 27C). Lastly, when the expression of *PORs* was examined in *pifq* GNLox seedlings, all *POR* genes were strongly upregulated (Figure 27C). From these results, it was concluded that B-GATAs are able to induce the expression of *POR* genes in etiolated seedlings. Furthermore, at least for *PORB* and *PORC*, it seems that the PIF proteins function antagonistically with GNL in the regulation of *PORs*, *PORA* and *PORC* expression was even higher than in *pifq* GNLox seedlings than in *pifq* (Figure 27C).

4.3.5 The B-GATAs GNC and GNL may protect de-etiolated seedlings from photooxidation through transcriptional upregulation of the carotenoid biosynthesis pathway

Carotenoids have multiple functions in plants as accessory proteins for the LHCs, as precursors for plant hormones such as abscisic acid and strigolactones, and as protectors against photooxidation (Ruiz-Sola & Rodríguez-Concepción 2012). Interestingly, the carotenoid pathway is markedly upregulated during the de-etiolation process (Welsch et al. 2000). Therefore, it was hypothesized that B-GATAs may also contribute to the protection against photooxidation of etiolated seedlings through the carotenoid pathway. To this end, the expression of all genes encoding for enzymes in the carotenoid biosynthesis pathway was examined in the RNA-seq experiments with B-GATAs GNC and GNL. Strikingly, 13 of the 21 genes of the carotenoid pathway had been found to be upregulated after GNC induction by Dex.

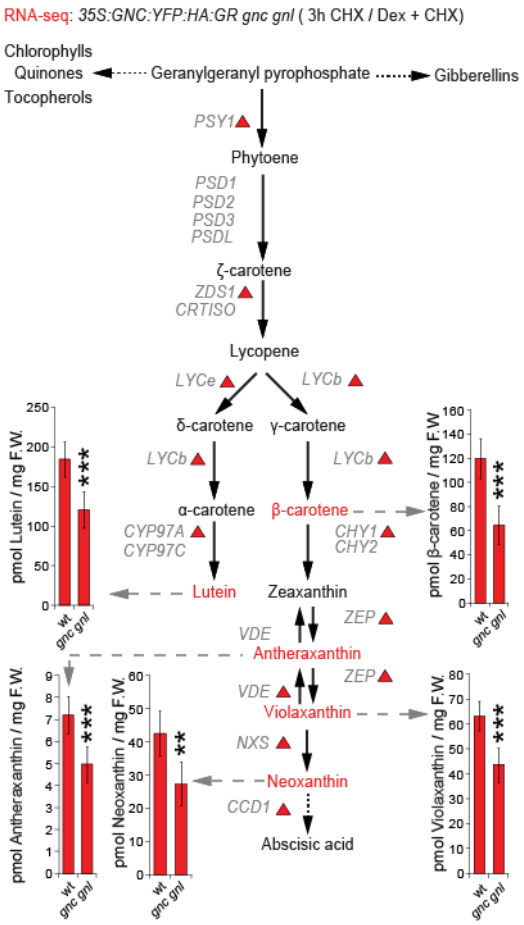

Figure 28: The levels of intermediates in the carotenoid pathway are reduced in the *gnc gnl* double mutant as determined by HPLC. Schematic representation of the carotenoid biosynthesis pathway. Intermediates colored red are those, which were quantified by HPLC analysis of 10-d-old light-grown seedlings. The bar-diagrams display the difference in carotenoid intermediates between wt and the *gnc gnl* double mutant. Genes with a role in each step of the pathway are depicted with grey italic letters. Student's *t*-test: **P < 0.01, ***P < 0.001. Red arrowheads show differentially expressed genes in the RNA-seq experiment with *35S:GNC:YFP:HA:GR gnc gnl*.

(Figure 28 and Appendix Table 9). This suggested that GNL is able to help in the protection against photooxdation after light exposure through upregulation of genes, which play a role in carotenoids biosynthesis.

To explain further the role of B-GATAs in carotenoid production, the levels of some basic carotenoids in the *gnc gnl* double mutant seedlings were quantified by Dr. Boris Hedtke from the group of Prof. Dr. Bernhard Grimm. The amounts of lutein, antheraxanthin, neoxanthin violaxanthin and β-caroten were quantified by HPLC as part of our collaboration in 10-d-old light-grown seedlings. All five carotenoids quantified in this study, were statistically significantly reduced in *gnc gnl* seedlings compared to wt (Figure 28). These results underline the positive contribution of GNC and GNL in carotenoid biosynthesis.

4.4 GOLDEN2-LIKE (GLK) transcription factors

4.4.1 GNC and GNL induce the expression of *GLK1* and *GLK2*

GLK transcription factors are important regulators of photosynthesis, chlorophyll biosynthesis, chloroplast development and retrograde signaling (Waters et al. 2008). Their pivotal role in chlorophyll biosynthesis is visible from the very pale green color of the *glk1 glk2* double mutant, not only in seedlings but also in adult plants (Figure 30A). It was postulated, from the NGS results, that GNC and GNL, could possibly influence the regulation of *GLKs*. The ChIP-seq experiment suggested that *GLK1* but not *GLK2* was a target of GNL (Figure 29). Moreover, the RNA-seq for GNC showed that *GLK2*, but not *GLK1*, was strongly induced after the application of Dex and CHX (Figure 14 and Appendix Table 9). To further clarify the binding of B-GATAs to *GLK* promoters, independent ChIP experiments with GNL were performed. It was revealed that GNL binds to the promoter of *GLK1* on a position close to the start codon (Figure 29B and D). Though, when the position of the peak identified based on the analysis of the NGS data of ChIP-seq was examined (Figure 29A), no binding of GNL was detected (Figure 29B and E). The ChIP-seq data also suggested that GNL did not bind to the promoter of the *GLK2* gene, a result also verified by independent ChIP (Figure 29C and F). Nevertheless, when *35S:GNL:YFP:HA:GR gnc gnl* seedlings were used for the

ChIP, GNL bound to the promoter of *GLK2* in a region in close proximity to the start codon after 4 h treatment with Dex (Figure 29C and G). In summary, these results suggest that both of B-GATAs may bind to the promoters of *GLK1* and *GLK2*.

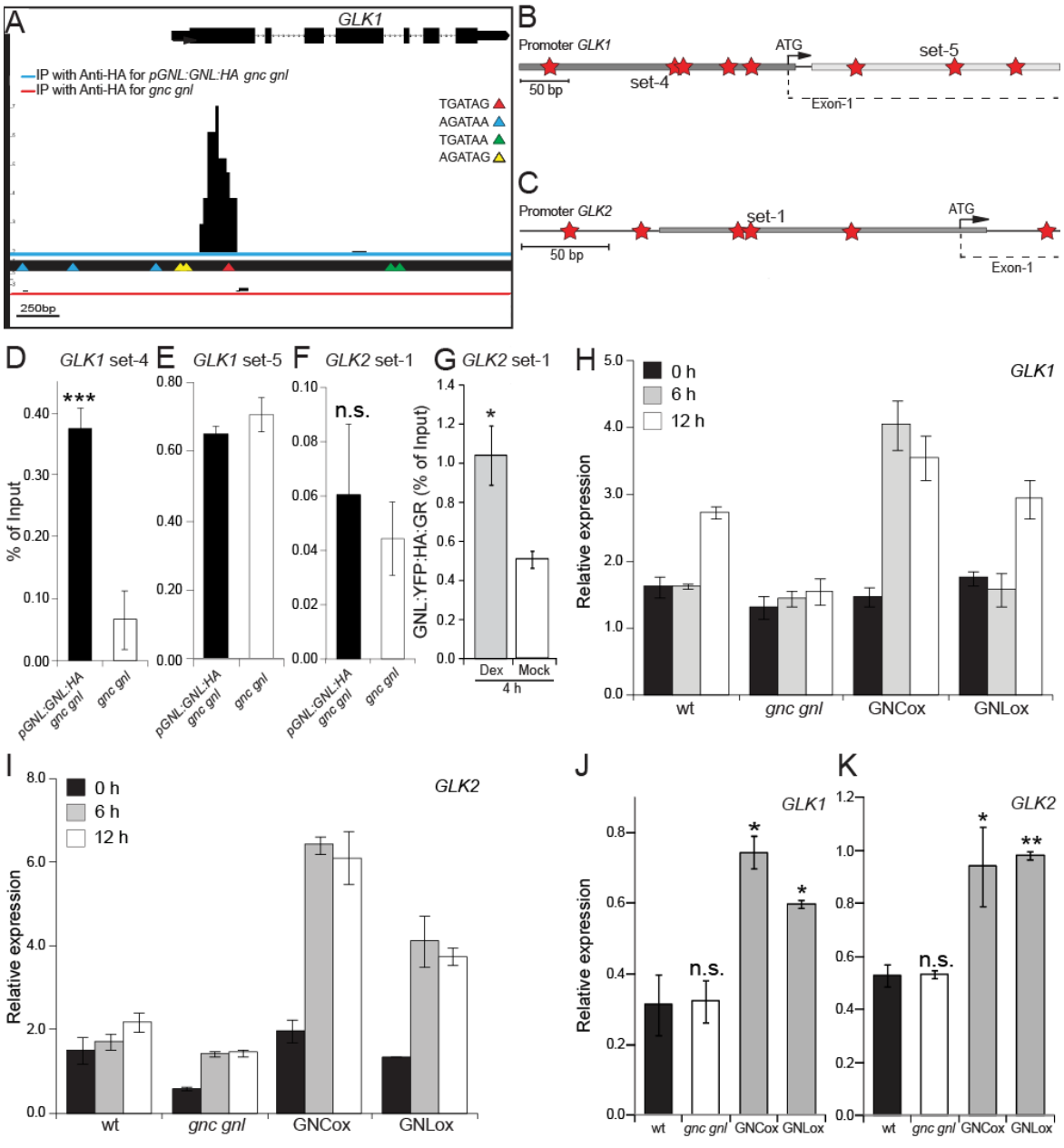

Figure 29: The B-GATAs GNC and GNL may regulate the expression of the *GLK1* and *GLK2* transcription factors. (**A**) Identified peak from the ChIP-seq with *pGNL:GNL:HA gnc gnl* transgenic line and the *gnc gnl* double mutant, associated to *GLK1* gene. The blue line corresponds to the chromatin immunoprecipitation of GNL:HA, and the red line corresponds to the ChIP of the *gnc gnl* double mutant (negative control). Colored arrowheads depict different variants of GATA motifs where GNL:HA can potentially bind. (**B**-**C**) Schematic representation of the *GLK1* and *GLK2* promoters. The red stars show locations of GATA boxes; the grey boxes represent regions tested by qRT-PCR after ChIP, for the binding of GNL:HA. (**D**, **E**) Results from qRT-PCRs

analysis of ChIP with *pGNL:GNL:HA gnc gnl* transgenic line and the *gnc gnl* double mutant to detect binding sites of GNL:HA on the promoter of *GLK1*. (**F**) Results from qRT-PCRs analysis after ChIP with *the pGNL:GNL:HA gnc gnl* transgenic line and the *gnc gnl* double mutant to detect binding sites of GNL:HA on the promoter of *GLK2*. (**G**) Results from qRT-PCRs analysis after ChIP with the *35S:GNL:YFP:HA:GR gnc gnl* transgenic line after 4 h treatment with Dex, to detect binding sites of GNL:YFP:HA:GR on the promoter of *GLK2*. The amplicons of each ChIP-qRT-PCR correspond to the regions with the grey boxes on the promoter of the *GLK* genes, designated as set-1, 4, 5. (**H**, **I**) Relative transcript levels of *GLK1* and *GLK2* in 6-d-old dark-grown seedlings, followed by light exposure for 0, 6 and 12 h. Data shown are averages and standard errors of one biological replicate with four technical replicates. (**J**, **K**) Relative transcript levels of *GLK1* and *GLK2* in 10-d-old light-grown seedlings. Data shown are averages and standard errors of three biological replicates each one with three technical replicates. Student's *t*-test: *P < 0.05, **P < 0.01, ***P < 0.001; n.s., not significant.

The next question was whether these respective binding events can lead to a transcriptional regulation of the *GLK1* and *GLK2* genes. Therefore, a qRT-PCR experiment with dark-grown seedlings after light exposure was performed. Both *GLK1* and *GLK2* were strongly induced in GNCox and GNLox seedling after light exposure (Figure 29H and I). Additionally, qRT-PCR experiments performed with seedlings grown under constant white light, confirmed the upregulation of both *GLKs* by GNC and GNL (Figure 29J and K). The overall conclusion from the previous data was that GNC and GNL could control the transcription of *GLKs* by binding to their promoters.

4.4.2 GLKs are downstream of GNC and GNL regarding greening

Since there is a relationship between B-GATAs and *GLKs* at the molecular level, the genetic relationship between them was investigated. For that reason, genetic crosses were conducted among different genotypes of *B-GATAs* and *GLKs*.

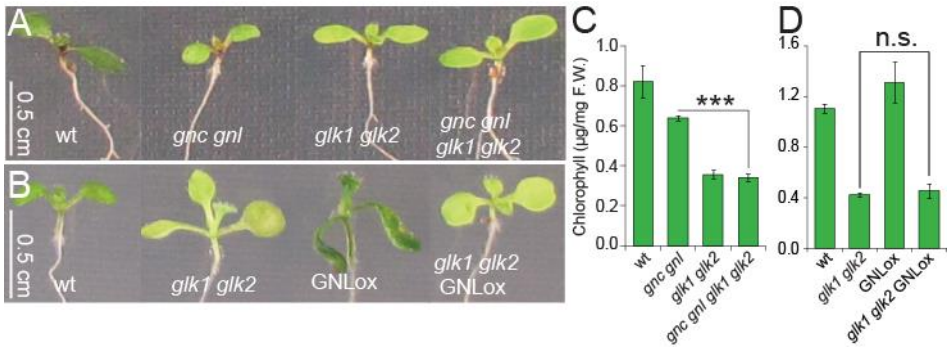

Figure 30: The *GLK* transcription factors function downstream or in parallel with B-GATAs *GNC* and *GNL* in the chlorophyll biosynthesis pathway. (**A**-**B**) Representative photographs of 7-d-old light-grown seedlings. (**C**-**D**) Results of the quantification of chlorophyll a and b in 7-d-old light-grown seedlings. Student's *t*-test: ***P < 0.001; n.s., not significant.

The *gnc gnl glk1 glk2* quadruple mutant showed equal chlorophyll levels to the *glk1 glk2* double mutant (Figure 30A and C). Furthermore, *glk1 glk2* GNLox was not able to promote chlorophyll levels higher than the *glk1 glk2* double mutant (Figure 30B and D). Taken together, these findings suggested that the GLK transcription factors function downstream or in parallel of the B-GATA GNC and GNL in the control of greening.

4.4.3 B-GATAs and GLKs have common but also distinct target genes with regard to greening

To investigate further how greening regulators are controlled by B-GATAs and GLK transcription factors, a qRT-PCR experiment was conducted with 10-d-old light-grown seedlings of the *gnc gnl and glk1 glk2* mutants as well as their quadruple mutant. Interestingly, when we compared the gene expression changes in the *gnc gnl* and *glk1 glk2* double mutant with those of the quadruple mutant, we noted an essentially additive defect in the expression of all genes tested. When gene expression was strongly reduced in both double mutants (*HEMA1*, *GUN4*, *GUN5*, *CRD1*, *CAO*), the defect was enhanced in the quadruple mutant (Figure 31).

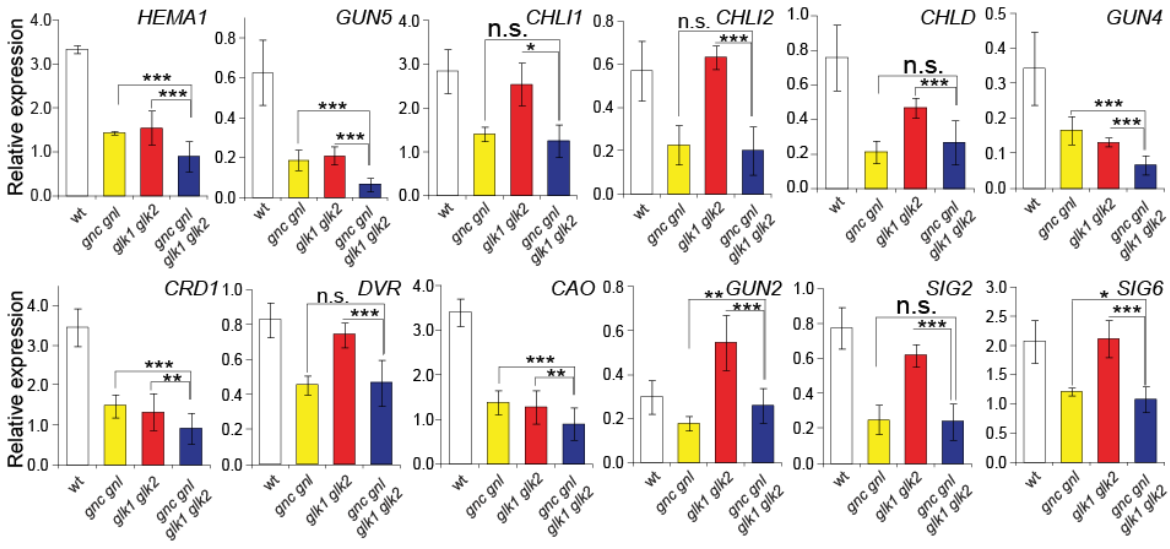

Figure 31: B-GATAs and GLKs have common but also distinct target genes regarding greening. Relative transcript levels of genes related to greening in 10-d-old light-grown seedlings. Data shown are averages and standard errors of ≥ two biological replicates with each one four technical replicates. Student's *t*-test: *P < 0.05, **P < 0.01, ***P < 0.001; n.s., not significant.

When the expression defect was strong in the *gnc gnl* mutant but not or only weakly impaired in the *glk1 glk2* mutant (*CHLI1*, *CHLI2*, *DVR*, *GUN2*, *SIG2* and *SIG6*), the expression changes in the quadruple mutant were very similar to those observed in *gnc gnl* (Figure 31). Among the twelve genes tested, *CHLD* was the only one exception from this rule, since its expression was strongly reduced in both mutants but as strongly impaired in the quadruple as in the *gnc gnl* double mutant (Figure 31).

In summary, it can be concluded that the GATA and the GLK factors regulate partially overlapping and partially distinct gene sets but that their combined defect cannot exacerbate the chlorophyll formation defects observed in the *glk1 glk2* mutant. Furthermore, the strong reduction of several of these genes specifically in the *gnc gnl* double mutant supports our conclusion that the effects of the GATAs on greening may be explained by the direct regulation of a specific gene set by the GATAs.

4.5 Sigma factors (SIGs), the regulators of the chloroplast transcription

Chlorophyll biosynthesis is regulated not only by nuclear-encoded but also by chloroplast-encoded genes. The transcription in the chloroplasts is controlled by two different types of polymerases, the plastid-encoded polymerase (PEP) and the nuclear-encoded polymerase (NEP). The binding specificity of PEP to the chloroplast gene-promoters is given by a set of nuclear-encoded proteins named sigma factors (SIGs). The Arabidopsis genome encodes six different sigma factors (Börner et al. 2015) but only *sig2* (*sig2-1*) and *sig6* (*sig6-2*) mutants show severe defects in chlorophyll biosynthesis, being very pale green compared to wt (Kanamaru & Tanaka 2004; Loschelder et al. 2006). Therefore, it was decided to study these mutants, alongside with B-GATA mutants, to elucidate possible interactions between them in the context of greening. The potential transcriptional regulation of *SIG2* and *SIG6* by GNC and GNL would reveal signals that are able to be transduced from the nucleus to the chloroplasts through B-GATAs and SIGs.

4.5.1 GNC and GNL control the expression of *SIG2*

SIG2 was not found to be a target of GNL in the ChIP-seq, though it was strongly induced in the RNA-seq for GNC (Figure 14B and Appendix Table 9). Independent, ChIP experiments revealed, however, a binding of GNL to the promoter of *SIG2* (Figure 32A-C). Additionally, a qRT-PCR experiment with 6-d-old dark-grown seedlings followed by 0, 6 12 h light exposure showed that *the gnc gnl* double mutant displayed significantly reduced levels of the *SIG2* expression (Figure 32D). Moreover, it was found that expression of *SIG2* was strongly induced in GNCox, and to a lesser degree in GNLox seedlings (Figure 32D). In sum, it seems that the B-GATA GNL binds to the *SIG2* promoter and that GNL as well as GNC are able to upregulate the expression of *SIG2*.

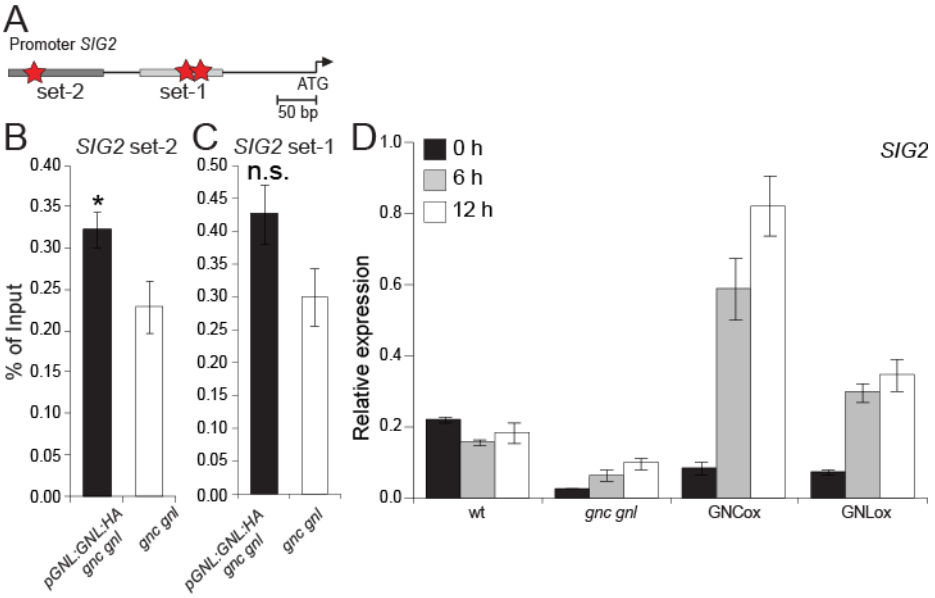

Figure 32: GNL directly controls the expression of *SIG2*. (**A**) Schematic representation of the *SIG2* promoter. The red stars show locations of GATA boxes; the grey boxes represent regions tested by qRT-PCR of ChIP experiment, for the binding of GNL:HA. (**B** - **C**) Results from the ChIP-qRT-PCRs analysis with the *pGNL:GNL:HA gnc gnl* transgenic line and the *gnc gnl* double mutant. (**D**) Relative transcript levels of *SIG2* in 6-d-old dark-grown seedlings followed by 0, 6 and 12 h light exposure. The data shown are the averages and standard errors of one biological replicate with four technical replicates. Student's *t*-test: *P < 0.05; n.s., not significant.

4.5.2 GNL induces greening independently from SIG2

sig2 GNLox was obtained through a genetic cross and was used to investigate the genetic relationship between *SIG2* and *GNL*. Initially, the development of *sig2* GNLox plants was followed, with particular focus on greening, from the stage of

young seedlings until the stage of adult plants. The *sig2* mutant displayed a very pale green color over its entire lifespan, indicating a severe defect in the chlorophyll biosynthesis (Figure 33A to H). The first 6-d following germination, the *sig2* GNLox seedlings appeared to be similar to *sig2* mutants but as the development of the plants progressed, the greening of the *sig2* GNLox was closer to that of the wt, in the cotyledons and the hypocotyl but not the emerging true leaves (Figure 33D-J).

When the chlorophyll levels of 7-d-old seedlings were quantified, *sig2* GNLox had slightly but statistically significantly increased chlorophyll content (Figure 33K). Furthermore, when the chlorophyll of 20 and 38-d-old plants was measured, *sig2* GNLox had higher chlorophyll levels than the *sig2* mutant (Figure 33L). Additionally, to test whether SIG2 was able to induce greening in wt and *gnc gnl* background, transgenic lines of SIG2ox and *gnc gnl* SIG2ox were generated (Figure 33N). The quantification of chlorophyll in 7-d old seedlings showed that neither SIG2ox nor *gnc gnl* SIG2ox was able to increase the chlorophyll levels higher than the *gnc gnl* double mutant (Figure 33O). Taken together, these results suggested that B-GATAs can control the expression of *SIG2*. Moreover, GNL is able to induce greening in the absence of *SIG2*, in a tissue-specific manner. Thus, GNL either induces greening through the upregulation of *SIG6*, another sigma factor with a prominent role in greening, when SIG2 is not present or GNL is able to induce greening through an independent pathway.

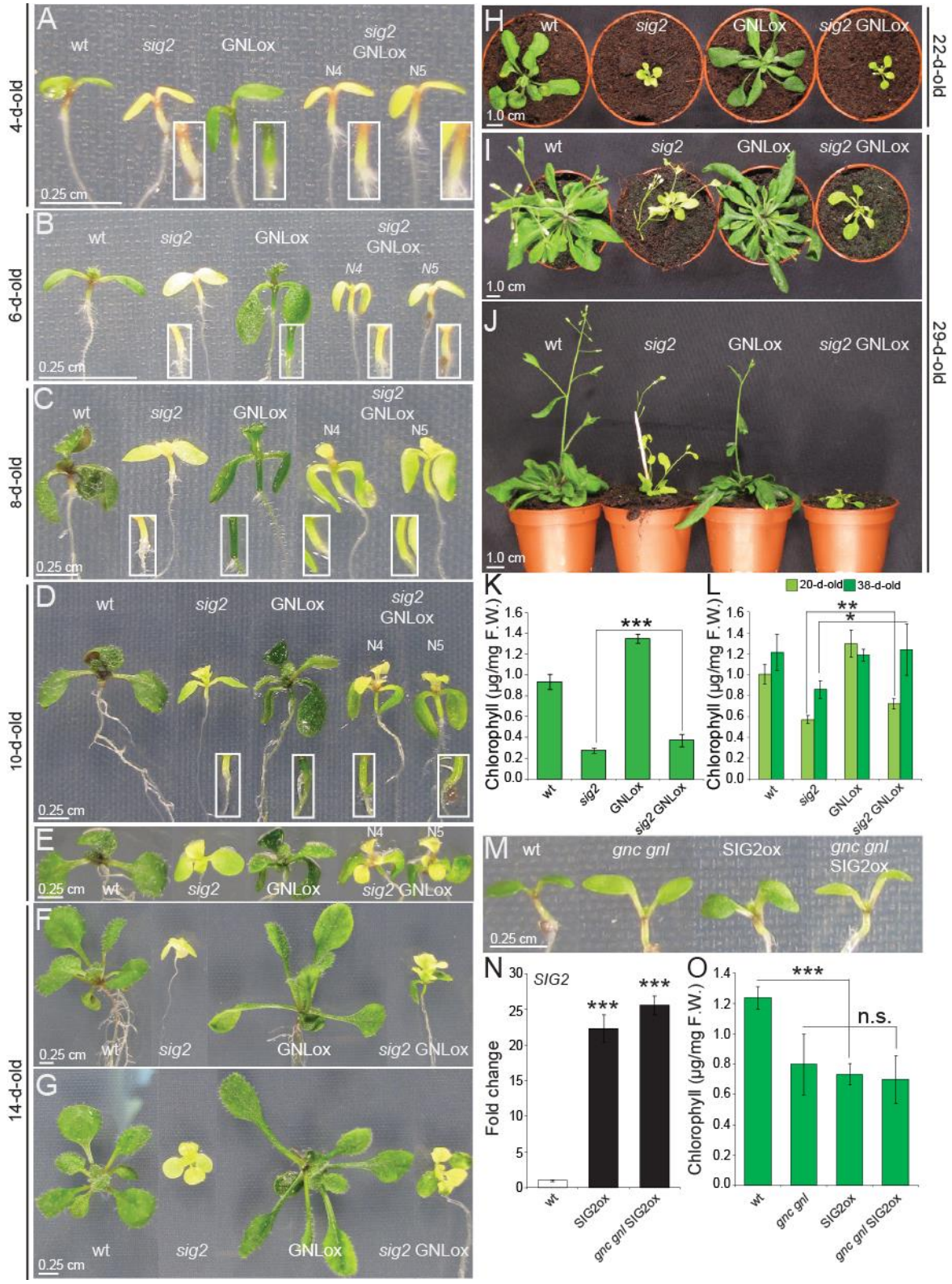

Figure 33: GNL partially induces greening independently from *SIG2* in a tissue-specific manner. (**A**-**E**) Representative photographs of 4, 6, 8 and 10-d-old light grown seedlings. All the insets show an enlargement of the hypocotyl region in the corresponding seedlings. (**F**-**J**) Representative photographs of 14, 22 and 29-d-old adult plants. (**K**) Results of the quantification

of chlorophyll a and b of 7-d-old light-grown seedlings. (**L**) Results of the quantification of chlorophyll a and b in 20-d-old and 38-d-old adult plants. (**M**) Representative photographs of 7-d-old light-grown seedlings. (**N**) Relative transcript levels of *SIG2* in 7-d-old light-grown seedlings of the transgenic SIG2ox and *gnc gnl* SIG2ox lines. The data shown are the averages and standard errors of four technical replicates. (**O**) Results of the quantification of chlorophyll a and b in 7-d-old light-grown seedlings. Student's *t*-test: *P < 0.05, **P < 0.01, ***P < 0.001; n.s., not significant.

4.5.3 The B-GATAs GNC and GNL control the expression of *SIG6*

Another member of the sigma factor family that contributes to chlorophyll biosynthesis is SIG6. Similar to *SIG2*, *SIG6* did not appear to be a target of GNL in the ChIP-seq but was found strongly upregulated in the RNA-seq for GNC (Figure 14 and Appendix Table 9).

Independent ChIP experiments revealed that GNL bound to two different positions in the *SIG6* promoter (Figure 34A-C). A qRT-PCR with 6-d-old dark-grown seedlings followed by exposure to light showed similar results as in the case of *SIG2*. The *gnc gnl* seedlings showed downregulation of the *SIG6*, but the GNCox and GNLox seedlings displayed strong upregulation of *SIG6* (Figure 34D). Much more prevalent was the induction of *SIG6* in GNCox seedlings. It was thus concluded, that the expression of *SIG6* could be directly controlled by the B-GATAs GNC and GNL.

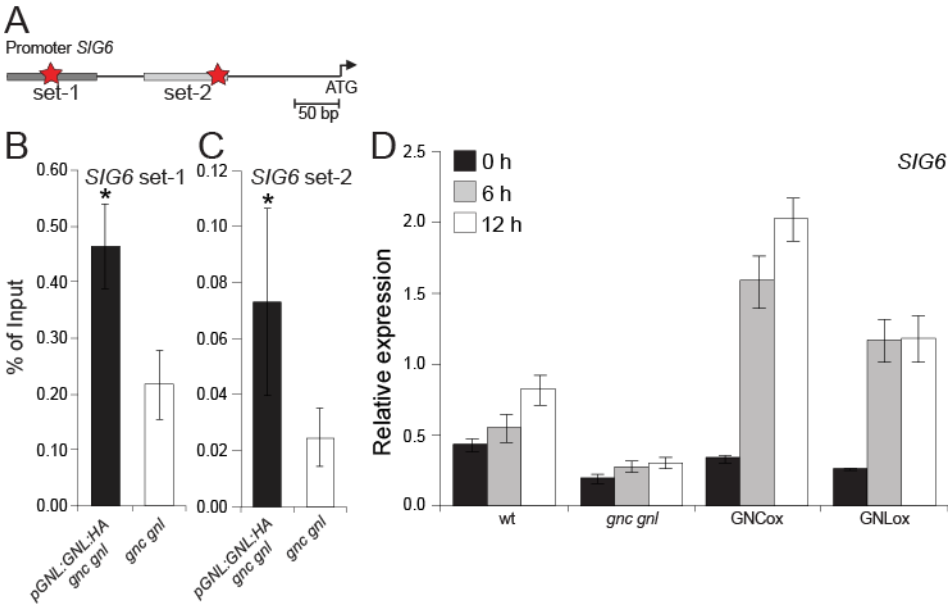

Figure 34: GNL controls the expression of *SIG6*. (**A**) Model of the *SIG6* promoter. The red stars show locations of GATA boxes; grey boxes represent regions tested by qRT-PCR of ChIP experiment for the binding of GNL:HA. (**B**-**C**) Results from qRT-PCR analysis of a ChIP with a *pGNL:GNL:HA gnc gnl* transgenic line and the *gnc gnl* double mutant. The amplicons of each ChIP-qRT-PCR correspond to the regions with the grey boxes on the promoter of the *SIG6* gene,

designated as set-1, -2. (**D**) Relative transcript levels of *SIG6* in 6-d-old dark-grown seedlings, followed by short 0, 6 and 12 h light exposure for. Data shown are averages and standard errors of one biological replicate with four technical replicates. Student's *t*-test: *P < 0.05; n.s., not significant.

4.5.4 GNL promotes greening independently from SIG6

To further investigate the genetic interaction between *GNC* and *GNL* with *SIG6*, genetic crosses were performed. The triple mutant *sig6 gnc gnl* displayed similar chlorophyll levels as the *sig6* single mutant (Figure 35A and H), indicating that *SIG6* functions downstream of *GNC* and *GNL*. Already early in their development, the *sig6* GNLox seedlings were greener than the *sig6* mutant (Figure 35B and C). When chlorophyll levels were measured, 7-d-old *sig6* GNLox seedlings showed a chlorophyll content higher than the *sig6* mutant and similar to wt (Figure 35D and I). This was a different result as observed in *sig2* GNL seedlings, which when at the same age, had chlorophyll levels just slightly higher than the *sig2* mutant (Figure 33). As development continued, it became obvious that the *sig6* mutant as well as *sig6* GNLox recovered from the pale green phenotype (Figure 35D, F, G and J).

The chlorophyll levels of adult plants were quantified, and it was found that 20-d-old and 38-d-old *sig6* GNLox plants displayed higher levels of chlorophyll than the *sig6* mutant (Figure 35J). In conclusion, all the previous results proposed that GNL is able to induce greening independent from SIG6, as it had been observed for *sig2* GNLox. The difference with *sig6* GNLox seedlings was that this could occur even earlier during the development than *sig2* GNLox seedlings. Next, it was tested whether SIG6 was able to induce greening in the wt and the *gnc gnl* background. Therefore, transgenic lines of SIG6ox and *gnc gnl* SIG6ox were generated (Figure 35K).

The quantification of chlorophyll in 7-d old seedlings showed that SIG2ox had slightly higher levels of chlorophyll compared to wt, but *gnc gnl* SIG2ox shown similar levels with *gnc gnl* (Figure 35L). The emerging hypothesis from these results could be similar to that phrased for *SIG2*. Either GNL could induce greening by the upregulation of *SIG2* or *SIG6* when either of these *SIG* genes is absent. Or GNL could act through an independent pathway.

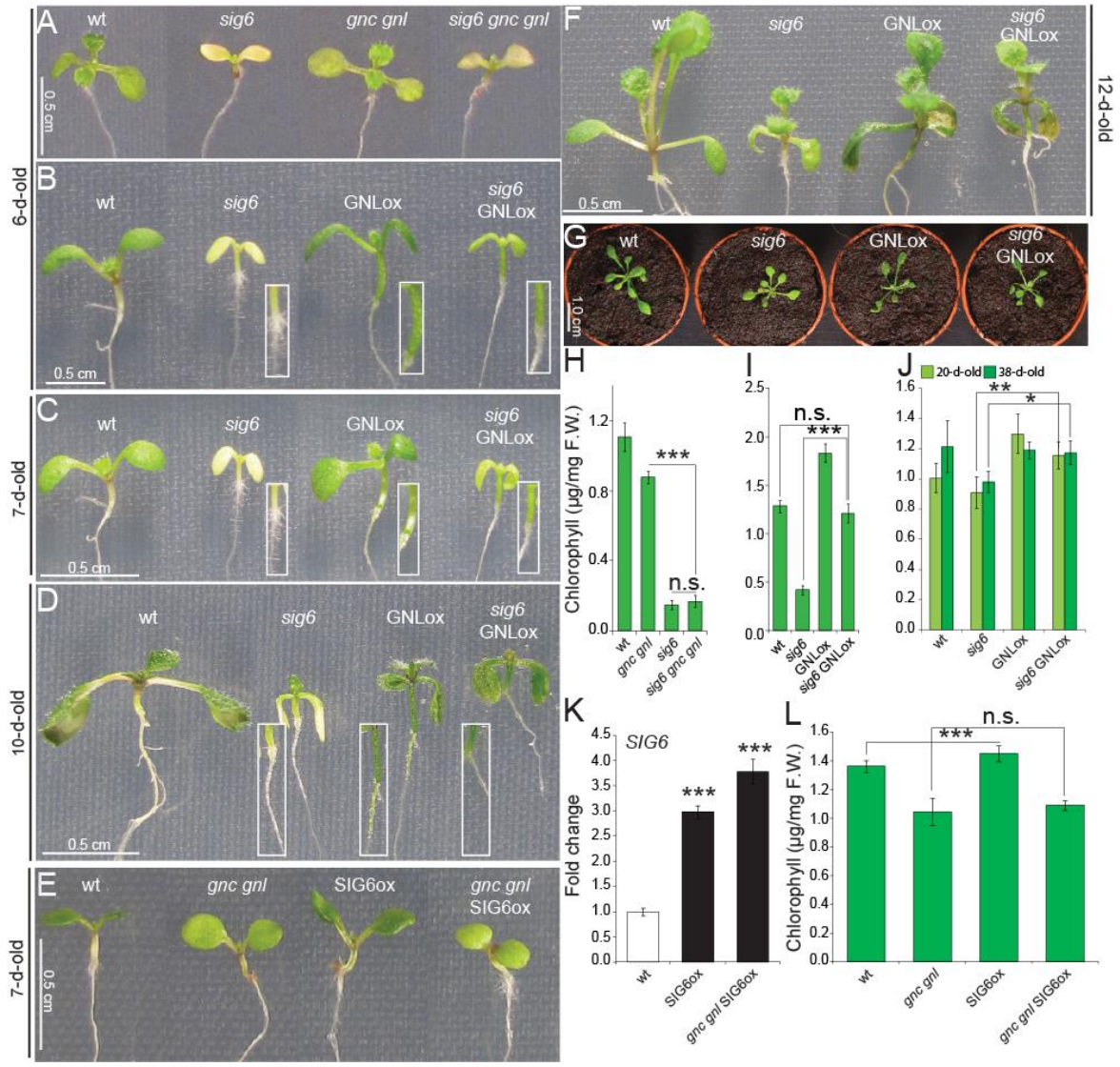

Figure 35: GNL can induce, at least partially, greening independently from *SIG6*. (**A**-**F**) Representative photographs of 6, 7, 10-d-old light grown seedlings. All the insets show enlargement of the hypocotyl region of the corresponding seedlings. (**G**) Representative photographs of 20-d-old adult plants. (**H**-**I**) Results of the quantification of chlorophyll a and b of 7-d-old light-grown seedlings. (**J**) Results of the quantification of chlorophyll a and b of 20-d-old and 38-d-old adult plants. (**K**) Relative transcript levels of *SIG6* in 7-d-old light-grown seedlings of transgenic line of SIG6ox wt and *gnc gnl* SIG6ox. Data shown are averages and standard errors of four technical replicates. (**L**) Results of the quantification of chlorophyll a and b of 7-d-old light-grown seedlings. Student's *t*-test: *P < 0.05, **P < 0.01, ***P < 0.001; n.s., not significant.

4.5.5 GNC and GNL regulate the expression of *SIG2* and *SIG6* in a cytokinin-dependent manner

GNC and *GNL* are cytokinin-induced genes (Ranftl et al. 2016). Therefore, it was hypothesized that the regulation of the *SIG2* and *SIG6* genes by GNC and GNL

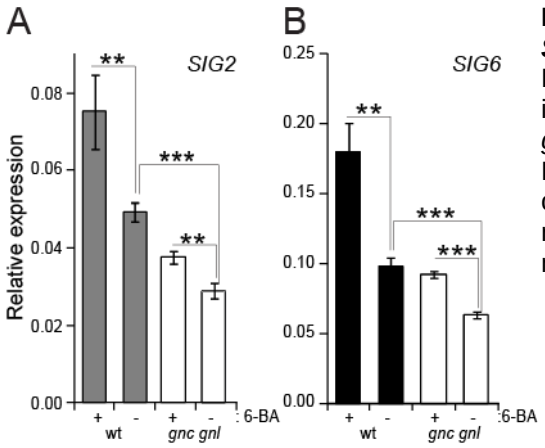

Figure 36: Cytokinin-dependent regulation of *SIG2* and *SIG6* via the B-GATA's GNC and GNL. Relative transcript levels of (**A**) *SIG2* and (**B**) *SIG6* in 10-d-old light-grown seedlings of wt and the *gnc gnl double* mutant, followed by 8 hr treatment with 6-BA. Data shown are averages and standard errors of one biological replicate with three technical replicates. Student's *t*-test: **P < 0.01, ***P < 0.001; n.s., not significant.

could be cytokinin-dependent. To test this, light-grown seedlings of wt and *gnc gnl* were treated for 8 h with the cytokinin 6-BA. Then, a qRT-PCR was performed to check the expression of *SIG2* and *SIG6*, which were both found to be strongly upregulated after the treatment with 6-BA in the wt, indicating that *SIG2* and *SIG6* are cytokinin-induced genes (Figure 36A, B). Furthermore, this induction was strongly compromised, independently from the application of 6-BA, in the *gnc gnl* seedlings (Figure 36A, B). Nevertheless, the expression of *SIG2* and *SIG6* in the *gnc gnl* seedlings treated with 6-BA was not abolished completely (Figure 36A, B). These results indicate that *SIG2* and *SIG6* are controlled by the GNC and GNL in a cytokinin-dependent manner. However, the fact that the *gnc gnl* seedlings showed a small increase in their expression after 6-BA treatment suggests that there might be other factors, possibly other GATA transcription factors, which contribute to the cytokinin-dependent upregulation of *SIG2* and *SIG6*.

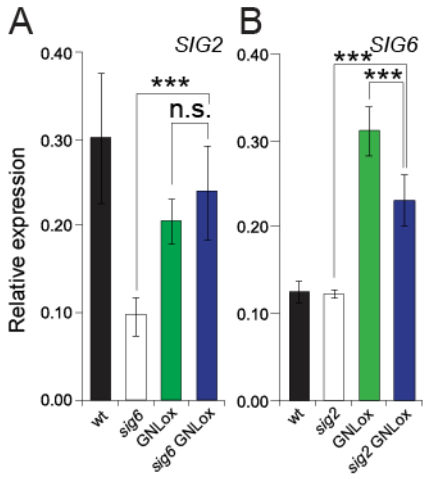

Figure 37: Dynamic transcriptional regulation of *SIG2* and *SIG6* by GNL, in order to promote greening. Relative transcript levels of (**A**) *SIG2* and (**B**) *SIG6* in 10-d-old light-grown seedlings. Data shown are averages and standard errors of three biological replicates with each one four technical replicates. Student's *t*-test: ***P < 0.001; n.s., not significant.

4.5.6 GNL dynamically readjusts the expression of SIG2 and SIG6 in order to promote greening

A partial rescue of the chlorophyll phenotype was observed in *sig2* GNLox and *sig6* GNLox seedlings compared to *sig2* and *sig6* mutants. Therefore, it was assumed that GNL may compensate for the loss of one *SIG* gene through the upregulation of the respective other. To test this hypothesis, a qRT-PCR was performed with using light-grown seedlings to check the expression of *SIG6* in *sig2* GNLox seedlings, and vice versa, the expression of *SIG2* in *sig6* GNLox seedlings. *SIG2* was severely downregulated in *sig6* indicating that SIG6 is able to activate, possibly indirectly, the expression of *SIG2* (Figure 37A). Moreover, the expression of *SIG2* was upregulated in *sig6* GNLox seedlings compared to the *sig6* mutant (Figure 37B). On the other hand, the *sig2* mutant showed similar expression of *SIG6* with wt but *sig2* GNLox seedlings compared to *sig2* showed an increased expression of *SIG6* (Figure 37B). The overall conclusions of these results are that GNL is able to readjust *SIG* expression levels through the upregulation of *SIG2* and *SIG6* genes in the *sig6* and *sig2* mutants, respectively.

4.5.7 SIG2 and SIG6 promote a signal, which suppresses the expression of *GNC* and *GNL*

As part of a hypothetical cross regulation among the SIGs and B-GATAs, it was hypothesized that SIG2 and SIG6 could influence the expression of *GNC* and *GNL*. To this end, the expression of *GNC* and *GNL* was tested in *sig2* and *sig6*

mutants. The expression of *GNL* was not affected in the *sig2* seedlings and only slightly increased in *sig6* (Figure 38A). In turn, the expression of *GNC* was significantly increased in both *sig2* and *sig6* mutants (Figure 38B). It was thus concluded that SIG2 and SIG6 can repress the expression of *GNC*, possibly indirectly, but to a lesser degree also the expression of *GNL*.

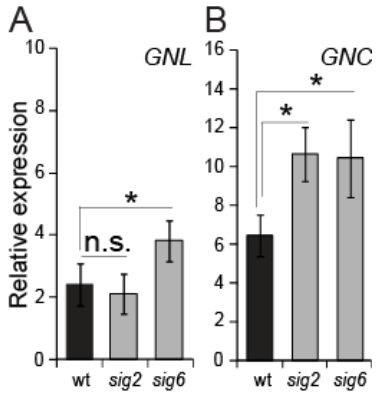

Figure 38: Transcriptional regulation of the B-GATA *GNC* and *GNL* by SIG2 and SIG6. Relative transcript levels of (**A**) *GNL* and (**B**) *GNC* in 10-d-old light-grown seedlings. Data shown are averages and standard errors of two ≥ biological replicates, each one with three technical replicates. Student's *t*-test: *P < 0.01; n.s., not significant.

4.6 Retrograde signaling, the communication between chloroplasts and the nucleus

Close to 90% of the proteins in chloroplasts are encoded in the nucleus, translated in the cytosol and then delivered to the chloroplasts (Woodson & Chory 2008). This implies the existence of communication or signaling between the nucleus and chloroplast. The signaling from the nucleus to the chloroplasts is called anterograde, that from the chloroplasts to the nucleus is retrograde. Chlorophyll biosynthesis takes place in the chloroplast with many necessary proteins delivered from the nucleus. For the coordination of this process many factors have been proposed to play a role (Woodson & Chory 2008). Among them, are some intermediates of the chlorophyll biosynthesis pathway such as Mg-proto-IX (Waters & Langdale 2009). *gun* mutants seem to have disturbed communication between the chloroplasts and the nucleus (Susek et al. 1993). The knowledge about transcription factors, which play a role in the retrograde signaling, is quite restricted.

4.6.1 GNC and GNL can influence the communication between chloroplasts and the nucleus

Carotenoids are essential molecules for photosynthesis. Under normal conditions, blocking carotenoid biosynthesis in the chloroplasts will stop the synthesis of any RNA in the nucleus related to photosynthesis. In the case of defective communication among chloroplasts and the nucleus, the signal from the chloroplasts, which informs the nucleus to stop the transcription of such photosynthesis genes will not be delivered. NF (norflurazon) is a chemical that effectively blocks carotenoid biosynthesis. The fact that GNC and GNL are regulators of the *GUN* genes led to the hypothesis that B-GATAs might also play a role in retrograde signaling. To test this, genetic crosses were performed between the *gnc gnl* double mutant and the single mutants of *gun2*, *gun4* and *gun5*. The triple mutant progenies of these crosses, *gun2 gnc gnl*, *gun4 gnc gnl* and *gun5 gnc gnl*, were subjected to a treatment with NF and the status of chloroplast to nucleus communication was examined by testing the expression of the nuclear encoded *Lhcb* genes. The *gun2*, *gun4* and *gun5* single mutants showed strong upregulation of the *Lhcb2* gene reflecting their previously reported *genomes uncoupled* (*gun*) defect in retrograde signaling. The *gnc gnl* double mutant showed no *gun* phenotype and even displayed reduced levels of *Lhcb2* compared to the wt (Figure 39B). Interestingly, when the expression of *Lhcb2* was followed in the *gun2 gnc gnl*, *gun4 gnc gnl* and *gun5 gnc gnl* triple mutants, all mutant combinations showed a suppression of the *gun* phenotype inviting the conclusion that GNC and GNL are part of the retrograde signaling pathway.

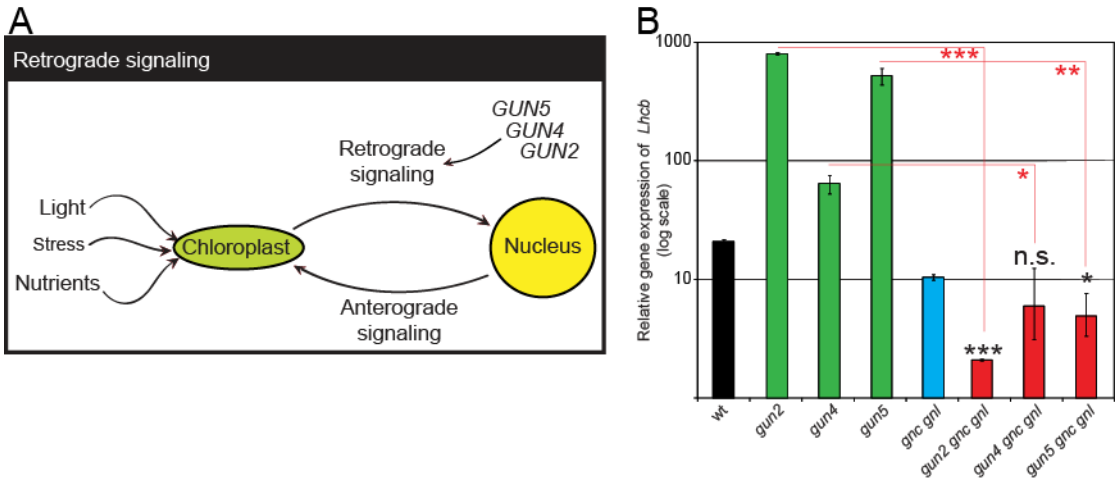

Figure 39: GNC and GNL are positive regulators of retrograde signaling and function downstream or independently of *GUN2*, *GUN4* and *GUN5*. (**A**) Model of the communication between chloroplasts and the nucleus. (**B**) Relative transcript levels of the *Lhcb2* gene in 10-d-old seedlings grown under strong white light and on medium with NF (norflurazon). The data shown are the averages and standard errors of two biological replicates with each one four technical replicates. For each genotype, the relative expression of the NF-treated samples is normalized to the relative expression of the untreated samples. The black asterisks depict statistically significant differences between *gnc gnl* and the crosses with *gun2 gnc gnl*, *gun4 gnc gnl* and *gun5 gnc gnl*. The red asterisks depict statistically significant differences between mutants *gun2*, *gun4* and *gun5* and corresponding genetic combinations. The blue asterisks depict statistically significant differences between GNLox and the other GNLox genotypes. Student's *t*-test: *P < 0.05, **P < 0.01, ***P < 0.001; n.s., not significant.

4.7 B-GATAs GNC and GNL can affect overall photosynthesis

From the results, which were presented in this thesis so far, it is clear that the regulation of chlorophyll biosynthesis by B-GATAs ultimately leads to the increase of chlorophyll levels. Because the main function of chlorophyll is the capture of light energy from the sun, which then can be converted through the photosynthesis to accessible energy for plant, one important question was if the function of GNC and GNL can affect the photosynthesis overall. To answer this question, basic parameters of photosynthesis such as assimilation of CO_2 and the yield of PSII were measured in various GATA genotypes, by Dr. Christian Blume from the lab of Prof. Dr. Christoph Peterhänsel. When the assimilation of CO_2 was quantified in 7-week-old plants, a statistically significant reduction was found in the *gnc gnl* double mutant for 400 ppm as well as for 100 ppm CO_2 compared to wt (Figure 40A). Additionally, the efficiency of PSII was found strongly reduced in

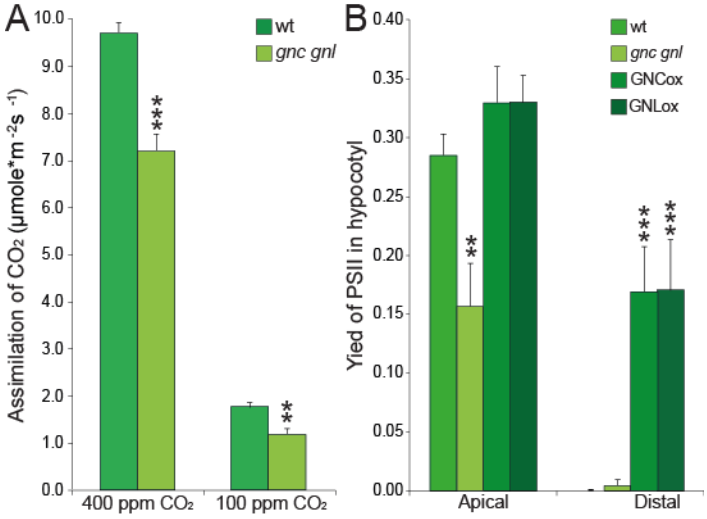

Figure 40: GNC and GNL are positive regulators of photosynthesis. (**A**) Assimilation of CO_2 in 7-week-old plants of wt, *gnc gnl*. The data shown are the averages and standard errors of at least four individuals per genotype. (**B**) Yield of PSII measured in the apical and distal parts of 7-d-old wt, *gnc gnl*, GNCox and GNLox seedlings, grown under long day conditions. The data shown are the averages and standard errors of ten individuals per genotype. Student's *t*-test: **P < 0.01, ***P < 0.001; n.s., not significant.

the *gnc gnl* double mutant compared to wt, but not significantly different in the GNCox and GNLox, for the apical part of the hypocotyl of 7-d-old seedlings (Figure 40B).

In contrast, the efficiency of PSII measured for the distal part of the hypocotyl, was found to be markedly increased in GNCox and GNLox seedlings compared to wt (Figure 40B). From these results it can be concluded that the B-GATAs GNC and GNL can positively affect the overall status of photosynthesis, in mature adult plants but in young seedlings too.

5. Discussion

Greening is regulated and fine-tuned in a complex way. Many pathways are interlinked in order to control greening in plants. The major goal of this study was to elucidate the contribution of the B-GATA transcription factors GNC and GNL in the greening of Arabidopsis. To reach this goal, different approaches were combined such as the analysis of pre-existing microarray data, NGS experiments (ChIP-seq and RNA-seq), genetic, molecular and physiological experiments. The main outcome of this effort was that GNC and GNL are able to promote greening by controlling the transcription of important players with various roles in the regulation of greening. The overall conclusion of this study is that GNC and GNL can regulate greening at least six distinct levels: through regulation of the chlorophyll biosynthesis pathway, the heme/phytochrome pathway, transcription factors with roles in greening like PIFs and GLKs, chloroplast transcription via the regulation of SIG factors and finally through their participation in retrograde signaling.

5.1 The transcriptional regulation of greening before and after the research conducted in this thesis

The landscape of the transcriptional regulation of greening, before and after the work performed for this thesis is depicted in Figure 41. This scheme includes the known transcription factors/regulators and their contribution to the various steps of the chlorophyll biosynthesis pathway as blurred colored circles. Bright blue circles illustrate the contribution, which GNC and GNL discovered to have in greening, from the results of this thesis solely. Moreover, Figure 41 shows the regulatory role, which GNC and GNL have in the regulation known regulators of greening such as the GLKs, PIFs, SIGs. The following discussion, attempts to discuss the most important conclusions for each step in the regulation of greening by the B-GATAs GNC and GNL.

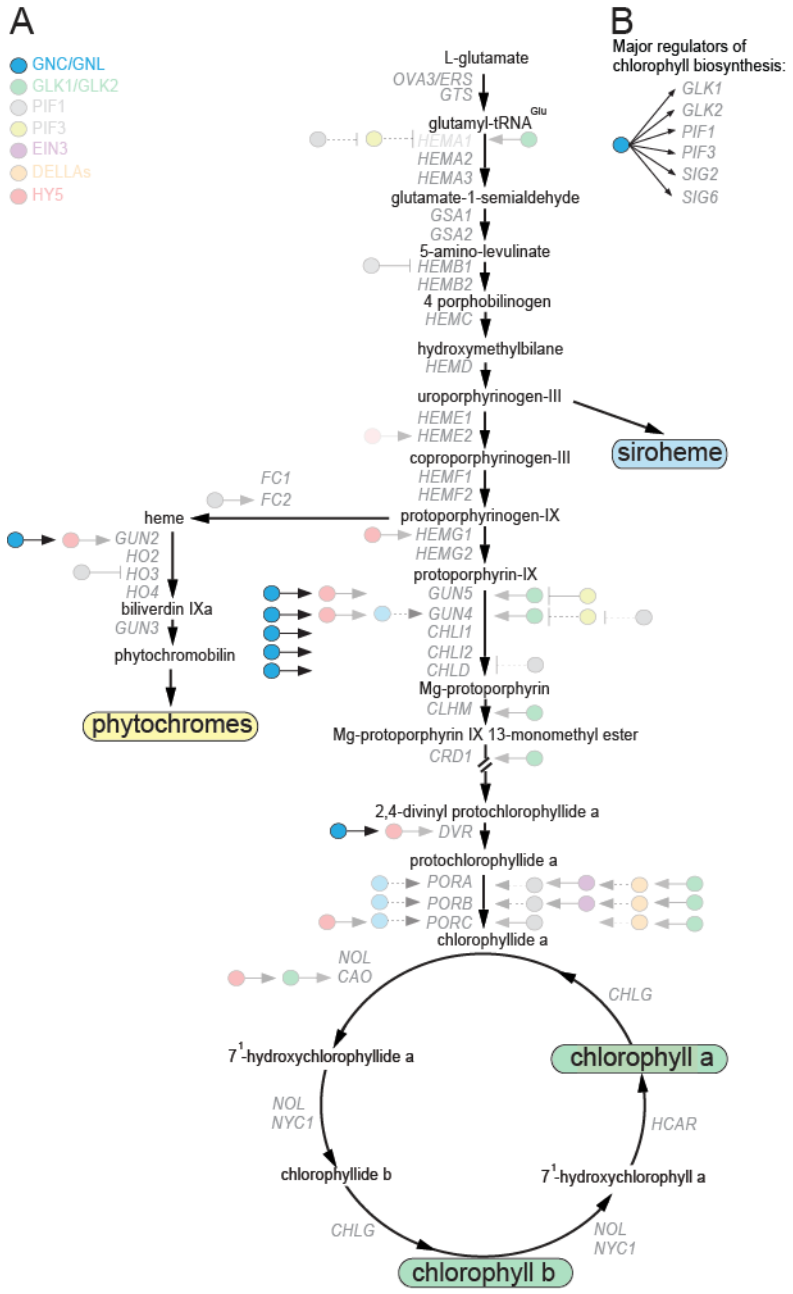

Figure 41: Contribution of B-GATAs GNC and GNL to the transcriptional regulation of greening, before and after, the research conducted in this thesis. (**A**) Schematic representation of the tetrapyrrole pathway with known transcriptional regulators (blurred colored circles) before the research performed for this thesis and with depicting the regulatory role of GNC and GNL contributed solely from the research performed in this thesis (bright blue circles). Horizontal arrow such: (→) indicates induction of gene expression , (⊣) : indicates repression of gene expression and (⇝): indicates presence of additional steps not presented in this figure, horizontal arrows with dashed lines represent transcriptional regulation not supported by chromatin immunoprecipitation. (**B**) Schematic representation of the transcriptional regulation of known greening regulators by the B-GATAs GNC and GNL after the research conducted in this thesis.

5.2 Combinatorial analysis of metabolomics together with ChIP-seq and RNA-seq reveals the major role of GATAs to the transcriptional control of many greening related genes

Despite the obvious implication of GNC and GNL in chlorophyll biosynthesis, there were no metabolic data (metabolomics) available (e.g., HPLCs) in the literature to describe the direct implication of B-GATAs in the synthesis of intermediate metabolites of the chlorophyll pathway. Therefore, the quantification of such intermediate metabolites in the wt and the *gnc gnl* double mutant was performed (Figure 7). As the results from the HPLC analysis show, all the chlorophyll metabolites were found to be significantly reduced in the *gnc gnl* double mutant compared to wt. This underlines the significance of the transcriptional regulation of the genes encoding enzymes in chlorophyll biosynthesis pathway by the B-GATAs.

In an effort to find genes with a prominent role in greening, which could directly be regulated by GNC and GNL, a RNA-seq experiment was performed by Dex-inducible translational fusion variants of GNC and GNL. This experiment was conducted with simultaneous application of Dex and CHX, an inhibitor of protein synthesis in order to minimize any effects, which might have the synthesis of new proteins. The results of the RNA-seq experiment with GNC are in line with the results found in the analyzed microarray data performed with the *GNC* and *GNL* overexpression lines and additionally underlines the direct implication of B-GATAs in the control of the expression of the chlorophyll biosynthesis genes (Appendix Table 9). The genes encoding for enzymes in chlorophyll branch found to be directly upregulated by GNC were: *CAO*, *CHLD*, *CHLG*, *CHLI1*, *CHLI2*, *CHLM*, *CRD1*, *DVR*, *GUN4*, *GUN5*, *NYC1*, *PORB* and *PORC* (Appendix Table 9). Additionally, in the same RNA-seq experiment were found genes, which encode for proteins with known regulatory functions in greening, such as *GLK1*, *GLK2*, *PIF1*, *PIF3*, *SIG2* and *SIG6* (Appendix Table 9). Overall the results from the RNA-seqs in combination with the ChIP-seq and the HPLC, helped to structure the initial hypothesis through which B-GATAs can contribute to the greening of Arabidopsis. The knowledge gained from these omics studies provided, in other words, the base of further molecular, physiological and genetic experiments,

which were performed afterwards in this thesis in order to study in depth the contribution of B-GATAs in greening. The most prominent results of these experiments are addressed later in the discussion.

Since, at least to my knowledge, there were no data available so far for the binding of Arabidopsis B-GATAs factors in genome wide scale, an effort was made to identify target genes of GNL at the genome-wide level through a ChIP-seq experiment. This effort identified some interesting targets regarding genes, which contribute to greening such as *HEME2*, *CHLD*, *CHLM*, *GUN5*, *FC1*, *GLK1* and *PIF3* (Appendix Table 9). However, it had been expected that the number of GNL target genes provided by the ChIP-seq with a role in greening would be much bigger. This, because the number of genes related to greening, which were found to be differentially expressed in the microarray analysis of *35S:GNC:GFP* (GNCox) and *35S:YFP:GNL* (GNLox) impressively covered the majority of genes implicated in the tetrapyrrole and chlorophyll pathway (Appendix Table 9). A possible cause of these unexpected results of the ChIP-seq can be the relative low expression of *GNL* whose expression was driven by a native *GNL* promoter fragment. However, it had been decided to use the native promoter to eliminate any possible off-target effects, which could be obtained if use a strong promoter such as the cauliflower mosaic virus promoter (*CaMV 35S*) had been used. Due to financial limitation, the ChIP-seq experiment could not be repeated, but definitely a repetition ChIP-seq with GNL with a much more elegant system, such as *35S:GNL:YFP:HA:GR gnc gnl* Dex inducible plants (described in this thesis), would potentially shed more light in the direct targets of GNL. Lastly it must not be overlooked an interesting result, which came from the ChIP-seq analysis, which was the binding of the GNL to genes of the B-GATAs *GNC*, *GNL* and *GATA17* (Figure 10). Taken in to account that the overexpressors of *GNC*, *GNL* and *GATA17* show dark green phenotype, and that *gnc gnl gata17 gata17l* quadruple mutant has lower chlorophyll levels than wt, this results may be interpreted as a cross regulation between GATAs, which promote greening in Arabidopsis (Behringer et al. 2014; Ranftl et al. 2016).

5.3 B-GATAs control the transcription of key enzymes in the chlorophyll biosynthesis pathway

Transcription factors such as GLKs, which control the expression of genes in the chlorophyll biosynthesis pathway, seem to do so by upregulating the transcription of genes in various steps of the pathway simultaneously, potentially in a coordinated manner (Figure 5) (Lee et al. 2007; Waters et al. 2009). It seems that B-GATAs follow the same way of regulation as the other greening related transcription factors, more specifically in the transcription of MgCh subunits and *DVR* regarding the chlorophyll branch.

The first step of chlorophyll biosynthesis, the metalation of Proto-IX with the Mg^{2+} ion, is crucial for the synthesis of chlorophyll. This step is catalyzed by the MgCh enzymatic complex, which is formed by three different subunits, GUN5, CHLI, CHLD, and one regulatory protein, GUN4. Previous studies have shown that genes that encode proteins in the MgCh enzyme are light-regulated (Stephenson et al., 2008). *GUN5* had been shown to be repressed by PIF3 and that this repression is mediated by HDA15 (Liu et al. 2013). The research conducted for this thesis shows the implication of B-GATA GNC and GNL in the direct regulation of all genes encoding MgCh subunits. All four genes are upregulated by GNC and GNL, and in most of the cases, this transcriptional regulation is linked with the direct binding of GNL to the promoters of these genes (Figure 41). Additionally, *GUN4* was found to be a direct target of GNL and strongly induced by GNC and GNL as well (Figure 20). This result is in line with a previous study that found GNC and GNL upregulating *GUN4* expression, though it was not able to conclude if the B-GATAs can bind to the promoter of the *GUN4* gene directly (Hudson et al. 2011).

Furthermore, when *GNL* is overexpressed in the mutants of *GUN5* (*gun5* or *cch1*) and *GNC* overexpressed in the mutant of *CHLI1* (*cs*), are able to suppress, at least partially, the greening defects of these mutants (Figure 17 and 19). This is probably either because of the upregulation of the only partially compromised *GUN5* in the *gun5* mutant or due to the more global promoting function of GNL and GNC in other steps of the pathway.

DVR is responsible for converting divinyl protochlorophyllide *a* or divinyl chlorophyllide to monovinyl protochlorophyllide *a* or monovinyl chlorophyllide, a reaction, which occurs downstream of the Mg-protoIX metalation and upstream from the conversion of protochlorophyllide a to chlorophyllide a in the chlorophyll pathway (Figure 41). The *dvr/pcb2* mutant shows severe defects in greening, a fact which underlines the importance of this enzyme in the chlorophyll biosynthesis (Nakanishi et al. 2005). The research in this thesis shows that GNC and GNL are able to regulate the expression of *DVR* and moreover that GNL, in particular, can bind directly to two different positions of the *DVR* promoter (Figure 22). These results, together with the fact that overexpression of *DVR* in the *gnc gnl* double mutant background can suppress the pale green phenotype of *gnc gnl* (Figure 22), reveal the crucial role of *DVR* regulation by the B-GATAs.

5.4 The chlorophyll and the heme pathway are converging on B-GATAs

Prior to this study, the information about the transcriptional regulation of the heme pathway, which leads to the synthesis of the phytochromobilins, the chromophores of the phytochromes, was quite restricted. One known important aspect was the regulation of *GUN2* by the HY5 transcription factor (Figure 5) (Lee et al. 2007). GUN2 encodes for an oxygenase, which catalyzes the second step of the heme pathway, which is the conversion of heme to biliverdin IXa, and has also an implication in the retrograde signaling (Figure 5) (Davis et al. 1999; Susek et al. 1993). The results of this thesis show that B-GATAs are able to control the expression of *GUN2* (Figure 23). It was also shown that GNLox could, at last partially, induce greening in *gun2* GNLox seedlings, mainly in the hypocotyls, thus overriding the defects in phytochrome function due to the *gun2* mutation (Figure 24).

Moreover, the expression of *GNC* and *GNL* was reduced in the *gun2* mutant and when DP, an inhibitor of heme pathway was applied to young seedlings (Figure 25). These lines of evidence are in agreement with the previously noted transcriptional regulation of B-GATAs, and GNL in particular, by phytochromes (Ranftl et al. 2016). Nevertheless, the possibility that heme and/or biliverdin IXa metabolites could influence the expression of B-GATAs independently from the

phytochrome pathway cannot be excluded either. Moreover, it is already mentioned that heme can be exported from chloroplasts and change the expression of genes, which are related to photosynthesis, and encoded by the nuclear genome (Thomas & Weinstein 1990; Woodson et al. 2011). Therefore, it could also be hypothesized that *GNC* and *GNL* are such candidate genes. Nevertheless, the precise mechanism under which this regulation takes place it is not yet known, and it could be a subject of future research.

5.5 B-GATAs function downstream of PIFs regarding greening

This study shows that GNLox can induce greening in *pif1*, *pif3* and *pifq* mutants (Figure 26). This indicates that B-GATAs can function downstream of PIFs. Interestingly, a previous study from our lab had shown that PIFs act also upstream of B-GATAs (Richter et al. 2010).

PIF3 is involved in the suppression of the chlorophyll biosynthesis gene *GUN5* in dark-grown seedlings (Liu et al. 2013). Thus, it has been proposed that PIF3 plays a role in the downregulation of the chlorophyll biosynthesis pathway in the dark, in order to protect seedlings from the effects of photooxidation caused by light exposure. These effects occur as a result of the over accumulation of some chlorophyll intermediates, such as protochlorophyllide (Cheminant et al. 2011). In line with these findings, this study reveals that GNLox etiolated seedlings show 40% more surviving plants compared to wt after two additional days of light exposure (Figure 27). This correlates with the markedly lower levels of protochlorophyllide in GNLox seedlings during their etiolated growth (Figure 27). The way through which this low accumulation of protochlorophyllide can be achieved in GNLox seedlings by the influence of B-GATAs is probably through the upregulation of *POR* genes, which are encoding for enzymes responsible for the catabolism of protochlorophyllide to chlorophyllide (Figure 27). Carotenoids have also been proposed to confer protection against photooxidation to etiolated seedlings (Cheminant et al. 2011). This study additionally shows that B-GATAs are not only able to induce expression of the majority of carotenoid biosynthesis genes but also that most of the carotenoids show a severe reduction in the *gnc gnl* double mutant seedlings (Figure 28). Overall, these results suggest that B-

GATAs are able to control the chlorophyll biosynthesis pathway by acting downstream of PIF in the dark. Moreover, B-GATAs have a protective role against the harmful effects of photooxidation by the upregulation of the *POR* genes and the carotenoid biosynthesis pathway (Figure 28).

5.6 The interplay between B-GATAs and GLK transcription factors promotes greening

Until now, there were no transcription factors discussed in the literature that are able to directly control the expression of *GLK1* and *GLK2* genes, which encode for transcription factors with a pivotal role in greening. This study shows that B-GATA GNL can bind to the promoters of *GLK1* and *GLK2* and that may induce their expression (Figure 29). The absence of additive phenotype regarding greening in the *gnc gnl glk1 glk2* quadruple mutant when compared to *glk1 glk2* indicates that GNC, GNL and GLKs function in the same pathway (Figure 30). Moreover, GNLox seedlings are not able to induce greening in the *glk1 glk2* double mutant background, indicating that GNL operates upstream of or in parallel to GLKs (Figure 30). Further experiments in this study showed that chlorophyll biosynthesis genes such as *HEMA1*, *GUN5*, *GUN4*, *CRD1* and *CAO* are regulated in an additive manner by B-GATAs and GLKs. On the other hand, other genes related to greening such as *CHLI1*, *CHLI2*, *CHLD*, *DVR*, *GUN2*, *SIG2* and *SIG6*, are controlled exclusively by GNC and GNL but not by GLKs (Figure 31).

5.7 The B-GATAs GNC and GNL induce greening by controlling the chloroplast transcription via the upregulation of SIG2 and SIG6 chloroplast proteins

SIGs control the expression of chloroplast genes by their association with the PEP enzyme (Börner et al. 2015). Until now, there was no information about the transcriptional regulation of *SIG* genes. Here, it was hypothesized that *SIG2* and *SIG6* might be targets GNL. This scenario was, indeed, true since GNL is able to associate with the promoters of both *SIGs* and therefore, can induce their expression (Figures 32 and 34). Further genetic experiments revealed that there

is an interplay between B-GATAs and *SIGs* regarding greening, which underlines for the first time the role of SIG2 and SIG6 as mediators of signals related to greening through the B-GATAs (Figures 33 and 36). Moreover, it was also shown that *SIG2* and *SIG6* are upregulated by GNC and GNL in a cytokinin-dependent manner (Figure 37). This study establishes a novel association between the hormone cytokinin and the transcriptional regulation of *SIGs*. Finally, it was also shown that a negative feedback loop might exist through which SIG2 and SIG6 can repress the expression of *GNC* and *GNL* (Figure 38). This negative feedback regulation can be explained as part of a control mechanism through which greening can be potentially fine-tuned.

5.8 B-GATAs are positive regulators of the retrograde signaling

The communication between chloroplasts and the nucleus (retrograde signaling), which can eventually lead to the regulation of some nuclear encoded genes, is important for the proper development of plants. So far very few transcription factors have been suggested to participate in retrograde signaling. The co-ordination of the genome of the chloroplast and the nucleus play an important role in the chlorophyll biosynthesis and photosynthesis. Therefore, after the discovery of the relationship between *GUN2*, *GUN4* and *GUN5* genes with GNC and GNL it was hypothesized that this link can potentially affect retrograde signaling, since all of the *GUN* genes, studied in this thesis, have a role in the retrograde signaling (Sussek et al. 2003). Genetic analysis of *GUN* mutants in the *gnc gnl* double mutant revealed the role of GNC and GNL as positive regulators of retrograde signaling, a fact, which so far was completely unknown (Figure 39). The direct implication of B-GATAs in retrograde signaling open a whole new level in the regulatory roles, of B-GATAs, which can be extended far beyond the chlorophyll biosynthesis, since this communication could mediate signals related to stress, hormones synthesis etc. Further experiments will be needed to fully explain the specific role(s) that these two B-GATAs potentially have in retrograde signaling.

5.9 Model of the proposed contribution of B-GATAs in greening of Arabidopsis

The major question and the core of the research conducted in this thesis was how the B-GATA GNC and GNL can promote greening in Arabidopsis. It can be concluded that GNC and GNL are able to control greening not only in a just linear way, such as by regulate genes related to chlorophyll biosynthesis pathway. Instead, they do so by being able to coordinate, synchronize and promote the expression of genes, which can induce greening in many different ways (Figure 42). Such complex regulation of greening is in line with the importance of chlorophyll production for the survival of the plants that do not solely rely on the upregulation of a single pathway. Moreover, the results, which are presented in this thesis, could shape a model that can be used, either partially or as a whole, to expand our knowledge in regulation of the chlorophyll biosynthesis also in other photosynthetic organisms. This can be a subject of future research, and could shed more light on the evolutionary conservation of the regulation of the chlorophyll biosynthesis mechanism.

Different colored letters represent proteins with an implication in different pathways which contribute to greening in Arabidopsis. The light-blue letters refer to the transcription factors with a positive role in greening. The purple letters refer to proteins, which regulate transcription in the chloroplast. The green letters refer to enzymes, which catalyze steps in the chlorophyll biosynthesis pathway. The red letters refer to GUN2, an enzyme which play a role in the heme/phytochromes pathway. The brown letters refer to PIF transcription factors, which play a role in greening. (→): indicates induction of gene expression and (⊣) : indicates repression of gene expression.

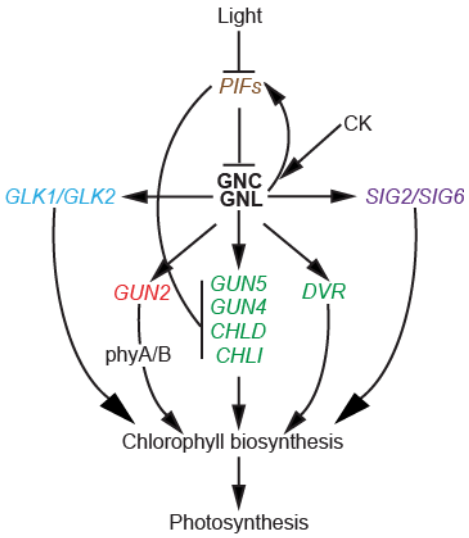

Figure 42: Proposed model of the mechanism through which GNC and GNL contribute to greening in Arabidopsis.

6. Literature

Adhikari, N.D. et al., 2011. GUN4-porphyrin complexes bind the ChlH/GUN5 subunit of Mg-Chelatase and promote chlorophyll biosynthesis in Arabidopsis. *The Plant cell*, 23(4), pp.1449–1467.

Adhikari, N.D. et al., 2009. Prophyrins promote the association of GENOMES UNCOUPLED 4 and a Mg-chelatase subunit with chloroplast membranes. *Journal of Biological Chemistry*, 284(37), pp.24783–24796.

Al-Sady, B. et al., 2006. Photoactivated Phytochrome Induces Rapid PIF3 Phosphorylation Prior to Proteasome-Mediated Degradation. *Molecular Cell*, 23(3), pp.439–446.

Allison, L. a, 2000. The role of sigma factors in plastid transcription. *Biochimie*, 82(6–7), pp.537–548.

An, Y. et al., 2014. Poplar GATA transcription factor PdGNC is capable of regulating chloroplast ultrastructure, photosynthesis, and vegetative growth in Arabidopsis under varying nitrogen levels. *Plant Cell, Tissue and Organ Culture (PCTOC)*, 119(2), pp.313–327.

Bailey, P.C. et al., 2003. Update on the basic helix-loop-helix transcription factor gene family in Arabidopsis thaliana. *The Plant Cell*, 15(11), pp.2497–502.

Behringer, C. et al., 2014. Functional diversification within the family of B-GATA transcription factors through the LLM-domain. *Plant Physiology*, 166(September), pp.293–305.

Behringer, C. & Schwechheimer, C., 2015. B-GATA transcription factors â€“ insights into their structure, regulation, and role in plant development. *Frontiers in Plant Science*, 6(February), pp.1–12.

Bensmihen, S. et al., 2004. Analysis of an activated ABI5 allele using a new selection method for transgenic Arabidopsis seeds. *FEBS Letters*, 561(1–3), pp.127–131.

Berry, J.O. et al., 2013. Photosynthetic gene expression in higher plants. *Photosynthesis Research*, 117(1–3), pp.91–120.

Bi, Y.M. et al., 2005. Genetic analysis of Arabidopsis GATA transcription factor gene family reveals a nitrate-inducible member important for chlorophyll synthesis and glucose sensitivity. *Plant Journal*, 44(4), pp.680–692.

Börner, T. et al., 2015. Chloroplast RNA polymerases: Role in chloroplast biogenesis. *Biochimica et Biophysica Acta*, 1847(9), pp.761–769.

Cheminant, S. et al., 2011. DELLAs regulate chlorophyll and carotenoid biosynthesis to prevent photooxidative damage during seedling deetiolation in Arabidopsis. *The Plant Cell*, 23(5), pp.1849–1860.

Cheng, Y.-C. & Fleming, G.R., 2009. Dynamics of Light Harvesting in Photosynthesis. *Annual Review of Physical Chemistry*, 60(1), pp.241–262.

Claeys, M. et al., 2012. Motifsuite: Workflow for probabilistic motif detection and assessment. *Bioinformatics*, 28(14), pp.1931–1932.

Davis, S.J., Kurepa, J. & Vierstra, R.D., 1999. The Arabidopsis thaliana HY1 locus, required for phytochrome-chromophore biosynthesis, encodes a protein related to heme oxygenases. *Proceedings of the National Academy of Sciences of the United States of America*, 96(11), pp.6541–6546.

Davison, P. a. et al., 2005. Structural and biochemical characterization of Gun4 suggests a mechanism for its role in chlorophyll biosynthesis. *Biochemistry*, 44(21), pp.7603–7612.

Earley, K.W. et al., 2006. Gateway-compatible vectors for plant functional genomics and proteomics. *Plant Journal*, 45(4), pp.616–629.

Evans, T., Reitman, M. & Felsenfeld, G., 1988. An erythrocyte-specific DNA-binding factor recognizes a regulatory sequence common to all chicken globin genes. *Proceedings of the National Academy of Sciences of the United States of America*, 85(16), pp.5976–5980.

Fitter, D.W. et al., 2002. GLK gene pairs regulate chloroplast development in diverse plant species. *Plant Journal*, 31(6), pp.713–727.

Frick, G. et al., 2003. An Arabidopsis porB porC double mutant lacking light-dependent NADPH:protochlorophyllide oxidoreductases B and C is highly chlorophyll-deficient and developmentally arrested. *Plant Journal*, 35(2), pp.141–153.

Fujiwara, M. et al., 2000. Three new nuclear genes, sigD, sigE and sigF, encoding putative plastid RNA polymerase factors in Arabidopsis thaliana. *FEBS Letters*, 481(1), pp.47–52.

Hall, L.N. et al., 1998. GOLDEN 2: a novel transcriptional regulator of cellular differentiation in the maize leaf. *The Plant Cell*, 10(6), pp.925–36.

Hirashima, M. et al., 2006. Pigment shuffling in antenna systems achieved by expressing prokaryotic chlorophyllide a oxygenase in Arabidopsis. *Journal of Biological Chemistry*, 281(22), pp.15385–15393.

Huang, Y.-S. & Li, H.-M., 2009. Arabidopsis CHLI2 can substitute for CHLI1. *Plant Physiology*, 150(2), pp.636–645.

Hudson, D. et al., 2011. GNC and CGA1 modulate chlorophyll biosynthesis and glutamate synthase (GLU1/FD-GOGAT) expression in Arabidopsis. *PLoS ONE*, 6(11).

Hudson, D. et al., 2013. Rice cytokinin GATA transcription Factor1 regulates chloroplast development and plant architecture. *Plant Physiology*, 162(1), pp.132–44.

Huq, E. et al., 2004. Phytochrome-interacting factor 1 is a critical bHLH regulator of chlorophyll biosynthesis. *Science (New York, N.Y.)*, 305(5692), pp.1937–1941.

Huq, E., Al-Sady, B. & Quail, P.H., 2003. Nuclear translocation of the photoreceptor phytochrome B is necessary for its biological function in seedling photomorphogenesis. *Plant Journal*, 35(5), pp.660–664.

Ishizaki, Y. et al., 2005. A nuclear-encoded sigma factor, Arabidopsis SIG6, recognizes sigma-70 type chloroplast promoters and regulates early chloroplast development in cotyledons. *Plant Journal*, 42(2), pp.133–144.

Jagendorf, A. & Uribe, E., 1966. ATP formation caused by acid-base transition of spinach chloroplasts. *Proceedings of the National Academy of Sciences of the United States of America*, 55, pp.170–177.

Kanamaru, K. & Tanaka, K., 2004. Roles of Chloroplast RNA Polymerase Sigma Factors in Chloroplast Development and Stress Response in Higher Plants. *Bioscience, Biotechnology, and Biochemistry*, 68(11), pp.2215–2223.

Kaufmann, K. et al., 2010. Chromatin immunoprecipitation (ChIP) of plant transcription factors followed by sequencing (ChIP-SEQ) or hybridization to whole genome arrays (ChIP-CHIP). *Nature Protocols*, 5(3), pp.457–472.

Kiba, T. et al., 2005. Combinatorial microarray analysis revealing Arabidopsis genes implicated in cytokinin responses through the His → Asp phosphorelay circuitry. *Plant and Cell Physiology*, 46(2), pp.339–355.

Klermund, C. et al., 2016. LLM-Domain B-GATA Transcription Factors Promote Stomatal Development Downstream of Light Signaling Pathways in Arabidopsis thaliana Hypocotyls. *The Plant Cell*, 28(3), pp.646–660.

Kobayashi, K. et al., 2008. Functional analysis of *Arabidopsis thaliana* isoforms of the Mg-chelatase CHLI subunit. *Photochemical & photobiological sciences : Official journal of the European Photochemistry Association and the European Society for Photobiology*, 7(10), pp.1188–1195.

Kobayashi, K. et al., 2012. Regulation of Root Greening by Light and Auxin/Cytokinin Signaling in Arabidopsis. *The Plant Cell*, 24(3), pp.1081–1095.

Kobayashi, K. & Masuda, T., 2016. Transcriptional Regulation of Tetrapyrrole Biosynthesis in Arabidopsis thaliana. *Frontiers in Plant Science*, 7(December), pp.1–17.

Kohchi, T. et al., 2001. The Arabidopsis HY2 gene encodes phytochromobilin synthase, a ferredoxin-dependent biliverdin reductase. *The Plant Cell*, 13(2), pp.425–436.

Krishna, S.S., Majumdar, I. & Grishin, N. V., 2003. Structural classification of zinc fingers. *Nucleic Acids Research*, 31(2), pp.532–550.

Larkin, R.M. et al., 2003. GUN4, a regulator of chlorophyll synthesis and intracellular signaling. *Science (New York, N.Y.)*, 299(5608), pp.902–906.

Lee, J. et al., 2007. Analysis of transcription factor HY5 genomic binding sites revealed its hierarchical role in light regulation of development. *The Plant Cell*, 19(3), pp.731–49.

Leivar, P. & Quail, P.H., 2011. PIFs: Pivotal components in a cellular signaling hub. *Trends in Plant Science*, 16(1), pp.19–28.

Li, R. et al., 2008. SOAP: Short oligonucleotide alignment program. *Bioinformatics*, 24(5), pp.713–714.

Liu, X. et al., 2013. PHYTOCHROME INTERACTING FACTOR3 associates with the histone deacetylase HDA15 in repression of chlorophyll biosynthesis and photosynthesis in etiolated Arabidopsis seedlings. *The Plant Cell*, 25(4), pp.1258–73.

Loschelder, H. et al., 2006. Dual temporal role of plastid sigma factor 6 in Arabidopsis development. *Plant Physiology*, 142(2), pp.642–650.

Lowry, J. a & Atchley, W.R., 2000. Molecular evolution of the GATA family of transcription factors: conservation within the DNA-binding domain. *Journal of Molecular Evolution*, 50(2), pp.103–115.

Lysenko, E. a., 2007. Plant sigma factors and their role in plastid transcription. *Plant Cell Reports*, 26(7), pp.845–859.

Mara, C.D. & Irish, V.F., 2008. Two GATA transcription factors are downstream effectors of floral homeotic gene action in Arabidopsis. *Plant Physiology*, 147,

pp.707–718.

Mochizuki, N., Brusslan, J. a, Larkin, R., Nagatani, a, et al., 2001. Arabidopsis genomes uncoupled 5 (GUN5) mutant reveals the involvement of Mg-chelatase H subunit in plastid-to-nucleus signal transduction. *Proceedings of the National Academy of Sciences of the United States of America*, 98(4), pp.2053–2058.

Mochizuki, N., Brusslan, J. a, Larkin, R., Nagatani, A., et al., 2001. Arabidopsis genomes uncoupled 5 (GUN5) mutant reveals the involvement of Mg-chelatase H subunit in plastid-to-nucleus signal transduction. *Proceedings of the National Academy of Sciences of the United States of America*, 98(4), pp.2053–2058.

Monte, E. et al., 2004. The phytochrome-interacting transcription factor, PIF3, acts early, selectively, and positively in light-induced chloroplast development. *Proceedings of the National Academy of Sciences of the United States of America*, 101(46), pp.16091–16098.

Moon, J. et al., 2008. PIF1 directly and indirectly regulates chlorophyll biosynthesis to optimize the greening process in Arabidopsis. *Proceedings of the National Academy of Sciences of the United States of America*, 105(27), pp.9433–9438.

Moran, R., 1982. Formulae for determination of chlorophyllous pigments extracted with n,n-dimethylformamide. *Plant Physiology*, 69(6), pp.1376–1381.

Muiño, J.M. et al., 2011. ChIP-seq Analysis in R (CSAR): An R package for the statistical detection of protein-bound genomic regions. *Plant Methods*, 7(1), p.11.

Nagata, N. et al., 2005. Identification of a vinyl reductase gene for chlorophyll synthesis in Arabidopsis thaliana and implications for the evolution of Prochlorococcus species. *The Plant Cell*, 17(1), pp.233–240.

Naito, T. et al., 2007. Characterization of a unique GATA family gene that

responds to both light and cytokinin in Arabidopsis thaliana. *Bioscience, Biotechnology, and Biochemistry*, 71(6), pp.1557–1560.

Nakanishi, H. et al., 2005. Characterization of the Arabidopsis thaliana mutant pcb2 which accumulates divinyl chlorophylls. *Plant and Cell Physiology*, 46(3), pp.467–473.

Nelson, N. & Yocum, C.F., 2006. Structure and Function of Photosystems I and Ii. *Annual Review of Plant Biology*, 57(1), pp.521–565.

Omichinski, J.G. et al., 1993. NMR structure of a specific DNA complex of Zn-containing DNA binding domain of GATA-1. *Science (New York, N.Y.)*, 261(5120), pp.438–446.

Parks, B.M. & Quail, P.H., 1991. Mutants of Arabidopsis Are Defective in Phytochrome Chromophore Biosynt hesis. *Plant Cell*, 3(November), pp.1177–86.

Powell, Ann l. t. et al., 2012. Uniform ripening Encodes a Golden. *Science*, 336(June), pp.1711–1715.

Ranftl, Q.L. et al., 2016. LLM-Domain Containing B-GATA Factors Control Different Aspects of Cytokinin-Regulated Development in Arabidopsis thaliana 1. 170(April), pp.2295–2311.

Reyes, J.C., Muro-Pastor, M.I. & Florencio, F.J., 2004. The GATA family of transcription factors in Arabidopsis and rice. *Plant Physiology*, 134(4), pp.1718–1732.

Richter, R. et al., 2010. The GATA-type transcription factors GNC and GNL/CGA1 repress gibberellin signaling downstream from DELLA proteins and phytochrome-interacting factors. *Genes and Development*, 24(18), pp.2093–2104.

Rossini, L. et al., 2001. The maize golden2 gene defines a novel class of transcriptional regulators in plants. *The Plant cell*, 13(5), pp.1231–44.

Ruiz-Sola, M.Á. & Rodríguez-Concepción, M., 2012. Carotenoid biosynthesis in Arabidopsis: a colorful pathway. *Arabidopsis Book*, 10, p.e0158.

Susek, R.E., Ausubel, F.M. & Chory, J., 1993. Signal transduction mutants of Arabidopsis uncouple nuclear CAB and RBCS gene expression from chloroplast development. *Cell*, 74(5), pp.787–799.

Tanaka, R. & Tanaka, A., 2007. Tetrapyrrole biosynthesis in higher plants. *Annual Review of Plant Biology*, 58, pp.321–346.

Thijs, G. et al., 2002. A Gibbs sampling method to detect overrepresented motifs in the upstream regions of coexpressed genes. *Journal of computational biology : A Journal of Computational Molecular Cell Biology*, 9(2), pp.447–464.

Thijs, G. et al., 2001. A higher-order background model improves the detection of promoter regulatory elements by Gibbs sampling. *Bioinformatics (Oxford, England)*, 17(12), pp.1113–1122.

Tsuzuki, T. et al., 2011. Mg-chelatase H subunit affects ABA signaling in stomatal guard cells, but is not an ABA receptor in Arabidopsis thaliana. *Journal of Plant Research*, 124(4), pp.527–538.

Waters, M.T. et al., 2009. GLK transcription factors coordinate expression of the photosynthetic apparatus in Arabidopsis. *The Plant Cell*, 21(4), pp.1109–1128.

Waters, M.T. & Langdale, J. a, 2009. The making of a chloroplast. *The EMBO journal*, 28(19), pp.2861–2873.

Waters, M.T., Moylan, E.C. & Langdale, J. a., 2008. GLK transcription factors regulate chloroplast development in a cell-autonomous manner. *Plant Journal*, 56(3), pp.432–444.

Welsch, R. et al., 2000. Regulation and activation of phytoene synthase, a key enzyme in carotenoid biosynthesis, during photomorphogenesis. *Planta*, 211(6), pp.846–54.

Woodson, J.D. & Chory, J., 2008. Coordination of gene expression between organellar and nuclear genomes. *Nature reviews. Genetics*, 9(5), pp.383–395.

Woodson, J.D., Perez-Ruiz, J.M. & Chory, J., 2011. Heme synthesis by plastid ferrochelatase i regulates nuclear gene expression in plants. *Current Biology*, 21(10), pp.897–903.

Appendix

Table 9: List of genes related to tetrapyrrole pathway, regulators of chlorophyll biosynthesis, chloroplast division, photosynthesis, import-export chloroplast machinery and carotenoids biosynthesis, presented in microarrays, RNA-seqs and ChIP-seq.

			Microarray (Fold Change)		RNA-seq (Fold Change/F.C.)		ChIP-seq: *pGNL:GNL:HA gnc gnl* (Peak Score)						
	Locus	Gene Name	*35:GNC:GFP*	*35:YFP:GNL*	*35S:GNC:YFP:HA:GR gnc gnl* (F. c. threshold 2.45)	*35S:GWL:YFP:HA:GR gnc gnl* (F. c. threshold 1.2)	Max Score	Upstream 3 kb	Upstream 2 kb	Upstream 1 kb	Intragenic	Downstream 1 kb
Tetrapyrrole pathway	Upstream of chlorophyll branch	AT1G69740	*HEMB1/ALAD1*	-	-	-	-	-	-	-	-	-	-
		AT1G44318	*HEMB2ALAD2*	-	-	-	-	-	-	-	-	-	-
		AT5G63570	*GSA1*	1.51	2.15	-	-	-	-	-	-	-	-
		AT3G48730	*GSA2*	1.67	2.38	2.45	-	-	-	-	-	-	-
		AT5G26710	*GTS*	1.22	1.36	-	-	-	-	-	-	-	-
		AT1G58290	*HEMA1*	-2.04	-1.60	3.20	-	-	-	-	-	-	-
		AT1G09940	*HEMA2*	-1.20	-1.30	-3.30	-	-	-	-	-	-	-
		AT2G31250	*HEMA3*	2.48	2.43	-	-	-	-	-	-	-	-
		AT5G08280	*HEMEC*	1.49	2.08	-	-	-	-	-	-	-	-
		AT2G26540	*HEMED*	1.47	1.73	-	-	-	-	-	-	-	-
		AT1G03475	*HEMF1/LIN2*	1.44	1.91	-	-	-	-	-	-	-	-
		AT4G03205	*HEMF2/CPO2*	-	-	-	-	-	-	-	-	-	-
		AT4G01690	*HEMG1/PPO1*	1.27	1.55	-	-	-	-	-	-	-	-
		AT5G14220	*HEMG2/PPO2*	1.21	1.58	-	-	-	-	-	-	-	-
		AT5G64050	*OVA3/ERS*	1.48	2.17	-	-	-	-	-	-	-	-
		AT3G14930	*HEME1*	-	1.83	-	-	-	-	-	-	-	-
		AT2G40490	*HEME2*	1.38	1.73	-3.30	-	-	-	-	-	-	-
	Chlorophyll biosynthesis branch	AT1G44446	*CAO*	-	-	3.50	-	-	-	-	-	-	-
		AT1G08520	*CHLD*	-	-	2.50	11.06	3.13	-	-	11.06	2.07	-
		AT3G51820	*CHLG*	1.58	1.88	-	-	-	-	-	-	-	-
		AT4G18480	*CHLI1*	1.41	1.82	3.40	-	-	-	-	-	-	-
		AT5G45930	*CHLI2*	1.36	1.69	4.70	-	-	-	-	-	-	-
		AT4G25080	*CHLM*	-	-	4.70	7.04	5.22	2.94	2.03	7.04	1.12	-
		AT3G56940	*CRD1/CHL27*	-	-	5.50	-	-	-	-	-	-	-
		AT5G18660	*DVR/PCB2*	1.39	2.11	4.90	-	-	-	-	-	-	-
		AT1G04620	*HCAR*	2.28	2.13	2.47	-	-	-	-	-	-	-
		AT3G59400	*GUN4*	-	-	3.70	-	-	-	-	-	-	-
		AT5G13630	*GUN5/CHLH*	-	-	2.50	9.03	2.62	4.59	-	9.03	-	-
		AT5G04900	*NOL*	1.44	1.70	-	-	-	-	-	-	-	-
		AT4G13250	*NYC1*	-1.29	-	3.30	-	-	-	-	-	-	-
		AT5G54190	*PORA*	-	-	-	-	-	-	-	-	-	-
		AT4G27440	*PORB*	1.43	1.71	4.70	-	-	-	-	-	-	-
		AT1G03630	*PORC*	1.53	1.88	4.70	-	-	-	-	-	-	-
	Heme branch (Phytochromobilin synthesis)	AT5G26030	*FC1*	-	-	-	7.04	-	-	1.12	7.04	-	-
		AT2G30390	*FC2*	-	-	3.80	-	-	-	-	-	-	-
		AT2G26670	*GUN2/HO1*	1.36	1.48	2.80	-	-	-	-	-	-	-
		AT2G26550	*HO2*	1.58	1.91	-	-	-	-	-	-	-	-
		AT1G69720	*HO3*	-	-	-	-	-	-	-	-	-	-
		AT1G58300	*HO4*	-	-4.00	-	-	-	-	-	-	-	-
		AT3G09150	*GUN3/HY2*	1.97	2.32	-	-	-	-	-	-	-	-
	Regulators of Chlorophyll biosynthesis	AT3G14110	*FLU*	1.42	1.92	-	-	-	-	-	-	-	-
		AT2G20570	*GLK1*	-	-	-	7.94	5.22	1.58	1.12	7.94	-	-
		AT5G44190	*GLK2*	-	-	5.80	-	-	-	-	-	-	-
		AT2G20180	*PIF1*	-	-	4.20	-	-	-	-	-	-	-
		AT1G09530	*PIF3*	-1.55	-1.94	2.50	9.76	1.12	2.49	-	1.12	9.76	-
		AT1G08540	*SIG2*	1.54	1.74	3.10	-	-	-	-	-	-	-
		AT2G36990	*SIG6*	1.65	1.90	4.40	-	-	-	-	-	-	-
	Chloroplast division	AT5G24020	*MIND*	1.47	2.01	-	-	-	-	-	-	-	-
		AT1G75010	*ARC3*	1.85	2.29	-	-	-	-	-	-	-	-
		AT1G20830	*MCD1*	1.34	1.51	-	-	-	-	-	-	-	-
		AT5G53280	*PDV1*	-	1.54	3.90	-	-	-	-	-	-	-
		AT2G16070	*PDV2*	1.35	1.62	-2.47	-	-	-	-	-	-	-
		AT5G42480	*ARC6*	1.68	2.01	-	8.00	8.00	-	-	3.60	-	-
		AT3G19720	*ARC5*	1.17	1.24	4.87	-	-	-	-	-	-	-

Table 9: continue

			Microarray (Fold Change)		RNA-seq (Fold Change)		ChIP-seq: *pGNL:GNL:HA gnc gnl* (Peak Score)					
		Locus	Gene Name	*35:GNC:GFP*	*35:YFP:GNL*	*35S:GNC:YFP:HA:GR gnc gnl* (F. C. threshold 2.45)	*35S:GNL:YFP:HA:GR gnc gnl* (F. C. threshold 1.2)	Max Score	Upstream 3 kb	Upstream 2 kb	Upstream 1 kb	Intragenic	Downstream 1 kb
Photosynthesis	Cc (Calvin cycle)	AT1G67090	*RBCS*	-	-	4.32	1.20	-	-	-	-	-	-
		AT1G43670	*FBP*	-	-	3.22	-	-	-	-	-	-	-
		AT3G55440	*TPI*	-1.08	-1.11	-2.99	-	8.03	2.22	1.86	8.03	3.33	2.22
		AT1G79550	*PGK*	-	-	-	-	-	-	-	-	-	-
		AT1G16300	*GAPDH*	-	-	-	-	-	-	-	-	-	-
		AT1G14030	*FBA*	1.91	2.46	3.25	-	7.89	1.01	1.01	7.89	0.00	0.00
		AT3G63180	*TKL*	-	-	-	-	-	-	-	-	-	-
		AT5G61410	*RPE*	-	-	-	-	-	-	-	-	-	-
		AT1G32060	*PRK*	-	1.41	6.57	-	7.36	4.06	0.00	7.36	3.33	1.86
		AT3G55800	*SBP*	-	-	4.76	-	-	-	-	-	-	-
	PSII	AT5G66570	*PSBO1*	-	1.19	5.41	-	8.05	7.06	1.63	0.00	8.05	1.63
		AT3G50820	*PSBO2*	-	-	10.07	-	-	-	-	-	-	-
		AT1G06680	*PSBP-1*	-	-	6.74	-	7.06	0.00	2.12	2.12	7.06	1.63
		AT2G30790	*PSBP-2*	-1.57	-1.79	-	-	-	-	-	-	-	-
		AT4G21280	*PSBQ-1*	-	1.30	4.86	-	-	-	-	-	-	-
		AT4G05180	*PSBQ-2*	-1.25	-	6.00	-	-	-	-	-	-	-
		AT1G79040	*PSBR*	-	-	5.50	-	-	-	-	-	-	-
		AT1G44575	*PSBS*	-	1.22	3.26	-	-	-	-	-	-	-
		AT3G21055	*PSBTN*	-	1.25	7.43	-	-	-	-	-	-	-
		AT2G30570	*PSBW*	-	-	6.93	-	-	-	-	-	-	-
		AT2G06520	*PSBX*	-	-	8.73	-	-	-	-	-	-	-
		AT1G67740	*PSBY*	-	1.19	5.02	-	-	-	-	-	-	-
	PSI	AT4G02770	*PSAD-1*	-	-	5.04	-	7.55	1.63	0.00	3.11	7.55	2.12
		AT1G03130	*PSAD-2*	-	-	4.48	-	12.04	2.49	0.00	0.00	12.04	2.94
		AT4G28750	*PSAE-1*	-	-	8.30	-	7.73	3.69	1.49	1.49	7.73	2.96
		AT2G20260	*PSAE-2*	-	-	4.87	-	-	-	-	-	-	-
		AT1G31330	*PSAF*	-	-	5.48	-	-	-	-	-	-	-
		AT1G55670	*PSAG*	-	-	5.34	-	8.40	8.40	1.12	0.00	0.00	6.13
		AT3G16140	*PSAH-1*	-	-	3.77	-	7.06	4.10	1.14	1.70	7.06	2.12
		AT1G52230	*PSAH-2*	-	1.23	6.01	-	-	-	-	-	-	-
		AT1G30380	*PSAK*	-	-	6.76	-	-	-	-	-	-	-
		AT4G12800	*PSAL*	-	-	3.92	-	-	-	-	-	-	-
		AT5G64040	*PSAN*	-1.41	-	8.47	-	-	-	-	-	-	-
		AT1G08380	*PSAO*	-	-	6.37	-	-	-	-	-	-	-
	LHC	AT3G54890	*LHCA1*	-	-	6.33	-	-	-	-	-	-	-
		AT3G61470	*LHCA2*	-1.29	-1.16	6.41	-	-	-	-	-	-	-
		AT1G61520	*LHCA3*	-	-	4.47	-	-	-	-	-	-	-
		AT3G47470	*LHCA4*	-1.34	-	5.48	-	8.54	0.00	2.12	0.00	8.54	0.00
		AT1G45474	*LHCA5*	-	-	4.36	-	-	-	-	-	-	-
		AT1G19150	*LHCA6*	-	-	6.58	-	-	-	-	-	-	-
		AT1G29920	*LHCB1.1*	-	-	-	-	-	-	-	-	-	-
		AT1G29910	*LHCB1.2*	-	1.14	8.99	-	-	-	-	-	-	-
		AT1G29930	*LHCB1.3*	-	-	8.61	-	-	-	-	-	-	-
		AT2G34430	*LHCB1.4*	-	-	18.70	-	-	-	-	-	-	-
		AT2G34420	*LHCB1.5*	-	-	9.61	-	-	-	-	-	-	-
		AT2G05100	*LHCB2.1*	-	-	5.18	-	-	-	-	-	-	-
		AT2G05070	*LHCB2.2*	-	-	8.57	-	-	-	-	-	-	-
		AT3G27690	*LHCB2.3*	-2.08	-2.48	13.63	-	-	-	-	-	-	-
		AT5G54270	*LHCB3*	-1.21	-	9.21	-	7.00	1.12	0.00	7.00	3.33	0.00
		AT5G01530	*LHCB4.1*	-	-148.77	3.83	-	8.54	6.57	0.00	1.14	8.54	0.00
		AT3G08940	*LHCB4.2*	-1.25	-1.26	7.11	-	7.55	2.62	1.14	6.07	7.55	3.11
		AT2G40100	*LHCB4.3*	-	-	-	-	-	-	-	-	-	-
		AT4G10340	*LHCB5*	-	-	7.38	-	-	-	-	-	-	-
		AT1G15820	*LHCB6*	-	-	4.98	-	-	-	-	-	-	-

Table 9: continue

			Microarray (Fold Change)		RNA-seq (Fold Change)		ChIP-seq: *pGNL:GNL:HA gnc gnl* (Peak Score)						
		Locus	Gene Name	*35:GNC:GFP*	*35:YFP:GNL*	*35S:GNC:YFP:HA:GR gnc gnl* (F. C. threshold 2.45)	*35S:GNL:YFP:HA:GR gnc gnl* (F. C. threshold 1.2)	Max Score	Upstream 3 kb	Upstream 2 kb	Upstream 1 kb	Intragenic	Downstream 1 kb
Import-export chloroplast machinery	TIC- apparatus	AT1G06950	*Tic110*	2.05	-	-	-	-	-	-	-	-	-
		AT2G24820	*Tic55-II*	1.50	1.66	4.19	-	8.05	1.63	2.12	8.05	4.10	2.62
		AT5G16620	*Tic40*	1.84	2.33	-	-	-	-	-	-	-	-
		AT2G15290	*Tic21*	1.46	1.92	-	-	-	-	-	-	-	-
		AT3G23710	*Tic22*	1.30	1.65	-	-	-	-	-	-	-	-
		AT1G04940	*Tic20-I*	1.94	2.37	11.20	-	-	-	-	-	-	-
		AT2G47840	*Tic20-II*	1.79	2.57	-	-	-	-	-	-	-	-
		AT4G03320	*Tic20-IV*	2.06	1.79	-11.15	-	-	-	-	-	-	-
		AT5G55710	*Tic20-V*	-	-	2.47	-	-	-	-	-	-	-
		AT3G18890	*Tic62*	-	-	-	-	-	-	-	-	-	-
		AT4G23430	*Tic32*	-	-	3.00	-	-	-	-	-	-	-
		AT3G48870	*HSP93*	-	-	-	-	-	-	-	-	-	-
	TOC- apparatus	AT4G02510	*Toc159*	1.48	1.87	3.51	-	-	-	-	-	-	-
		AT1G02280	*Toc33*	1.71	2.35	4.47	-	-	-	-	-	-	-
		AT5G05000	*Toc34*	1.35	1.62	-	-	7.55	7.55	4.22	2.12	2.62	0.00
		AT1G35860	*Toc75-I*	-	-	-	-	-	-	-	-	-	-
		AT3G46740	*Toc75-III*	1.55	2.20	-	-	-	-	-	-	-	-
		AT4G09080	*Toc75-IV*	1.57	1.87	-	-	-	-	-	-	-	-
		AT5G19620	*Toc75-V*	1.49	1.76	-	-	-	-	-	-	-	-
		AT1G08980	*Toc64-I*	1.31	1.48	5.02	-	-	-	-	-	-	-
		AT3G17970	*Toc64-III*	1.66	2.34	-	-	7.55	1.63	5.58	0.00	7.55	2.12
		AT2G16640	*Toc132*	1.20	1.46	3.03	-	-	-	-	-	-	-
		AT5G20300	*Toc90*	1.34	1.43	-	-	-	-	-	-	-	-
		AT3G16620	*Toc120*	-	1.36	-	-	-	-	-	-	-	-
		AT3G12580	*HSP70*	2.16	2.39	-	-	-	-	-	-	-	-

			Microarray (Fold Change)		RNA-seq (Fold Change)		ChIP-seq: *pGNL:GNL:HA gnc gnl* (Peak Score)						
		Locus	Gene Name	*35:GNC:GFP*	*35:YFP:GNL*	*35S:GNC:YFP:HA:GR gnc gnl* (F. C. threshold 2.45)	*35S:GNL:YFP:HA:GR gnc gnl* (F. C. threshold 1.2)	Max Score	Upstream 3 kb	Upstream 2 kb	Upstream 1 kb	Intragenic	Downstream 1 kb
Carotenoid biosynthesis genes		AT5G17230	*PSY1*	1.46	1.38	3.33	-	-	-	-	-	-	-
		AT1G06570	*PSD1*	-1.33	-1.34	-	-	-	-	-	-	-	-
		AT3G11945	*PSD2*	-	1.34	-	-	-	-	-	-	-	-
		AT4G14210	*PSD3*	1.66	1.83	-	-	-	-	-	-	-	-
		AT3G09580	*PDS like*	-	-	-	-	-	-	-	-	-	-
		AT3G04870	*ZDS1*	-	1.53	2.47	-	-	-	-	-	-	-
		AT1G06820	*CRTISO*	1.29	1.49	-	-	-	-	-	-	-	-
		AT5G57030	*LYCe*	1.35	1.54	3.85	-	-	-	-	-	-	-
		AT3G10230	*LYCb*	-	1.33	3.89	-	-	-	-	-	-	-
		AT3G53130	*CYP97C1*	1.76	2.35	-	-	-	-	-	-	-	-
		AT1G31800	*CYP97A3*	1.41	1.53	2.89	-	-	-	-	-	-	-
		AT4G25700	*CHY1*	2.00	2.03	3.21	-	-	-	-	-	-	-
		AT5G52570	*CHY2*	-	-	-	-	-	-	-	-	-	-
		AT5G67030	*ZEP*	-	-1.63	3.62	-	-	-	-	-	-	-
		AT1G08550	*VDE*	1.88	1.64	4.34	-	-	-	-	-	-	-
		AT1G67080	*NXS*	-	1.42	4.41	-	-	-	-	-	-	-
		AT3G63520	*CCD1/NECD1*	-	-	2.96	-	-	-	-	-	-	-

Table 10: List of genes from the overlap of ChIP-seq with *pGNL:GNL:HA gnc gnl* and the RNA-seq with *35S:GNC:YFP:HA:GR gnc gnl* for 3 h Dex and CHX (filtered with fold change threshold/F.C. 2.45 and FDR < 0.01).

		RNA-seq: *35S:GNC:YFP:HA:GR gnc gnl* 3 h CHX / Dex + CHX			ChIP-seq: *pGNL:GNL:HA*					
Locus	Gene name	Fold change (F.C.)	P-value	FDR	Max score	Up-stream 3Kb	Up-stream 2Kb	Up-stream 1Kb	Intragenic	Down-stream 1Kb
AT1G01260	AT1G01260	-2.7	1.4E-08	1.6E-07	14.31	1.12	0	14.31	4.31	2.49
AT1G01430	*TBL25*	5.3	3.4E-06	2.7E-05	7.73	3.69	4.06	1.86	2.96	7.73
AT1G02150	AT1G02150	2.7	3.9E-06	3.1E-05	12.49	12.49	0	0	2.03	5.22
AT1G02470	AT1G02470	-10.7	2.4E-04	1.4E-03	15.45	0	7.55	15.45	1.14	3.6
AT1G02475	AT1G02475	3.2	2.9E-07	2.8E-06	15.45	1.14	4.59	2.12	15.45	1.14
AT1G02640	*BXL2*	3.4	3.4E-05	2.3E-04	12.04	12.04	0	0	0	2.49
AT1G03130	*PSAD-2*	4.5	1.8E-11	2.8E-10	12.04	2.49	0	0	12.04	2.94
AT1G03870	*FLA9*	3.6	8.1E-09	9.6E-08	11.58	0	1.12	1.12	0	11.58
AT1G03900	*NAP4*	2.8	3.7E-10	5.1E-09	10.67	10.67	1.12	0	4.31	0
AT1G03905	AT1G03905	-2.8	1.8E-04	1.1E-03	10.67	10.67	1.12	1.58	0	0
AT1G04120	*MRP5*	3.0	5.4E-05	3.6E-04	7.41	2.07	0	0	7.41	3.13
AT1G04350	AT1G04350	4.4	4.1E-08	4.4E-07	7.36	0	1.54	1.54	3.13	7.36
AT1G04620	AT1G04620	2.5	1.4E-03	6.7E-03	8.83	8.83	1.49	3.33	6.38	1.49
AT1G04640	*LIP2*	4.5	5.4E-04	2.8E-03	8.83	8.83	2.96	0	4.06	0
AT1G05140	AT1G05140	4.6	7.0E-05	4.5E-04	10.67	0	1.58	0	10.67	1.58
AT1G05150	AT1G05150	2.7	5.3E-04	2.8E-03	10.67	0	0	0	10.67	1.12
AT1G05990	*RHS2*	-32.7	3.1E-56	1.0E-54	10.39	0	10.39	1.12	1.12	0
AT1G06680	*PSBP-1*	6.7	0.0E+00	0.0E+00	7.06	0	2.12	2.12	7.06	1.63
AT1G07080	AT1G07080	3.2	9.1E-09	1.1E-07	10.22	1.12	1.58	0	4.31	10.22
AT1G08520	*ALB1*	2.5	4.0E-09	4.9E-08	11.06	3.13	0	0	11.06	2.07
AT1G08920	*ESL1*	3.3	0.0E+00	0.0E+00	8.05	3.6	2.12	4.59	3.6	8.05
AT1G09150	AT1G09150	3.3	2.2E-04	1.3E-03	9.76	2.03	9.76	1.12	3.4	3.4
AT1G09310	AT1G09310	7.9	2.9E-15	5.9E-14	9.93	9.93	0	1.49	0	1.86
AT1G09530	*PIF3*	2.5	3.8E-04	2.1E-03	9.76	1.12	2.49	0	1.12	9.76
AT1G10090	AT1G10090	2.5	4.6E-05	3.1E-04	12.5	1.49	12.5	1.86	1.86	1.86
AT1G10170	*NFXL1*	-14.5	2.8E-63	9.6E-62	7.06	7.06	1.63	0	3.11	2.62
AT1G10950	*TMN1*	3.2	1.8E-10	2.5E-09	7.73	7.73	2.96	4.43	4.43	3.33
AT1G11680	*CYP51G1*	4.2	6.9E-11	1.0E-09	9.53	0	0	0	9.53	1.14
AT1G11700	AT1G11700	4.8	2.6E-07	2.5E-06	9.57	9.57	3.69	0	4.06	0
AT1G12050	AT1G12050	3.8	2.3E-05	1.6E-04	9.53	0	3.11	4.1	3.6	9.53
AT1G12310	AT1G12310	2.9	1.3E-09	1.7E-08	9.31	3.85	0	0	9.31	0
AT1G12780	*UGE1*	4.3	3.1E-13	5.4E-12	7.06	2.12	1.63	0	7.06	3.6
AT1G13930	AT1G13930	8.2	0.0E+00	0.0E+00	9.31	2.03	1.12	3.4	9.31	0
AT1G13980	*GN*	4.1	2.5E-04	1.4E-03	9.93	0	0	5.53	9.93	0
AT1G14030	AT1G14030	3.2	2.1E-03	9.5E-03	7.89	1.01	1.01	7.89	0	0
AT1G14040	AT1G14040	-33.7	9.5E-39	2.9E-37	7.89	7.89	1.01	1.01	1.01	0
AT1G14700	*PAP3*	10.8	1.7E-04	9.9E-04	9.57	3.69	0	1.12	9.57	2.59
AT1G14710	AT1G14710	3.0	2.4E-11	3.6E-10	10.52	2.62	2.62	1.14	10.52	2.12
AT1G14920	*GAI*	2.6	9.7E-04	4.8E-03	9.53	0	2.3	1.63	9.53	2.67
AT1G17600	AT1G17600	-3.7	1.6E-04	9.5E-04	10.02	0	1.14	1.63	10.02	2.62
AT1G18260	AT1G18260	2.5	2.5E-04	1.4E-03	7.06	0	0	5.08	7.06	0
AT1G18300	*NUDT4*	5.3	0.0E+00	0.0E+00	7.36	1.01	0	7.36	1.54	0
AT1G18710	*MYB47*	8.8	5.8E-06	4.6E-05	7.73	1.12	7.73	3.33	4.79	4.79
AT1G19050	*ARR7*	2.8	0.0E+00	0.0E+00	8.85	8.85	0	0	2.03	2.49
AT1G19210	AT1G19210	3.1	3.7E-05	2.5E-04	8.85	8.85	0	1.27	1.58	0
AT1G19350	*BES1*	8.0	0.0E+00	0.0E+00	10.52	3.11	2.62	1.63	10.52	2.62
AT1G19660	AT1G19660	2.9	2.0E-15	4.1E-14	7.06	1.14	3.11	7.06	2.62	0
AT1G19670	*CLH1*	9.7	0.0E+00	0.0E+00	7.06	1.14	0	4.59	3.11	7.06
AT1G20330	*SMT2*	2.5	2.2E-16	4.9E-15	8.85	8.85	0	2.94	2.49	0
AT1G20340	*DRT112*	9.1	0.0E+00	0.0E+00	8.85	8.85	0	2.49	7.04	2.94
AT1G20350	*TIM17-1*	-14.5	4.7E-40	1.4E-38	8.85	8.85	0	1.58	1.12	2.49
AT1G21050	AT1G21050	6.9	0.0E+00	0.0E+00	7.06	0	0	2.62	7.06	2.12
AT1G21120	AT1G21120	-53.5	2.0E-80	7.4E-79	9.57	9.57	4.43	1.49	1.12	0
AT1G21130	AT1G21130	-5.2	2.7E-55	9.0E-54	9.57	1.12	2.59	0	3.33	9.57
AT1G21440	AT1G21440	5.9	2.1E-10	2.9E-09	8.85	4.76	2.28	4.19	4.31	8.85
AT1G21500	AT1G21500	6.4	0.0E+00	0.0E+00	9.57	2.96	2.96	9.57	0	2.59
AT1G21680	AT1G21680	3.0	3.8E-10	5.1E-09	7.06	2.62	7.06	1.14	5.08	1.63
AT1G22610	AT1G22610	2.7	8.1E-06	6.2E-05	8.85	4.31	1.58	8.85	2.03	0

		RNA-seq: *35S:GNC:YFP:HA:GR gnc gnl* 3 h CHX / Dex + CHX			ChIP-seq: *pGNL:GNL:HA*					
Locus	**Gene name**	**Fold change (F.C.)**	**P-value**	**FDR**	**Max score**	**Up-stream 3Kb**	**Up-stream 2Kb**	**Up-stream 1Kb**	**Intragenic**	**Down-stream 1Kb**
AT1G23400	*CAF2*	3.0	1.3E-04	8.2E-04	8.1	8.1	0	0	2.22	1.49
AT1G26850	AT1G26850	3.4	0.0E+00	0.0E+00	7.36	0	1.49	0	7.36	3.33
AT1G27090	AT1G27090	2.7	1.4E-08	1.6E-07	8.85	2.03	2.03	0	8.85	0
AT1G27480	AT1G27480	10.7	6.8E-07	6.2E-06	7.36	0	7.36	0	1.49	1.12
AT1G28130	*GH3.17*	3.2	4.7E-04	2.5E-03	9.03	1.63	0	1.14	9.03	1.14
AT1G28190	AT1G28190	-9.9	6.6E-26	1.7E-24	7.79	0	0	2.12	7.79	2.12
AT1G28440	*HSL1*	5.0	4.6E-09	5.5E-08	7.55	1.63	0	3.03	7.55	1.14
AT1G28470	*NAC010*	-4.0	2.8E-05	1.9E-04	7	2.96	7	2.96	1.49	0
AT1G29310	AT1G29310	2.6	9.0E-04	4.5E-03	8.85	1.58	8.85	1.58	4.31	1.12
AT1G29660	AT1G29660	3.7	6.7E-13	1.2E-11	11.4	1.86	1.12	5.16	3.33	11.4
AT1G31320	*LBD4*	9.9	1.8E-03	8.2E-03	13.6	1.49	13.6	0	2.22	0
AT1G32060	*PRK*	6.6	0.0E+00	0.0E+00	7.36	4.06	0	7.36	3.33	1.86
AT1G32080	AT1G32080	4.1	9.3E-07	8.3E-06	7.06	1.63	7.06	2.12	1.63	0
AT1G32350	*AOX1D*	-114.4	2.3E-28	6.2E-27	8.85	1.12	0	2.94	2.03	8.85
AT1G32990	*PRPL11*	2.9	0.0E+00	0.0E+00	7.36	0	0	1.49	6.63	7.36
AT1G35720	*ANNAT1*	6.5	0.0E+00	0.0E+00	7.89	7.89	1.01	1.62	0	0
AT1G36640	AT1G36640	-6.6	8.1E-08	8.3E-07	8.83	0	0	0	8.83	0
AT1G42970	*GAPB*	3.9	1.6E-15	3.3E-14	8.85	0	2.49	1.58	8.85	2.03
AT1G43710	emb1075	4.2	5.1E-15	1.0E-13	8.85	0	0	0	2.94	8.85
AT1G44920	AT1G44920	3.7	1.5E-08	1.7E-07	16.54	2.96	3.69	16.54	1.49	2.22
AT1G45201	*TLL1*	5.9	0.0E+00	0.0E+00	11.03	4.43	2.59	0	1.49	11.03
AT1G45230	AT1G45230	5.2	4.4E-06	3.6E-05	7.06	2.12	2.12	0	7.06	2.12
AT1G47128	*RD21*	4.2	0.0E+00	0.0E+00	7	2.59	2.22	7	4.06	3.69
AT1G49660	*CXE5*	6.9	4.2E-14	7.9E-13	8.03	0	0	8.03	0	1.49
AT1G51680	*4CL1*	2.6	2.0E-06	1.7E-05	10.52	1.14	0	0	10.52	3.6
AT1G51790	AT1G51790	-3.8	1.7E-08	1.9E-07	9.48	2.96	2.59	9.48	1.86	0
AT1G52150	ATHB-15	3.6	9.8E-04	4.9E-03	8.54	2.22	8.54	0	4.43	2.22
AT1G52190	AT1G52190	6.2	8.0E-08	8.3E-07	10.35	0	10.35	0	2.59	1.12
AT1G52290	AT1G52290	3.8	9.2E-09	1.1E-07	7	4.43	1.82	7	1.12	3.69
AT1G52410	*TSA1*	7.7	0.0E+00	0.0E+00	10.02	3.11	3.11	3.11	3.6	10.02
AT1G52870	AT1G52870	5.2	5.4E-14	1.0E-12	7.36	4.43	5.53	1.49	7.36	6.26
AT1G53060	AT1G53060	-5.8	3.9E-07	3.6E-06	7.06	2.12	1.14	1.63	7.06	0
AT1G53230	*TCP3*	3.9	4.0E-05	2.7E-04	8.4	8.4	2.03	2.49	3.85	1.58
AT1G53920	*GLIP5*	-2.5	3.8E-05	2.5E-04	18.37	0	3.69	1.12	4.06	18.37
AT1G54610	AT1G54610	2.9	1.1E-04	6.8E-04	12.12	1.54	1.01	0	12.12	0
AT1G54730	AT1G54730	4.9	7.8E-04	4.0E-03	9.93	1.49	1.49	9.57	5.16	9.93
AT1G55390	AT1G55390	-3.3	8.5E-07	7.6E-06	9.03	0	1.63	1.14	9.03	2.62
AT1G55670	*PSAG*	5.3	0.0E+00	0.0E+00	8.4	8.4	1.12	0	0	6.13
AT1G56020	AT1G56020	3.8	7.2E-04	3.7E-03	7.06	1.63	0	0	7.06	0
AT1G56060	AT1G56060	-5.1	2.2E-18	5.1E-17	7.06	7.06	3.11	2.12	3.11	0
AT1G56170	*NF-YC2*	4.4	1.3E-03	6.1E-03	7.06	0	1.14	3.6	7.06	2.62
AT1G56190	AT1G56190	3.2	2.5E-08	2.8E-07	7.06	7.06	2.62	1.63	2.12	3.6
AT1G56220	AT1G56220	7.4	1.4E-10	2.0E-09	8.54	2.62	0	2.12	8.54	0
AT1G56520	AT1G56520	3.0	2.1E-07	2.1E-06	7.77	2.96	0	7.77	4.43	2.59
AT1G56660	AT1G56660	2.7	2.2E-05	1.5E-04	7	3.12	4.06	2.22	7	1.12
AT1G57990	*PUP18*	-3.3	2.5E-282	1.0E-280	8.4	4.31	8.4	3.09	1.58	0
AT1G58360	*AAP1*	4.5	2.3E-09	2.9E-08	13.24	13.24	4.06	4.06	1.86	0
AT1G59900	*E1 ALPHA*	2.5	1.1E-10	1.5E-09	9.03	1.14	2.62	2.62	9.03	1.63
AT1G59950	AT1G59950	-12.2	9.6E-09	1.1E-07	8.83	0	0	0	4.43	8.83
AT1G60270	*BGLU6*	3.2	7.8E-06	6.0E-05	8.03	2.96	8.03	2.08	1.49	2.22
AT1G62300	*WRKY6*	-3.2	7.2E-46	2.3E-44	8.1	8.1	1.49	2.22	2.22	2.59
AT1G62480	AT1G62480	5.1	0.0E+00	0.0E+00	8.1	2.59	1.86	8.1	0	0
AT1G62750	*SCO1*	4.0	0.0E+00	0.0E+00	8.54	0	8.54	1.14	6.57	2.12
AT1G62800	*ASP4*	4.4	1.7E-05	1.2E-04	9.2	0	1.12	1.49	9.2	2.22
AT1G64060	*RBOH F*	2.8	1.9E-04	1.1E-03	8.42	0	0	1.01	8.42	1.54
AT1G64065	AT1G64065	-2.5	2.6E-06	2.2E-05	7.89	0	1.54	0	7.89	1.54
AT1G64500	AT1G64500	4.8	1.5E-06	1.3E-05	7.89	0	2.07	1.54	1.54	7.89
AT1G64510	AT1G64510	3.2	0.0E+00	0.0E+00	7.89	0	0	2.07	7.89	1.54
AT1G64770	*NDF2*	3.5	6.3E-07	5.7E-06	10.3	0	1.86	3.69	10.3	0
AT1G65500	AT1G65500	-2.5	4.3E-04	2.3E-03	8.46	0	8.46	4.43	0	4.79

		RNA-seq: *35S:GNC:YFP:HA:GR gnc gnl* 3 h CHX / Dex + CHX			ChIP-seq: *pGNL:GNL:HA*					
Locus	**Gene name**	**Fold change (F.C.)**	**P-value**	**FDR**	**Max score**	**Up-stream 3Kb**	**Up-stream 2Kb**	**Up-stream 1Kb**	**Intragenic**	**Down-stream 1Kb**
AT1G65560	AT1G65560	5.4	4.5E-04	2.4E-03	8.54	0	0	8.54	1.14	3.11
AT1G65590	*HEXO3*	3.6	7.4E-05	4.8E-04	8.83	0	0	4.79	8.83	3.33
AT1G66140	*ZFP4*	5.0	2.1E-04	1.2E-03	7	3.33	7	1.12	2.22	2.22
AT1G67360	AT1G67360	2.4	8.0E-09	9.4E-08	8.4	2.49	1.58	0	8.4	2.49
AT1G67720	AT1G67720	2.6	5.2E-04	2.7E-03	14.27	14.27	2.22	2.22	2.22	0
AT1G68390	AT1G68390	-36.7	5.2E-43	1.6E-41	10.01	0	0	1.54	10.01	0
AT1G69310	*WRKY57*	3.4	3.7E-05	2.5E-04	7	0	1.49	5.16	7	2.96
AT1G69360	AT1G69360	2.9	4.6E-04	2.5E-03	7	4.06	1.86	7	2.96	0
AT1G69450	AT1G69450	2.6	8.3E-04	4.2E-03	7	7	2.6	0	2.96	4.79
AT1G69460	AT1G69460	2.9	2.8E-05	1.9E-04	7	1.86	1.49	0	7	2.6
AT1G69580	AT1G69580	3.2	7.8E-04	4.0E-03	10.3	0	0	0	10.3	3.69
AT1G70200	AT1G70200	3.8	4.4E-05	2.9E-04	8.4	1.58	3.85	2.49	8.4	4.31
AT1G70210	*CYCD1;1*	5.6	2.2E-04	1.3E-03	8.4	1.58	2.49	1.58	8.4	0
AT1G70420	AT1G70420	-4.4	1.9E-32	5.4E-31	7	1.49	7	3.69	3.33	1.12
AT1G70700	*TIFY7*	3.2	0.0E+00	0.0E+00	9.53	9.53	0	3.11	2.62	1.63
AT1G70940	*PIN3*	4.0	1.3E-13	2.4E-12	8.05	2.12	1.63	0	8.05	0
AT1G71170	AT1G71170	3.8	9.6E-08	9.8E-07	8.4	1.58	2.49	8.4	1.12	2.03
AT1G71480	AT1G71480	4.2	1.1E-07	1.1E-06	7.06	3.6	1.63	0	7.06	5.08
AT1G71710	AT1G71710	3.3	7.4E-05	4.8E-04	10.61	2.22	2.22	0	10.61	1.86
AT1G71870	AT1G71870	5.7	3.6E-05	2.5E-04	9.53	2.62	0	0	9.53	1.63
AT1G71980	AT1G71980	3.6	1.1E-05	8.2E-05	7.01	0	0	7.01	2.51	3.1
AT1G72140	AT1G72140	3.1	1.7E-07	1.7E-06	8.4	1.12	0	0	4.31	8.4
AT1G72190	AT1G72190	6.1	9.2E-04	4.6E-03	10.52	1.14	10.52	1.63	3.6	0
AT1G72210	AT1G72210	2.7	1.8E-03	8.3E-03	7.73	0	7.73	3.33	5.53	1.49
AT1G72240	AT1G72240	3.3	2.4E-08	2.7E-07	7.36	0	7.36	1.86	0	1.86
AT1G73120	AT1G73120	22.3	3.4E-11	5.1E-10	9.06	1.12	1.86	9.06	0	1.49
AT1G73130	AT1G73130	3.2	2.3E-04	1.3E-03	9.06	1.49	0	9.06	3.33	0
AT1G73540	NUDT21	6.4	0.0E+00	0.0E+00	9.2	1.12	1.49	1.12	2.59	9.2
AT1G74690	*IQD31*	4.0	2.6E-08	2.8E-07	8.05	2.62	2.12	0	8.05	0
AT1G74850	*PTAC2*	3.3	1.8E-03	8.3E-03	7.36	0	7.36	0	2.59	1.12
AT1G74870	AT1G74870	-92.7	1.8E-215	7.2E-214	7.06	7.06	2.62	1.63	2.62	5.08
AT1G75420	AT1G75420	4.2	1.1E-03	5.6E-03	7	1.12	4.43	7	2.22	0
AT1G75680	*GH9B7*	4.3	2.5E-11	3.8E-10	7.73	3.33	7.73	2.59	3.33	3.33
AT1G76440	AT1G76440	-3.4	5.8E-09	7.0E-08	7.36	1.12	7.36	1.49	1.86	2.96
AT1G76460	AT1G76460	2.7	8.9E-04	4.4E-03	7.36	3.33	1.12	0	2.22	7.36
AT1G76490	*HMG1*	2.8	0.0E+00	0.0E+00	12.98	3.6	0	0	12.98	2.62
AT1G76880	AT1G76880	3.2	6.7E-06	5.2E-05	9.53	0	0	0	9.53	1.13
AT1G77060	AT1G77060	3.5	0.0E+00	0.0E+00	7.73	7.73	3.33	2.59	2.22	1.12
AT1G77090	AT1G77090	3.9	3.1E-06	2.6E-05	11.5	3.11	0	2.12	11.5	1.63
AT1G77710	AT1G77710	2.7	8.7E-12	1.4E-10	8.83	4.92	1.12	2.59	0	8.83
AT1G78210	AT1G78210	3.1	2.6E-06	2.1E-05	8.1	8.1	2.96	4.06	2.22	2.22
AT1G78270	UGT85A4	5.1	9.3E-04	4.6E-03	12.49	1.63	4.59	1.14	12.49	2.12
AT1G78310	AT1G78310	-2.9	5.4E-04	2.9E-03	8.4	0	3.85	1.58	4.92	8.4
AT1G78370	*GSTU20*	8.8	0.0E+00	0.0E+00	8.4	0	2.49	8.4	1.12	1.58
AT1G78670	*GGH3*	4.2	1.9E-11	2.9E-10	7.06	0	2.62	1.57	4.1	7.06
AT1G78680	*GGH2*	3.8	9.5E-11	1.4E-09	7.06	4.1	1.63	2.12	7.06	3.6
AT1G78895	AT1G78895	-4.0	5.1E-22	1.3E-20	8.4	0	0	0	8.4	2.49
AT1G79110	AT1G79110	4.2	1.6E-05	1.2E-04	8.4	0	8.4	1.12	2.49	1.58
AT1G79310	*MC7*	3.6	0.0E+00	0.0E+00	7.06	1.14	5.08	1.14	7.06	0
AT1G79670	*RFO1*	-3.2	3.2E-07	3.0E-06	7.06	0	7.06	0	3.6	3.6
AT1G79680	*WAKL10*	-6.7	1.2E-38	3.7E-37	7.06	1.63	0	1.14	7.06	2.62
AT1G79700	AT1G79700	3.9	2.9E-04	1.6E-03	7.06	0	3.11	1.14	7.06	0
AT1G79870	AT1G79870	2.9	1.2E-06	1.1E-05	8.2	3.4	1.27	8.2	1.63	5.67
AT1G80440	AT1G80440	3.8	1.9E-14	3.7E-13	7.94	7.94	2.03	0	4.76	2.94
AT2G01520	*MLP328*	19.9	0.0E+00	0.0E+00	10.02	0	0	0	10.02	0
AT2G01620	*MEE11*	3.1	1.6E-04	9.5E-04	7.36	5.53	7.36	4.79	2.59	2.22
AT2G01670	*NUDT17*	3.9	0.0E+00	0.0E+00	8.1	0	0	2.96	8.1	3.33
AT2G01720	AT2G01720	2.5	4.1E-05	2.7E-04	7.06	2.12	0	3.6	7.06	1.14
AT2G02070	*IDD5*	3.2	1.8E-05	1.3E-04	7.94	7.94	0	5.22	6.13	0
AT2G03090	*EXPA15*	2.6	4.9E-07	4.5E-06	7	1.12	3.33	7	5.16	2.59

		RNA-seq: *35S:GNC:YFP:HA:GR gnc gnl* 3 h CHX / Dex + CHX			ChIP-seq: *pGNL:GNL:HA*					
Locus	**Gene name**	**Fold change (F.C.)**	**P-value**	**FDR**	**Max score**	**Up-stream 3Kb**	**Up-stream 2Kb**	**Up-stream 1Kb**	**Intragenic**	**Down-stream 1Kb**
AT2G03680	*SPR1*	3.7	5.8E-15	1.2E-13	9.03	1.14	0	0	4.59	9.03
AT2G04050	AT2G04050	-105.9	3.1E-18	7.2E-17	11.03	11.03	1.86	1.49	2.22	0
AT2G04680	AT2G04680	-16.6	3.7E-10	5.0E-09	13.24	1.12	0	13.24	4.06	2.22
AT2G05920	AT2G05920	3.8	0.0E+00	0.0E+00	7.36	0	0	0	7.36	0
AT2G13360	*AGT*	6.0	0.0E+00	0.0E+00	7.73	1.49	1.12	1.86	7.73	0
AT2G15320	AT2G15320	3.1	5.9E-04	3.1E-03	7.94	7.94	1.12	2.94	3.4	0
AT2G16720	*MYB7*	5.1	7.2E-04	3.7E-03	11.03	0	6.26	0	3.69	11.03
AT2G17120	*LYM2*	-3.2	2.2E-35	6.4E-34	7.55	0	0	0	2.12	7.55
AT2G19460	AT2G19460	-3.0	4.1E-08	4.4E-07	10.53	0	0	0	10.53	1.54
AT2G20300	*ALE2*	3.2	1.1E-04	7.1E-04	17.27	0	1.12	17.27	4.43	1.86
AT2G20800	*NDB4*	-118.5	1.5E-21	3.7E-20	7.73	1.12	2.96	7.73	1.12	1.86
AT2G20890	*PSB29*	3.9	0.0E+00	0.0E+00	7.94	4.76	2.03	0	7.94	2.49
AT2G21050	*LAX2*	2.6	1.1E-03	5.5E-03	8.05	1.14	4.1	8.05	1.63	2.62
AT2G21330	*FBA1*	8.9	0.0E+00	0.0E+00	7.36	1.86	0	1.12	7.36	1.49
AT2G21960	AT2G21960	4.1	1.5E-08	1.7E-07	7.94	4.31	7.94	1.12	2.49	1.58
AT2G22330	*CYP79B3*	29.9	0.0E+00	0.0E+00	9.93	9.93	3.33	0	4.79	0
AT2G22425	AT2G22425	2.9	4.6E-07	4.3E-06	11.4	1.86	11.4	1.86	1.49	1.12
AT2G22930	AT2G22930	17.1	1.3E-03	6.4E-03	8.05	0	0	1.14	8.05	2.12
AT2G24240	AT2G24240	-4.2	6.8E-04	3.5E-03	7.94	3.4	0	7.94	1.58	2.49
AT2G24330	AT2G24330	4.1	0.0E+00	0.0E+00	8.83	8.83	0	2.22	2.96	2.59
AT2G24820	*TIC55-II*	4.2	5.2E-10	7.0E-09	8.05	1.63	2.12	8.05	4.1	2.62
AT2G25490	*EBF1*	3.7	0.0E+00	0.0E+00	8.54	2.62	0	2.12	8.54	2.12
AT2G25625	AT2G25625	4.8	2.0E-04	1.2E-03	8.1	3.69	8.1	2.22	0	2.96
AT2G26110	AT2G26110	5.6	1.8E-05	1.3E-04	7.36	2.59	4.79	4.43	0	7.36
AT2G26580	*YAB5*	3.2	1.5E-04	8.8E-04	9.2	3.69	0	2.96	9.2	0
AT2G28000	*CPN60A*	3.2	0.0E+00	0.0E+00	7.36	2.59	2.96	7.36	2.96	0
AT2G28140	AT2G28140	8.1	3.5E-04	1.9E-03	7.36	1.12	2.22	3.33	2.59	7.36
AT2G28310	AT2G28310	4.5	1.1E-05	8.1E-05	8.46	3.69	2.22	8.46	1.49	3.69
AT2G28500	*LBD11*	7.6	1.2E-08	1.4E-07	7.36	2.22	1.49	1.49	3.69	7.36
AT2G29510	AT2G29510	6.4	0.0E+00	0.0E+00	7.94	2.49	1.12	0	7.94	3.4
AT2G30140	AT2G30140	-6.4	1.0E-16	2.3E-15	8.46	1.49	2.22	0	2.59	8.46
AT2G30250	*WRKY25*	-11.2	6.4E-110	2.4E-108	7.36	2.22	2.59	0	7.36	0
AT2G30590	*WRKY21*	2.5	1.1E-03	5.4E-03	7.94	2.03	0	1.58	7.94	1.12
AT2G31040	AT2G31040	2.6	1.5E-08	1.7E-07	29.75	3.69	2.59	29.75	0	4.79
AT2G31810	AT2G31810	2.8	0.0E+00	0.0E+00	7.94	2.03	0	2.94	7.94	1.12
AT2G32090	AT2G32090	3.5	1.1E-03	5.3E-03	9.2	9.2	0	3.33	2.96	2.22
AT2G32520	AT2G32520	2.7	3.4E-06	2.8E-05	7.94	1.58	1.58	0	7.94	1.09
AT2G32540	*CSLB04*	9.3	6.4E-04	3.3E-03	8.83	0	1.49	0	8.83	2.59
AT2G32560	AT2G32560	4.8	3.1E-15	6.4E-14	7.06	1.63	1.14	1.14	4.1	7.06
AT2G32580	AT2G32580	3.4	7.9E-08	8.2E-07	7.06	3.11	0	4.1	7.06	0
AT2G34310	AT2G34310	3.8	5.2E-06	4.1E-05	10.53	10.53	1.54	0	1.01	0
AT2G34620	AT2G34620	4.6	5.2E-04	2.8E-03	7.06	0	3.6	0	7.06	1.14
AT2G34680	*AIR9*	4.0	7.7E-06	5.9E-05	6.9	1.49	1.86	0	6.9	5.53
AT2G35330	AT2G35330	2.5	8.7E-04	4.4E-03	7.51	1.51	7.51	0	2.01	2.01
AT2G35780	*scpl26*	5.2	2.7E-08	2.9E-07	8.05	1.14	8.05	7.06	3.11	0
AT2G35795	AT2G35795	3.1	4.8E-04	2.6E-03	8.05	3.11	7.06	8.05	1.14	2.67
AT2G35800	AT2G35800	4.0	4.3E-05	2.9E-04	8.05	8.05	1.14	2.67	3.11	2.62
AT2G35820	AT2G35820	5.3	6.3E-05	4.1E-04	7	2.96	0	2.22	7	0
AT2G35830	AT2G35830	7.1	5.6E-12	8.9E-11	7	0	2.22	7	0	1.86
AT2G35840	AT2G35840	2.9	5.3E-05	3.5E-04	7	2.22	7	1.86	6.26	0
AT2G35860	*FLA16*	3.4	5.4E-10	7.2E-09	8.05	2.62	0	1.14	8.05	0
AT2G35940	*BLH1*	2.8	5.2E-07	4.8E-06	10.02	0	0	1.14	10.02	1.14
AT2G36130	AT2G36130	2.5	1.6E-03	7.4E-03	9.03	2.12	2.12	6.07	3.03	9.03
AT2G36145	AT2G36145	6.5	2.3E-11	3.4E-10	9.03	6.07	1.14	3.03	9.03	2.62
AT2G36570	AT2G36570	5.7	1.6E-03	7.5E-03	7.06	1.63	4.1	3.6	7.06	1.63
AT2G36720	AT2G36720	3.7	2.1E-04	1.2E-03	8.05	8.05	1.14	0	4.59	0
AT2G36750	UGT73C1	-4.4	1.7E-09	2.2E-08	7.25	7.25	1.49	2.22	3.33	1.86
AT2G36770	AT2G36770	-25.8	3.9E-33	1.1E-31	7.25	0	0	3.33	1.86	7.25
AT2G36790	UGT73C6	-15.5	1.4E-50	4.6E-49	9.57	0	2.59	9.57	2.59	0
AT2G36800	*DOGT1*	-6.6	1.4E-26	3.8E-25	9.57	0	1.86	0	2.59	9.57

		RNA-seq: *35S:GNC:YFP:HA:GR gnc gnl* 3 h CHX / Dex + CHX			ChIP-seq: *pGNL:GNL:HA*					
Locus	**Gene name**	**Fold change (F.C.)**	**P-value**	**FDR**	**Max score**	**Up-stream 3Kb**	**Up-stream 2Kb**	**Up-stream 1Kb**	**Intragenic**	**Down-stream 1Kb**
AT2G36830	*GAMMA-TIP*	6.7	0.0E+00	0.0E+00	9.2	1.49	3.33	2.59	0	9.2
AT2G36870	*XTH32*	7.9	1.2E-05	8.9E-05	7	0	0	7	4.79	0
AT2G36880	*MAT3*	2.9	0.0E+00	0.0E+00	7.51	6.51	0	7.51	1.99	0
AT2G37130	AT2G37130	8.9	0.0E+00	0.0E+00	7.51	0	7.51	6.51	0	0
AT2G37220	AT2G37220	3.3	0.0E+00	0.0E+00	7	1.12	3.33	1.86	7	4.06
AT2G37330	*ALS3*	4.4	9.6E-04	4.8E-03	7.94	1.12	1.63	1.12	7.94	0
AT2G37460	AT2G37460	22.8	1.1E-04	6.9E-04	13.6	0	1.49	4.43	13.6	1.12
AT2G37620	*ACT1*	3.3	1.4E-11	2.1E-10	12.98	1.14	2.62	0	4.59	12.98
AT2G37630	*AS1*	5.8	3.4E-07	3.2E-06	12.98	1.63	3.6	0	12.98	0
AT2G37750	AT2G37750	-3.5	1.2E-03	5.6E-03	7.73	2.22	2.59	7.73	1.86	0
AT2G37980	AT2G37980	-2.8	1.7E-03	7.8E-03	15.82	0	2.6	0	15.82	0
AT2G38530	*LTP2*	12.3	0.0E+00	0.0E+00	7.73	1.49	0	7.73	1.86	0
AT2G38540	*LP1*	5.7	0.0E+00	0.0E+00	7.73	7.73	1.86	1.12	2.22	1.86
AT2G38823	AT2G38823	-93.9	1.7E-93	6.4E-92	13.7	13.7	1.86	0	1.49	0
AT2G38970	AT2G38970	5.7	4.9E-04	2.6E-03	7.51	0	0	6.51	7.51	0
AT2G39010	*PIP2E*	9.4	0.0E+00	0.0E+00	7.06	1.63	0	2.12	7.06	0
AT2G39130	AT2G39130	2.7	3.1E-05	2.1E-04	7.89	7.89	0	0	1.54	0
AT2G39140	*SVR1*	3.2	8.2E-04	4.2E-03	7.89	0	0	0	7.89	0
AT2G39470	*PPL2*	4.2	1.2E-13	2.3E-12	7.06	7.06	1.14	4.1	1.14	6.07
AT2G39480	*PGP6*	-2.9	1.1E-13	2.1E-12	7	4.43	4.06	7	3.33	2.59
AT2G39518	AT2G39518	-3.1	2.4E-09	3.0E-08	8.1	2.22	1.12	0	4.43	8.1
AT2G40480	AT2G40480	6.4	7.8E-04	4.0E-03	7.89	0	0	7.89	1.54	1.54
AT2G40490	*HEME2*	3.4	7.1E-11	1.0E-09	7.89	7.89	1.01	1.54	5.77	0
AT2G41220	*GLU2*	2.8	4.2E-05	2.8E-04	8.11	0	1.86	0	4.43	8.11
AT2G41250	AT2G41250	3.5	9.9E-06	7.4E-05	10.52	0	3.6	0	10.52	4.59
AT2G42060	AT2G42060	-2.9	2.0E-06	1.7E-05	7.94	0	1.12	0	7.94	2.49
AT2G42320	AT2G42320	3.8	1.8E-04	1.1E-03	7.94	0	1.58	7.94	1.58	4.55
AT2G43360	*BIO2*	4.5	1.6E-06	1.4E-05	7.55	2.62	2.62	2.62	7.55	0
AT2G43535	AT2G43535	5.2	0.0E+00	0.0E+00	8.05	1.63	2.62	1.14	0	8.05
AT2G43540	AT2G43540	5.3	2.7E-06	2.3E-05	8.05	2.62	1.14	0	8.05	1.63
AT2G43550	AT2G43550	65.2	0.0E+00	0.0E+00	8.05	1.14	0	8.05	1.63	3.11
AT2G44140	AT2G44140	3.1	2.9E-07	2.7E-06	9.53	0	4.1	0	9.53	0
AT2G44490	*PEN2*	-4.4	2.7E-35	7.9E-34	7.94	0	2.03	0	7.94	0
AT2G44840	*ERF13*	3.1	0.0E+00	0.0E+00	7.73	0	3.69	7.73	2.08	0
AT2G45200	*GOS12*	3.4	7.6E-04	3.9E-03	7.36	3.69	4.06	0	7.36	0
AT2G45310	*GAE4*	3.4	6.4E-10	8.5E-09	7.06	1.14	0	2.12	7.06	3.11
AT2G45470	*FLA8*	8.3	0.0E+00	0.0E+00	10.02	0	2.62	1.14	10.02	3.6
AT2G45700	AT2G45700	2.9	1.1E-03	5.4E-03	7.06	7.06	0	0	6.07	3.11
AT2G45810	AT2G45810	3.6	2.3E-08	2.6E-07	8.54	3.11	0	1.63	8.54	2.12
AT2G46400	WRKY46	3.9	0.0E+00	0.0E+00	8.83	2.96	2.22	1.49	8.83	5.53
AT2G46560	AT2G46560	2.8	5.7E-04	3.0E-03	8.83	0	1.86	5.9	8.83	2.59
AT2G47130	AT2G47130	-4.0	3.1E-39	9.4E-38	10.52	10.52	0	1.63	7.06	0
AT2G47140	AT2G47140	-9.7	1.9E-27	5.1E-26	10.52	0	1.63	10.52	1.63	7.06
AT2G47150	AT2G47150	-10.1	5.9E-04	3.1E-03	10.52	0	0	1.63	10.52	0
AT2G47180	*GolS1*	3.3	8.2E-09	9.7E-08	11.01	2.12	0	1.63	11.01	3.6
AT2G47190	*MYB2*	-3.4	4.3E-08	4.6E-07	12.87	2.59	12.87	4.79	1.86	0
AT2G47450	*CAO*	4.3	4.5E-11	6.7E-10	8.05	2.12	2.62	3.11	8.05	1.94
AT2G47470	*UNE5*	4.4	0.0E+00	0.0E+00	8.54	6.07	0	5.08	3.6	8.54
AT2G47550	AT2G47550	-2.8	1.9E-11	3.0E-10	15.07	2.22	15.07	0	2.96	2.96
AT3G01290	AT3G01290	-2.4	3.3E-35	9.6E-34	7.06	0	6.57	0	3.6	7.06
AT3G02050	*KUP3*	5.3	1.1E-06	9.4E-06	7.49	7.49	0	0	2.03	0
AT3G02120	AT3G02120	3.1	7.5E-04	3.8E-03	10.52	0	0	1.14	0	10.52
AT3G02180	*SP1L3*	4.4	2.2E-10	3.0E-09	9.2	1.49	9.2	4.43	1.56	1.86
AT3G02510	AT3G02510	2.5	2.3E-04	1.3E-03	11.77	1.49	11.77	1.12	1.49	3.33
AT3G02730	*TRXF1*	5.2	0.0E+00	0.0E+00	7	1.49	3.33	7	2.96	1.86
AT3G02870	*VTC4*	2.5	5.7E-04	3.0E-03	7.55	5.08	0	0	7.55	1.63
AT3G03470	*CYP89A9*	7.3	1.9E-05	1.4E-04	9.03	3.11	0	0	9.03	2.12
AT3G04340	*emb2458*	4.9	8.0E-07	7.2E-06	7.55	0	7.55	2.62	1.63	2.62
AT3G04930	AT3G04930	3.1	2.2E-07	2.2E-06	10.02	3.11	3.11	1.63	10.02	0
AT3G04940	*CYSD1*	4.7	9.8E-07	8.7E-06	10.02	10.02	0	5.08	5.58	1.63

		RNA-seq: *35S:GNC:YFP:HA:GR gnc gnl* 3 h CHX / Dex + CHX			ChIP-seq: *pGNL:GNL:HA*					
Locus	**Gene name**	**Fold change (F.C.)**	**P-value**	**FDR**	**Max score**	**Up-stream 3Kb**	**Up-stream 2Kb**	**Up-stream 1Kb**	**Intragenic**	**Down-stream 1Kb**
AT3G05410	AT3G05410	6.1	2.2E-03	1.0E-02	7.76	3.33	1.49	0	7.76	1.86
AT3G05660	*RLP33*	-4.0	1.5E-03	7.2E-03	13.65	0	3.33	4.43	5.9	13.65
AT3G06430	EMB2750	5.1	1.6E-05	1.2E-04	7.06	3.11	6.32	1.63	7.06	1.63
AT3G06550	AT3G06550	2.5	2.5E-06	2.1E-05	7.36	1.86	2.59	7.36	3.33	0
AT3G06560	*PAPS3*	-52.1	8.9E-11	1.3E-09	7.36	0	1.12	7.36	2.59	1.12
AT3G07310	AT3G07310	4.4	1.3E-05	9.4E-05	8.05	4.59	0	1.14	8.05	2.12
AT3G07340	AT3G07340	3.3	1.7E-03	7.8E-03	7.06	2.62	1.14	1.63	7.06	1.63
AT3G07950	AT3G07950	2.7	2.8E-04	1.6E-03	7.55	0	2.12	0	7.55	7.06
AT3G08030	AT3G08030	4.9	0.0E+00	0.0E+00	7.55	7.06	4.1	2.12	7.55	1.63
AT3G08670	AT3G08670	4.0	3.3E-07	3.1E-06	11.4	2.96	1.86	2.22	11.4	3.33
AT3G08680	AT3G08680	2.5	2.8E-04	1.6E-03	11.4	1.86	4.06	11.4	3.33	2.22
AT3G08710	*TH9*	-2.5	7.2E-15	1.4E-13	7.73	0	4.79	2.59	1.86	7.73
AT3G08940	*LHCB4.2*	7.1	4.2E-09	5.1E-08	7.55	2.62	1.14	6.07	7.55	3.11
AT3G08943	AT3G08943	2.6	3.6E-04	2.0E-03	7.55	0	0	2.62	4.59	7.55
AT3G09010	AT3G09010	-11.5	1.2E-19	2.9E-18	7.55	7.55	2.12	0	0	0
AT3G09020	AT3G09020	-6.0	3.2E-68	1.1E-66	7.55	0	0	0	3.11	7.55
AT3G09210	*PTAC13*	3.2	5.6E-05	3.7E-04	8.05	8.05	4.1	0	3.11	3.6
AT3G09220	*LAC7*	8.0	4.1E-11	6.0E-10	8.05	0	0	0	8.05	1.14
AT3G09560	AT3G09560	2.9	1.4E-03	6.6E-03	7.51	1.01	0	0	7.51	3.01
AT3G09770	AT3G09770	2.6	8.0E-04	4.1E-03	9.03	0	1.14	0	9.03	3.11
AT3G09920	*PIP5K9*	-2.8	2.6E-07	2.6E-06	11.37	11.37	5.9	2.96	1.86	1.49
AT3G10190	AT3G10190	3.5	1.8E-03	8.2E-03	12.5	0	1.12	12.5	2.22	0
AT3G10410	*SCPL49*	3.7	1.5E-13	2.7E-12	7.55	3.11	7.55	0	3.6	2.62
AT3G10520	*HB2*	4.4	5.0E-10	6.7E-09	7.06	0	0	1.14	2.12	7.06
AT3G10810	AT3G10810	3.5	2.8E-04	1.6E-03	7.89	0	0	0	7.89	0
AT3G10840	AT3G10840	4.1	1.7E-03	7.8E-03	7.49	2.94	2.94	1.12	7.49	0
AT3G11110	AT3G11110	11.8	2.2E-04	1.3E-03	7.06	5.08	3.11	0	7.06	2.62
AT3G11410	*PP2CA*	2.6	7.1E-05	4.6E-04	9.03	1.63	2.62	1.63	9.03	0
AT3G11590	AT3G11590	3.8	1.8E-04	1.1E-03	7	7	7	0	2.22	3.33
AT3G11650	*NHL2*	3.0	6.8E-06	5.3E-05	8.05	3.11	2.62	2.12	8.05	0
AT3G11840	*PUB24*	-6.1	5.0E-70	1.8E-68	7.55	7.55	1.14	1.14	3.6	3.11
AT3G11880	AT3G11880	2.6	9.4E-09	1.1E-07	7.73	0	0	2.96	7.73	2.22
AT3G12345	AT3G12345	4.7	0.0E+00	0.0E+00	7.55	3.6	1.14	7.55	4.59	2.12
AT3G12780	*PGK1*	3.8	6.7E-16	1.4E-14	7.06	7.06	3.11	3.6	4.1	1.14
AT3G13060	*ECT5*	2.9	1.5E-05	1.1E-04	7.49	2.49	1.12	4.31	7.49	3.85
AT3G13330	*PA200*	-3.4	3.4E-17	7.7E-16	8.05	2.12	1.14	8.05	3.6	1.14
AT3G13500	AT3G13500	-77.6	6.9E-08	7.2E-07	7.06	1.63	2.62	0	7.06	0
AT3G14067	AT3G14067	5.1	5.0E-13	8.7E-12	7.49	2.49	3.4	0	7.49	2.94
AT3G14225	*GLIP4*	-14.9	6.9E-15	1.4E-13	8.05	0	8.05	0	1.63	2.12
AT3G14240	AT3G14240	5.1	4.2E-10	5.7E-09	7.06	4.1	2.12	0	7.06	4.59
AT3G14860	AT3G14860	3.8	5.8E-04	3.0E-03	7.06	0	7.06	1.14	6.07	6.07
AT3G15353	*MT3*	3.3	0.0E+00	0.0E+00	9.03	0	1.14	1.63	9.03	0
AT3G15518	AT3G15518	-5.9	1.5E-60	5.0E-59	7	2.59	7	3.63	1.86	1.12
AT3G15530	AT3G15530	6.3	0.0E+00	0.0E+00	9.53	2.62	2.62	0	9.53	3.6
AT3G16140	*PSAH-1*	3.8	0.0E+00	0.0E+00	7.06	4.1	1.14	1.7	7.06	2.12
AT3G16200	AT3G16200	3.2	6.1E-04	3.2E-03	7.55	0	1.14	0	7.55	1.63
AT3G16340	*PDR1*	5.8	4.2E-06	3.3E-05	8.46	1.12	1.86	1.86	8.46	2.96
AT3G16400	*NSP1*	3.1	0.0E+00	0.0E+00	22.23	0	4.43	1.49	22.23	3.33
AT3G16410	*NSP4*	3.0	4.9E-10	6.5E-09	7.36	3.33	3.33	0	0	7.36
AT3G16520	UGT88A1	3.1	1.3E-04	7.9E-04	8.54	0	0	3.6	6.07	8.54
AT3G16530	AT3G16530	-11.8	2.5E-29	6.8E-28	10.02	1.14	0	2.62	10.02	0
AT3G16770	*EBP*	10.4	1.3E-12	2.1E-11	7.51	1.51	0	0	7.51	0
AT3G16920	*CTL2*	2.7	1.5E-03	7.2E-03	26.08	1.49	26.08	1.86	4.79	0
AT3G17100	AT3G17100	2.6	2.7E-05	1.9E-04	7	0	4.43	7	2.22	1.12
AT3G17400	AT3G17400	-17.6	8.7E-04	4.4E-03	7.55	3.11	7.55	0	3.6	1.14
AT3G17410	AT3G17410	-3.8	1.4E-36	4.1E-35	7.55	7.55	0	3.6	3.11	2.12
AT3G17800	AT3G17800	6.4	0.0E+00	0.0E+00	7.55	3.6	2.12	1.14	7.55	3.11
AT3G17810	*PYD1*	3.8	1.0E-13	1.9E-12	7.55	1.14	7.55	1.14	3.6	0
AT3G17840	*RLK902*	3.4	4.6E-04	2.5E-03	8.05	1.63	0	1.63	8.05	1.14
AT3G17940	AT3G17940	2.7	3.1E-05	2.2E-04	7.55	7.55	5.58	1.63	2.12	2.12

		RNA-seq: *35S:GNC:YFP:HA:GR gnc gnl* 3 h CHX / Dex + CHX			ChIP-seq: *pGNL:GNL:HA*					
Locus	**Gene name**	**Fold change (F.C.)**	**P-value**	**FDR**	**Max score**	**Up-stream 3Kb**	**Up-stream 2Kb**	**Up-stream 1Kb**	**Intragenic**	**Down-stream 1Kb**
AT3G63170	AT3G63170	2.8	7.9E-04	4.0E-03	7.36	7.36	1.86	3.69	2.22	0
AT3G63440	*CKX6*	2.6	6.8E-07	6.2E-06	7.06	0	6.07	4.1	7.06	5.08
AT3G63450	AT3G63450	5.6	1.6E-04	9.4E-04	7.06	3.11	4.1	1.94	5.08	7.06
AT4G00030	AT4G00030	3.2	1.7E-04	1.0E-03	8.05	2.12	0	4.1	8.05	3.6
AT4G00490	*BAM2*	4.3	2.8E-04	1.6E-03	7.36	3.69	1.12	7.36	1.86	4.43
AT4G01210	AT4G01210	3.1	1.4E-05	1.0E-04	7.55	2.12	3.11	2.62	4.59	7.55
AT4G01870	AT4G01870	-2.6	7.5E-10	9.8E-09	7.55	0	2.62	1.63	7.55	2.67
AT4G02290	*GH9B13*	3.3	8.6E-04	4.3E-03	7.06	0	0	2.12	7.06	0
AT4G02725	AT4G02725	3.2	1.5E-04	9.0E-04	7.55	1.63	7.55	5.58	0	4.1
AT4G02770	*PSAD-1*	5.0	0.0E+00	0.0E+00	7.55	1.63	0	3.11	7.55	2.12
AT4G03520	*ATHM2*	2.8	0.0E+00	0.0E+00	7.36	1.12	1.49	7.36	2.22	1.49
AT4G04210	*PUX4*	2.8	1.2E-04	7.5E-04	7.55	0	0	1.14	7.55	1.14
AT4G04350	EMB2369	3.0	1.2E-03	5.6E-03	7.06	1.63	2.12	4.1	7.06	1.14
AT4G04890	*PDF2*	3.0	4.8E-04	2.6E-03	7.55	1.14	2.12	3.11	7.55	2.12
AT4G04940	AT4G04940	-2.7	1.2E-04	7.3E-04	7.06	7.06	0	1.63	3.6	1.14
AT4G04950	AT4G04950	3.1	9.5E-05	6.0E-04	7.06	0	1.14	0	7.06	3.6
AT4G08980	*FBW2*	3.7	7.6E-04	3.9E-03	7.06	1.14	0	5.08	7.06	0
AT4G11150	*TUF*	3.3	0.0E+00	0.0E+00	9.09	9.09	1.49	2.22	6.26	3.33
AT4G12420	*SKU5*	2.5	9.2E-09	1.1E-07	7.06	5.23	0	0	7.06	0
AT4G12690	AT4G12690	3.0	3.8E-04	2.1E-03	7.73	1.49	1.12	7.73	1.12	0
AT4G13395	*RTFL12*	8.2	0.0E+00	0.0E+00	12.5	4.79	1.49	12.5	0	1.49
AT4G13580	AT4G13580	12.0	2.1E-03	9.4E-03	7.73	0	6.63	7.73	0	1.49
AT4G14540	*NF-YB3*	5.3	1.8E-04	1.1E-03	8.97	5.16	2.22	2.96	0	8.97
AT4G15490	*UGT84A3*	5.2	4.3E-04	2.4E-03	9.93	4.06	9.93	1.49	2.59	1.49
AT4G15540	AT4G15540	3.2	3.7E-05	2.5E-04	7	1.49	7	0	1.86	2.22
AT4G15560	*CLA1*	3.1	0.0E+00	0.0E+00	8.83	3.33	1.49	6.26	2.22	8.83
AT4G16370	*OPT3*	4.1	5.1E-09	6.2E-08	8	1.01	8	0	2.51	0
AT4G16670	AT4G16670	-28.5	0.0E+00	0.0E+00	7.55	1.14	1.14	4.59	7.55	0
AT4G16680	AT4G16680	-37.8	1.1E-302	4.6E-301	8.24	8.24	0	1.01	3.66	2.6
AT4G16830	AT4G16830	3.9	1.5E-10	2.1E-09	7.04	7.04	1.58	0	1.12	0
AT4G17150	AT4G17150	3.2	1.1E-03	5.5E-03	7.06	7.06	0	0	3.6	2.12
AT4G18670	AT4G18670	4.3	1.5E-09	1.9E-08	7.06	4.1	0	0	7.06	1.14
AT4G18700	*CIPK12*	2.5	5.3E-06	4.2E-05	7.06	1.14	0	1.14	7.06	3.11
AT4G19720	AT4G19720	-17.5	2.5E-21	6.1E-20	9.31	0	4.06	4.06	1.12	9.31
AT4G20240	CYP71A27	5.5	1.5E-03	7.0E-03	8.46	8.46	2.59	0	5.9	0
AT4G20360	*RABE1b*	6.6	0.0E+00	0.0E+00	7.04	7.04	0	0	2.73	2.03
AT4G21920	AT4G21920	-31.7	9.0E-38	2.7E-36	8.54	2.62	0	2.12	0	8.54
AT4G22150	*PUX3*	4.1	3.3E-05	2.3E-04	15.07	4.06	0	1.86	15.07	1.12
AT4G22230	AT4G22230	3.7	2.0E-03	9.0E-03	11.03	2.96	11.03	2.59	0	1.86
AT4G22530	AT4G22530	-4.2	6.8E-05	4.4E-04	7.55	1.63	0	2.62	7.55	2.12
AT4G22540	*ORP2A*	3.9	1.8E-03	8.3E-03	7.55	2.12	1.14	0	3.6	7.55
AT4G23010	*UTR2*	-3.6	1.5E-44	4.6E-43	7.36	4.43	1.86	0	7.36	2.59
AT4G24210	*SLY1*	4.2	8.8E-04	4.4E-03	7.55	1.14	7.55	2.12	0	1.54
AT4G25080	*CHLM*	4.7	0.0E+00	0.0E+00	7.04	5.22	2.94	2.03	7.04	1.12
AT4G25490	*CBF1*	29.2	4.1E-08	4.4E-07	8.15	8.15	1.63	2.12	6.07	2.12
AT4G25500	*RSP35*	2.7	8.1E-07	7.3E-06	8.15	6.07	2.12	1.63	8.15	2.12
AT4G25570	*ACYB-2*	6.7	0.0E+00	0.0E+00	7.38	0	2.12	6.07	7.38	0
AT4G25640	*DTX35*	2.6	1.4E-11	2.1E-10	8.26	0	0	8.26	0	0
AT4G26130	AT4G26130	5.6	0.0E+00	0.0E+00	7	0	1.12	1.49	0	7
AT4G27030	*FADA*	4.1	1.1E-06	9.4E-06	7.06	0	2.62	0	7.06	0
AT4G28350	AT4G28350	-7.7	3.9E-27	1.0E-25	7.06	1.14	7.06	1.14	4.1	0
AT4G28740	AT4G28740	4.8	1.1E-04	6.7E-04	7.06	1.63	3.6	0	7.06	0
AT4G28750	*PSAE-1*	8.3	0.0E+00	0.0E+00	7.73	3.69	1.49	1.49	7.73	2.96
AT4G29100	AT4G29100	3.2	1.5E-04	9.2E-04	10.3	1.86	3.69	4.06	10.3	1.49
AT4G29840	*MTO2*	4.9	0.0E+00	0.0E+00	8.54	2.12	3.6	3.11	8.54	2.12
AT4G30210	*ATR2*	-4.0	7.7E-246	3.1E-244	7.06	3.11	1.63	1.63	7.06	5.08
AT4G30960	*SIP3*	3.1	8.4E-13	1.4E-11	8.05	3.11	3.6	1.63	8.05	1.63
AT4G31020	AT4G31020	-4.1	1.9E-05	1.4E-04	8.46	0	2.22	0	8.46	0
AT4G32260	AT4G32260	2.9	0.0E+00	0.0E+00	8.05	0	3.11	0	8.05	2.12
AT4G32920	AT4G32920	2.7	3.4E-04	1.9E-03	8.05	1.63	1.14	3.11	8.05	1.14

		RNA-seq:*35S:GNC:YFP:HA:GR gnc gnl* 3 h CHX / Dex + CHX			ChIP-seq: *pGNL:GNL:HA*					
Locus	**Gene name**	**Fold change (F.C.)**	**P-value**	**FDR**	**Max score**	**Up-stream 3Kb**	**Up-stream 2Kb**	**Up-stream 1Kb**	**Intragenic**	**Down-stream 1Kb**
AT3G17980	AT3G17980	-107.3	6.5E-15	1.3E-13	8.05	0	3.11	1.14	2.12	8.05
AT3G18080	BGLU44	3.8	0.0E+00	0.0E+00	20.43	1.12	1.12	0	1.86	20.43
AT3G18390	EMB1865	3.4	2.4E-07	2.3E-06	7.06	1.14	0	2.62	7.06	3.11
AT3G19100	AT3G19100	3.4	1.1E-08	1.3E-07	7.51	1.01	0	7.51	1.01	1.01
AT3G19820	*DWF1*	5.1	0.0E+00	0.0E+00	8.83	0	8.83	0	3.33	3.33
AT3G21220	*MKK5*	2.6	1.4E-10	1.9E-09	7.49	1.58	0	0	7.49	1.12
AT3G21550	*DMP2*	2.9	4.1E-04	2.2E-03	7.55	0	0	1.14	7.55	2.62
AT3G21750	UGT71B1	5.3	2.0E-05	1.4E-04	9.03	0	1.14	0	9.03	0
AT3G21780	UGT71B6	-3.5	3.5E-17	8.1E-16	7.06	1.63	0	7.06	4.1	2.62
AT3G22110	*PAC1*	2.5	5.6E-09	6.7E-08	7.36	2.22	0	7.36	3.33	0
AT3G22120	*CWLP*	5.3	0.0E+00	0.0E+00	7.36	0	0	2.22	0	7.36
AT3G23410	*FAO3*	2.8	1.2E-04	7.3E-04	7	0	2.59	7	2.22	0
AT3G23490	*CYN*	2.6	2.2E-07	2.2E-06	8.54	3.11	2.62	0	8.54	1.14
AT3G25980	*MAD2*	5.5	1.1E-03	5.4E-03	10.67	1.49	0	5.9	10.67	3.33
AT3G26180	*CYP71B20*	11.0	6.4E-09	7.6E-08	8.1	2.22	0	8.1	1.49	0
AT3G26650	*GAPA*	6.1	0.0E+00	0.0E+00	7.55	0	7.55	3.6	7.06	0
AT3G26830	*PAD3*	-19.1	5.4E-11	8.0E-10	9.2	1.86	0	9.2	2.22	0
AT3G28050	AT3G28050	8.6	2.4E-08	2.7E-07	7	0	1.86	3.69	7	2.22
AT3G43220	AT3G43220	3.2	2.6E-04	1.5E-03	9.93	1.12	9.93	2.96	2.59	0
AT3G43540	AT3G43540	2.5	1.5E-03	7.0E-03	10.3	0	0	10.3	3.33	2.22
AT3G43670	AT3G43670	8.3	2.3E-06	1.9E-05	7.55	7.55	1.14	0	0	0
AT3G44020	AT3G44020	6.5	2.0E-04	1.2E-03	11.03	0	1.12	11.03	0	3.33
AT3G45410	AT3G45410	-3.4	4.1E-04	2.3E-03	8.95	0	1.01	0	0	8.95
AT3G46550	*SOS5*	4.0	1.8E-07	1.8E-06	10.67	0	2.96	4.43	10.67	1.86
AT3G47470	*LHCA4*	5.5	1.0E-06	8.9E-06	8.54	0	2.12	0	8.54	0
AT3G48340	AT3G48340	3.1	3.6E-05	2.4E-04	8.83	2.59	3.33	0	8.83	5.16
AT3G48630	AT3G48630	-18.8	2.9E-05	2.0E-04	12.42	12.42	1.49	0	0	1.12
AT3G48640	AT3G48640	-9.3	7.0E-08	7.3E-07	12.42	3.33	3.33	7.73	0	12.42
AT3G49310	AT3G49310	2.9	8.7E-04	4.4E-03	7.49	0	0	1.58	0	7.49
AT3G50440	*MES10*	12.2	1.8E-06	1.5E-05	9.93	9.93	1.12	0	0	0
AT3G50740	*UGT72E1*	3.5	3.2E-08	3.5E-07	7.85	0	1.01	1.49	7.85	1.55
AT3G51420	*SSL4*	8.8	1.4E-08	1.6E-07	8.1	1.86	8.1	1.49	1.86	2.96
AT3G52060	AT3G52060	5.4	1.5E-08	1.7E-07	7.36	0	0	1.49	7.36	0
AT3G52430	*PAD4*	5.0	3.2E-13	5.6E-12	7.06	0	2.62	3.6	7.06	2.12
AT3G52610	AT3G52610	3.6	3.2E-05	2.2E-04	9.48	0	3.66	0	9.48	1.54
AT3G53160	*UGT73C7*	-9.8	5.9E-06	4.6E-05	8.54	2.62	1.63	2.62	8.54	0
AT3G53190	AT3G53190	4.9	1.4E-04	8.2E-04	9.57	2.96	2.59	9.57	4.06	4.06
AT3G53920	*SIGC*	4.1	2.9E-06	2.4E-05	9.32	7.73	2.22	1.86	9.32	1.49
AT3G53980	AT3G53980	21.5	1.7E-07	1.6E-06	8.46	2.96	8.46	1.49	0	0
AT3G54040	AT3G54040	-3.5	1.1E-15	2.2E-14	7.06	7.06	0	0	5.58	1.63
AT3G54050	*HCEF1*	5.6	0.0E+00	0.0E+00	7.06	5.58	1.14	0	7.06	0
AT3G54150	AT3G54150	-18.5	4.6E-42	1.4E-40	8.83	0	0	3.69	8.83	4.43
AT3G54826	AT3G54826	-2.7	1.0E-06	9.1E-06	8.15	1.63	1.14	8.15	4.1	0
AT3G55440	*TPI*	-3.0	5.1E-18	1.2E-16	8.03	2.22	1.86	8.03	3.33	2.22
AT3G55450	*PBL1*	-7.7	4.6E-58	1.6E-56	7.36	3.33	1.49	2.22	7.36	0
AT3G55620	emb1624	-27.1	9.3E-50	3.0E-48	11.08	1.63	11.08	6.07	3.11	0
AT3G55700	AT3G55700	-6.4	1.1E-03	5.4E-03	7.06	2.12	0	2.12	7.06	3.6
AT3G55770	AT3G55770	3.8	2.4E-15	5.0E-14	7.49	0	1.12	2.79	7.49	0
AT3G56110	*PRA1.B1*	3.0	4.2E-04	2.3E-03	7.49	0	0	7.49	3.4	1.27
AT3G56360	AT3G56360	5.8	0.0E+00	0.0E+00	8.54	1.14	4.1	4.59	8.54	0
AT3G56750	AT3G56750	2.9	1.9E-03	8.9E-03	7.55	7.55	1.14	5.58	2.62	1.63
AT3G57090	*BIGYIN*	-2.9	6.1E-18	1.4E-16	8.46	3.33	0	2.22	8.46	1.49
AT3G57320	AT3G57320	4.9	3.1E-04	1.7E-03	8.05	0	2.62	1.14	8.05	3.11
AT3G57630	AT3G57630	-3.0	1.4E-09	1.8E-08	8.54	0	8.54	4.1	1.14	2.62
AT3G61111	AT3G61111	-51.3	8.5E-06	6.5E-05	8.46	0	2.96	3.71	2.22	8.46
AT3G62010	AT3G62010	5.2	0.0E+00	0.0E+00	7.06	0	2.12	1.14	2.62	7.06
AT3G62150	*PGP21*	-3.6	2.7E-36	7.9E-35	8.05	4.59	8.05	3.11	2.12	0
AT3G62410	*CP12-2*	5.5	0.0E+00	0.0E+00	7.06	0	1.63	1.63	7.06	5.58
AT3G62600	ATERDJ3B	3.6	2.0E-07	1.9E-06	7.55	7.55	0	0	2.62	1.63
AT3G63160	AT3G63160	10.5	0.0E+00	0.0E+00	7.06	2.62	2.12	7.06	3.11	1.63

		RNA-seq: *35S:GNC:YFP:HA:GR gnc gnl* 3 h CHX / Dex + CHX			ChIP-seq: *pGNL:GNL:HA*					
Locus	**Gene name**	**Fold change (F.C.)**	**P-value**	**FDR**	**Max score**	**Up-stream 3Kb**	**Up-stream 2Kb**	**Up-stream 1Kb**	**Intragenic**	**Down-stream 1Kb**
AT4G33070	AT4G33070	-13.5	3.3E-59	1.1E-57	9.03	2.62	1.63	0	9.03	3.6
AT4G33150	AT4G33150	2.7	1.0E-03	5.1E-03	10.3	2.96	10.3	2.96	3.69	1.49
AT4G33160	AT4G33160	4.7	2.7E-08	3.0E-07	10.3	3.33	1.12	10.3	2.96	0
AT4G33380	AT4G33380	3.3	2.3E-05	1.6E-04	7.04	2.94	0	0	7.04	3.4
AT4G34215	AT4G34215	4.0	2.6E-05	1.8E-04	10.52	4.1	3.11	1.63	10.52	0
AT4G34220	AT4G34220	5.5	2.8E-04	1.6E-03	10.52	1.14	1.63	1.14	4.1	10.52
AT4G34610	*BLH6*	6.8	1.1E-03	5.4E-03	7	3.69	7	0	0	1.12
AT4G34620	*SSR16*	5.2	0.0E+00	0.0E+00	7.06	4.1	7.06	2.12	1.14	2.62
AT4G34640	*SQS1*	2.7	5.4E-07	5.0E-06	7.06	2.12	0	7.06	4.1	1.63
AT4G34830	*MRL1*	3.7	7.0E-07	6.4E-06	7.06	1.14	0	3.11	7.06	0
AT4G35060	AT4G35060	9.6	5.8E-05	3.8E-04	7.04	2.94	2.03	0	7.04	0
AT4G35250	AT4G35250	3.7	7.2E-10	9.5E-09	7.06	7.06	3.6	1.63	6.57	1.63
AT4G35720	AT4G35720	19.9	3.2E-06	2.6E-05	14.23	1.49	14.23	3.33	3.69	1.86
AT4G35760	AT4G35760	4.4	2.7E-06	2.2E-05	9.03	1.63	0	9.03	5.58	3.11
AT4G35770	*SEN1*	13.9	3.1E-09	3.8E-08	9.03	0	2.12	5.58	9.03	1.63
AT4G35780	AT4G35780	4.3	7.5E-06	5.8E-05	9.03	1.14	0	3.11	3.6	9.03
AT4G36220	*FAH1*	3.1	4.1E-05	2.8E-04	7.04	2.49	1.12	7.04	0	2.94
AT4G36360	*BGAL3*	2.8	1.4E-10	2.0E-09	7.55	2.62	1.63	2.62	7.55	2.12
AT4G36430	AT4G36430	-3.7	2.9E-07	2.8E-06	7.55	3.6	1.63	0	2.62	7.55
AT4G36580	AT4G36580	-4.9	8.5E-07	7.6E-06	7.36	1.54	0	0	7.36	0
AT4G36870	*BLH2*	4.0	1.8E-03	8.3E-03	8.54	0	1.63	0	8.54	1.63
AT4G36890	*IRX14*	3.6	1.3E-05	9.3E-05	8.1	1.49	8.1	2.22	4.43	0
AT4G37250	AT4G37250	3.1	9.1E-05	5.7E-04	9	1.51	2.01	1.01	9	0
AT4G37300	*MEE59*	3.3	0.0E+00	0.0E+00	7.55	2.62	0	1.63	4.1	7.55
AT4G37410	*CYP81F4*	5.8	0.0E+00	0.0E+00	12.93	0	12.93	1.49	1.49	2.22
AT4G37870	*PCK1*	3.0	0.0E+00	0.0E+00	7	7	2.59	1.86	3.69	0
AT4G37880	AT4G37880	2.5	5.7E-05	3.7E-04	7.55	1.63	0	3.03	7.55	0
AT4G37980	*ELI3-1*	5.8	2.6E-08	2.9E-07	10.67	2.96	10.67	1.12	3.69	1.49
AT4G38220	AT4G38220	4.4	1.9E-10	2.6E-09	8.05	5.08	0	3.6	8.05	6.57
AT4G38680	*GRP2*	3.3	3.8E-12	6.2E-11	7.55	7.55	0	3.03	7.55	0
AT4G38690	AT4G38690	5.2	2.8E-06	2.3E-05	7.55	0	0	3.11	7.55	3.03
AT4G38940	AT4G38940	-3.0	1.9E-17	4.3E-16	9.53	1.14	3.6	9.53	3.11	3.6
AT4G39090	*RD19*	3.4	0.0E+00	0.0E+00	7	7	1.49	5.9	2.96	2.59
AT4G39100	*SHL1*	3.4	1.1E-05	8.5E-05	7	0	3.33	1.12	7	2.96
AT4G39230	AT4G39230	-8.8	8.9E-35	2.6E-33	9.57	1.12	2.34	9.57	1.86	1.86
AT4G39800	*MIPS1*	3.3	8.7E-15	1.7E-13	7.55	0	4.1	1.14	7.55	0
AT4G39860	AT4G39860	3.5	1.2E-03	5.7E-03	12.87	2.59	1.12	12.87	2.59	0
AT4G40020	AT4G40020	-10.4	7.8E-13	1.3E-11	7	0	7	1.12	2.59	3.69
AT5G01530	*LHCB4.1*	3.8	0.0E+00	0.0E+00	8.54	6.57	0	1.14	8.54	0
AT5G01830	AT5G01830	-4.8	2.0E-11	3.0E-10	9.53	0	1.14	1.63	9.53	2.62
AT5G01840	*OFP1*	6.5	6.0E-06	4.7E-05	9.53	9.53	4.59	2.62	7.55	3.11
AT5G01890	AT5G01890	3.6	1.6E-04	9.4E-04	9	0	1.01	9	1.51	3.51
AT5G01920	*STN8*	3.3	3.7E-05	2.5E-04	10.02	0	1.63	0	10.02	2.12
AT5G01950	AT5G01950	-3.6	4.8E-27	1.3E-25	7.06	5.08	4.59	3.6	2.12	7.06
AT5G02120	*OHP*	9.1	0.0E+00	0.0E+00	7.36	1.45	1.49	7.36	2.96	2.22
AT5G02200	*FHL*	3.3	9.1E-05	5.8E-04	7.04	2.03	1.58	7.04	1.58	2.49
AT5G03140	AT5G03140	9.0	3.4E-05	2.3E-04	7.06	1.63	0	1.14	7.06	1.14
AT5G03200	AT5G03200	4.6	1.0E-04	6.5E-04	7.06	0	7.06	0	6.07	2.12
AT5G03204	AT5G03204	14.0	1.6E-05	1.2E-04	7.06	0	0	7.06	0	6.07
AT5G03260	*LAC11*	4.1	2.1E-03	9.4E-03	7.06	1.63	0	7.06	2.62	1.14
AT5G03545	*AT4*	3.1	6.9E-15	1.4E-13	14.96	1.14	14.96	0	1.63	0
AT5G03760	ATCSLA09	3.6	4.4E-04	2.4E-03	8.46	2.96	1.86	0	8.46	1.49
AT5G03940	CPSRP54	2.7	6.5E-08	6.8E-07	9.2	0	1.86	9.2	2.96	1.49
AT5G05010	AT5G05010	2.7	3.7E-12	5.9E-11	7.55	0	2.12	2.62	7.55	2.62
AT5G05690	*CPD*	5.2	4.3E-13	7.6E-12	8.05	0	1.14	2.12	8.05	1.21
AT5G06240	emb2735	4.2	5.3E-04	2.8E-03	7.06	1.14	7.06	0	2.62	2.12
AT5G06570	AT5G06570	-6.5	1.4E-04	8.3E-04	7.06	0	2.12	4.1	7.06	1.63
AT5G06750	AT5G06750	2.5	6.7E-06	5.2E-05	8.54	1.14	0	8.54	4.59	1.14
AT5G06960	*OBF5*	2.6	1.9E-03	8.7E-03	7.36	7.36	0	2.22	1.86	2.59
AT5G07020	AT5G07020	3.1	1.2E-13	2.3E-12	8.54	0	8.54	0	3.6	0

		RNA-seq: *35S:GNC:YFP:HA:GR gnc gnl* 3 h CHX / Dex + CHX			ChIP-seq: *pGNL:GNL:HA*					
Locus	**Gene name**	**Fold change (F.C.)**	**P-value**	**FDR**	**Max score**	**Up-stream 3Kb**	**Up-stream 2Kb**	**Up-stream 1Kb**	**Intragenic**	**Down-stream 1Kb**
AT5G07030	AT5G07030	11.0	0.0E+00	0.0E+00	8.54	0	0	0	8.54	0
AT5G08310	AT5G08310	-2.9	1.8E-03	8.3E-03	8.46	0	3.69	4.79	0	8.46
AT5G08690	AT5G08690	2.5	0.0E+00	0.0E+00	7.55	7.55	0	0	6.07	0
AT5G09530	AT5G09530	9.6	8.5E-07	7.6E-06	7.36	0	1.01	1.01	7.36	0
AT5G10100	AT5G10100	3.8	8.8E-04	4.4E-03	13.97	2.59	0	2.96	13.97	1.49
AT5G10520	*RBK1*	-5.0	3.7E-05	2.5E-04	9.57	1.49	2.96	1.86	9.57	2.59
AT5G10745	AT5G10745	4.6	2.9E-04	1.6E-03	10.02	0	1.63	10.02	2.12	4.1
AT5G10750	AT5G10750	2.8	0.0E+00	0.0E+00	10.02	10.02	0	4.1	4.1	1.63
AT5G10860	AT5G10860	2.8	0.0E+00	0.0E+00	8.05	3.6	1.14	0	3.11	8.05
AT5G11330	AT5G11330	3.6	1.8E-07	1.8E-06	7.55	7.55	1.14	2.12	4.1	3.6
AT5G11550	AT5G11550	9.5	2.1E-04	1.2E-03	10.02	1.63	5.08	1.63	10.02	3.11
AT5G11560	AT5G11560	2.7	1.7E-07	1.7E-06	10.02	1.14	0	5.08	5.08	10.02
AT5G11670	NADP-ME2	-3.3	3.4E-23	8.6E-22	7.55	4.1	2.12	0	7.55	1.63
AT5G11890	AT5G11890	3.1	1.2E-03	5.9E-03	8.54	0	1.14	1.63	8.54	3.6
AT5G11980	AT5G11980	2.5	1.4E-03	6.6E-03	7.06	1.63	0	3.6	7.06	1.14
AT5G12110	AT5G12110	4.7	7.3E-11	1.1E-09	7.55	0	1.14	7.55	2.12	5.58
AT5G13210	AT5G13210	-101.6	4.3E-49	1.4E-47	7	0	0	4.79	1.49	7
AT5G13390	*NEF1*	4.7	5.7E-09	6.8E-08	7.06	1.14	0	2.12	7.06	1.63
AT5G13630	*GUN5*	2.5	9.7E-14	1.8E-12	9.03	2.62	4.59	0	9.03	0
AT5G13770	AT5G13770	7.4	3.5E-10	4.8E-09	8.05	4.1	2.12	1.14	8.05	5.08
AT5G14060	CARAB-AK-LYS	3.0	2.2E-06	1.8E-05	9.09	0	9.09	2.51	4.01	1.66
AT5G14240	AT5G14240	2.5	1.1E-04	6.8E-04	7.06	1.63	2.62	7.06	2.62	1.14
AT5G14730	AT5G14730	-5.2	0.0E+00	0.0E+00	7.73	1.49	1.49	0	7.73	7.36
AT5G14740	*CA2*	4.1	4.9E-13	8.5E-12	7.73	0	0	7.73	7.36	0
AT5G14880	AT5G14880	3.7	5.4E-04	2.9E-03	8.46	1.86	2.96	8.46	1.49	2.59
AT5G15190	AT5G15190	4.3	1.9E-07	1.8E-06	8.05	2.62	1.14	5.08	8.05	0
AT5G16120	AT5G16120	2.5	8.8E-04	4.4E-03	7.06	3.6	1.14	3.6	7.06	1.63
AT5G16300	AT5G16300	2.7	8.8E-05	5.6E-04	7.55	1.63	1.14	3.6	7.55	1.63
AT5G16360	AT5G16360	3.3	0.0E+00	0.0E+00	7.06	1.63	3.6	7.06	3.11	0
AT5G16370	*AAE5*	2.6	2.6E-08	2.8E-07	7.06	2.12	4.1	1.63	3.6	7.06
AT5G17310	*UGP2*	3.0	2.3E-07	2.2E-06	18.74	1.49	4.06	0	5.9	18.74
AT5G17920	*ATMS1*	4.2	0.0E+00	0.0E+00	7.06	1.57	0	1.63	7.06	2.12
AT5G18650	AT5G18650	2.9	2.9E-08	3.1E-07	12.5	3.69	2.22	0	12.5	1.12
AT5G19020	*MEF18*	5.0	1.6E-04	9.7E-04	7.36	1.49	1.86	1.12	3.69	7.36
AT5G19290	AT5G19290	3.3	4.2E-06	3.4E-05	9.03	0	0	0	9.03	3.11
AT5G20500	AT5G20500	3.0	1.2E-08	1.4E-07	8.1	0	3.69	8.1	0	1.12
AT5G20590	*TBL5*	2.6	1.9E-03	8.6E-03	7.55	2.12	2.62	4.59	7.55	2.62
AT5G20700	AT5G20700	4.3	0.0E+00	0.0E+00	7.25	0	7.25	2.46	2.22	1.86
AT5G21070	AT5G21070	3.7	1.4E-06	1.2E-05	7.55	0	0	0	4.59	7.55
AT5G21930	*PAA2*	4.0	1.2E-07	1.2E-06	9.03	3.6	2.12	4.1	9.03	1.63
AT5G21960	AT5G21960	4.2	6.7E-16	1.4E-14	7.06	5.58	2.62	3.6	7.06	0
AT5G22050	AT5G22050	4.1	4.7E-07	4.4E-06	8.05	1.14	1.14	6.07	8.05	0
AT5G22830	*MGT10*	2.6	2.4E-04	1.4E-03	7.06	3.6	1.14	2.62	7.06	4.59
AT5G23020	*IMS2*	8.5	6.3E-11	9.2E-10	7	4.79	0	7	3.69	2.59
AT5G23240	AT5G23240	4.8	6.3E-06	4.9E-05	7.55	4.86	0	0	3.11	7.55
AT5G23920	AT5G23920	7.7	1.3E-08	1.5E-07	10	0	0	1.51	0	10
AT5G24300	*SSI1*	2.8	9.0E-08	9.2E-07	7	2.22	4.06	1.49	7	1.12
AT5G24314	*PTAC7*	5.9	1.4E-11	2.1E-10	7.73	0	1.12	7.73	0	1.86
AT5G24540	*BGLU31*	-13.8	3.4E-14	6.5E-13	7	7	6.63	4.06	1.86	2.96
AT5G25220	*KNAT3*	3.1	4.3E-04	2.3E-03	7.55	0	1.14	0	7.55	3.11
AT5G26360	AT5G26360	2.7	6.3E-12	1.0E-10	9.93	3.69	0	9.93	3.69	3.33
AT5G26570	ATGWD3	2.6	8.7E-07	7.8E-06	9.93	9.93	0	3.69	3.69	1.12
AT5G28237	AT5G28237	2.6	9.0E-05	5.7E-04	7.06	1.63	0	0	7.06	1.14
AT5G28630	AT5G28630	-3.3	2.7E-11	4.1E-10	10.5	10.5	1.51	1.51	2.01	1.01
AT5G33320	*CUE1*	2.7	2.9E-10	3.9E-09	7.89	0	1.01	2.07	7.89	1.01
AT5G35630	*GS2*	2.8	0.0E+00	0.0E+00	8.83	7	0	1.49	8.83	1.12
AT5G38280	*PR5K*	4.6	7.7E-06	5.9E-05	15.81	0	2.22	15.81	2.59	1.86
AT5G38430	AT5G38430	7.6	0.0E+00	0.0E+00	20.17	20.17	0	0	0	3.33
AT5G39570	AT5G39570	4.1	0.0E+00	0.0E+00	7.73	1.86	1.49	7.73	3.33	0
AT5G39580	AT5G39580	-9.0	3.3E-36	9.9E-35	8.05	4.59	0	0	8.05	1.63

		RNA-seq: *35S:GNC:YFP:HA:GR gnc gnl* 3 h CHX / Dex + CHX			ChIP-seq: *pGNL:GNL:HA*					
Locus	**Gene name**	**Fold change (F.C.)**	**P-value**	**FDR**	**Max score**	**Up-stream 3Kb**	**Up-stream 2Kb**	**Up-stream 1Kb**	**Intragenic**	**Down-stream 1Kb**
AT5G40610	AT5G40610	2.9	3.1E-08	3.3E-07	10.3	3.69	0	1.86	2.22	10.3
AT5G40950	*RPL27*	3.4	0.0E+00	0.0E+00	7.06	2.62	0	1.63	7.06	3.6
AT5G41340	*UBC4*	3.1	3.6E-04	2.0E-03	10.5	0	0	10.5	1.51	1.01
AT5G42290	AT5G42290	-5.8	1.7E-14	3.3E-13	7.73	0	4.43	7.73	3.33	2.22
AT5G42720	AT5G42720	4.9	4.4E-04	2.4E-03	7.73	0	0	7.73	3.69	0
AT5G42890	*SCP2*	2.5	1.3E-05	9.6E-05	7.73	2.59	7.73	2.96	2.22	2.22
AT5G43090	*PUM13*	-28.7	5.3E-04	2.8E-03	16.54	0	2.22	1.12	2.22	16.54
AT5G43180	AT5G43180	4.9	3.1E-05	2.1E-04	7.06	7.06	1.21	0	3.03	0
AT5G44260	AT5G44260	3.5	7.9E-04	4.0E-03	15.44	2.22	0	1.86	4.43	15.44
AT5G44820	AT5G44820	-5.3	7.3E-07	6.6E-06	7.06	0	0	0	7.06	0
AT5G45950	AT5G45950	6.4	7.8E-04	4.0E-03	8.1	8.1	2.59	2.96	1.86	2.22
AT5G46420	AT5G46420	2.6	3.2E-06	2.6E-05	8.46	1.86	0	3.33	8.46	2.96
AT5G46900	AT5G46900	7.9	9.0E-08	9.2E-07	7	1.86	3.69	7	0	2.59
AT5G47040	*LON2*	4.4	3.2E-14	6.0E-13	11.9	1.12	11.9	1.86	4.43	3.33
AT5G47870	AT5G47870	2.6	4.4E-04	2.4E-03	7.55	1.14	2.62	3.6	7.55	0
AT5G48180	*NSP5*	2.6	4.7E-14	8.9E-13	7.04	0	1.12	0	7.04	1.58
AT5G48530	AT5G48530	-3.8	1.4E-33	4.0E-32	7.73	0	2.22	0	7.73	0
AT5G48790	AT5G48790	2.5	4.7E-05	3.1E-04	7.55	2.62	7.55	0	2.12	4.1
AT5G48800	AT5G48800	7.2	3.3E-04	1.8E-03	7.55	7.55	0	0	1.63	3.11
AT5G49360	*BXL1*	28.7	0.0E+00	0.0E+00	7.06	0	0	1.14	7.06	1.63
AT5G49460	*ACLB-2*	3.0	7.8E-08	8.0E-07	7	7	4.06	6.26	1.86	1.49
AT5G49740	*FRO7*	15.7	1.9E-05	1.4E-04	7.06	2.62	1.14	0	7.06	0
AT5G50920	*CLPC1*	3.7	0.0E+00	0.0E+00	11.15	0	1.51	11.15	1.01	0
AT5G51830	AT5G51830	-3.3	1.1E-14	2.2E-13	8.1	4.79	2.22	8.1	1.86	3.33
AT5G52540	AT5G52540	3.3	1.2E-04	7.3E-04	7	2.96	7	0	1.86	4.06
AT5G52882	AT5G52882	3.3	6.7E-07	6.1E-06	10.01	0	0	1.54	10.01	5.25
AT5G53160	*RCAR3*	3.0	6.9E-10	9.2E-09	7.89	0	1.01	0	1.54	7.89
AT5G53170	*FTSH11*	2.8	6.2E-07	5.7E-06	7.89	0	0	3.13	7.89	0
AT5G54270	*LHCB3*	9.2	2.8E-06	2.3E-05	7	1.12	0	7	3.33	0
AT5G54370	AT5G54370	13.3	8.0E-07	7.2E-06	13.19	13.19	1.86	3.33	1.86	0
AT5G54600	AT5G54600	3.2	0.0E+00	0.0E+00	7.55	1.14	2.12	0	7.55	1.14
AT5G54770	*THI1*	6.7	0.0E+00	0.0E+00	9.53	1.14	3.6	0	9.53	2.12
AT5G54810	*TSB1*	-2.9	1.5E-38	4.5E-37	7.25	0	2.96	7.25	0	5.53
AT5G55270	AT5G55270	-91.1	1.3E-16	2.9E-15	8.83	6.26	1.49	8.83	0	2.22
AT5G55910	*D6PK*	3.1	1.5E-09	1.9E-08	39.66	2.22	4.06	1.49	39.66	0
AT5G56100	AT5G56100	6.7	1.8E-04	1.1E-03	9.03	2.62	3.11	0	9.03	0
AT5G56600	*PRF3*	3.6	4.6E-06	3.7E-05	7	1.12	1.49	1.12	7	2.96
AT5G56850	AT5G56850	4.7	4.0E-05	2.7E-04	82.61	82.61	1.12	0	4.79	1.49
AT5G56870	*BGAL4*	7.4	0.0E+00	0.0E+00	9.03	0	1.14	2.62	3.11	9.03
AT5G56890	AT5G56890	4.0	3.3E-06	2.7E-05	7.04	0	7.04	0	2.94	1.58
AT5G57330	AT5G57330	3.1	1.3E-07	1.3E-06	8.95	3.13	0	8.95	2.6	3.13
AT5G57815	AT5G57815	3.2	1.2E-06	1.0E-05	7.04	0	4.31	1.12	4.31	7.04
AT5G57900	*SKIP1*	3.6	3.7E-05	2.5E-04	11.5	0	1.01	11.5	1.51	0
AT5G57930	*APO2*	5.3	2.0E-08	2.2E-07	12	3.01	3.01	1.51	12	0
AT5G57940	*CNGC5*	2.8	1.3E-07	1.3E-06	7.06	1.63	0	7.06	4.1	2.12
AT5G58330	AT5G58330	2.6	0.0E+00	0.0E+00	8.05	1.63	2.12	8.05	5.08	1.63
AT5G58960	*GIL1*	4.1	1.1E-03	5.3E-03	9.03	2.3	4.59	0	9.03	0
AT5G59680	AT5G59680	-49.1	1.0E-23	2.6E-22	8.46	1.12	0	8.46	0	4.06
AT5G59750	AT5G59750	3.6	2.4E-04	1.4E-03	7.04	0	2.49	3.85	7.04	0
AT5G59780	*MYB59*	2.6	5.1E-04	2.7E-03	9.2	9.2	1.86	4.43	1.86	8.83
AT5G60200	*TMO6*	2.9	1.1E-05	8.3E-05	7.06	0	0	2.12	7.06	0
AT5G60360	*ALP*	5.6	0.0E+00	0.0E+00	11.77	11.77	1.49	2.96	4.06	3.69
AT5G61160	AACT1	-17.9	6.6E-16	1.4E-14	7.36	1.12	1.86	2.22	2.22	7.36
AT5G62140	AT5G62140	7.1	2.2E-03	9.7E-03	7.36	7.36	0	0	2.07	0
AT5G62150	AT5G62150	-6.2	5.1E-08	5.4E-07	7.36	0	0	2.6	7.36	3.66
AT5G62690	*TUB2*	5.2	0.0E+00	0.0E+00	9.93	1.86	9.93	3.33	1.49	2.59
AT5G63530	*FP3*	6.4	1.5E-06	1.3E-05	7.06	1.63	1.15	1.63	7.06	0
AT5G63670	*SPT42*	3.7	4.1E-06	3.3E-05	8.83	3.69	2.22	1.86	0	8.83
AT5G63690	AT5G63690	-4.7	7.0E-04	3.6E-03	7.55	0	1.14	1.14	7.55	2.12
AT5G63810	*BGAL10*	5.0	6.4E-06	5.0E-05	8.05	1.14	2.62	2.12	8.05	1.14

		RNA-seq: *35S:GNC:YFP:HA:GR gnc gnl* 3 h CHX / Dex + CHX			ChIP-seq: *pGNL:GNL:HA*					
Locus	**Gene name**	**Fold change (F.C.)**	**P-value**	**FDR**	**Max score**	**Up-stream 3Kb**	**Up-stream 2Kb**	**Up-stream 1Kb**	**Intragenic**	**Down-stream 1Kb**
AT5G64260	*EXL2*	2.5	0.0E+00	0.0E+00	7.55	0	1.14	1.63	7.55	0
AT5G64350	*FKBP12*	3.2	0.0E+00	0.0E+00	7	1.49	0	3.69	2.59	7
AT5G65100	AT5G65100	-61.4	1.8E-07	1.8E-06	24.5	24.5	0	0	1.51	0
AT5G65110	*ACX2*	-3.9	1.5E-14	2.9E-13	7.04	0	1.12	0	7.04	2.94
AT5G65320	AT5G65320	-18.0	2.7E-04	1.5E-03	7	1.12	7	0	1.49	0
AT5G65600	AT5G65600	-24.5	3.7E-39	1.1E-37	7.73	7.73	3.33	1.49	6.26	1.12
AT5G65990	AT5G65990	4.3	9.6E-06	7.2E-05	7.25	7.25	0	1.86	2.59	0
AT5G66560	AT5G66560	4.0	7.9E-04	4.0E-03	7.06	0	1.63	0	7.06	1.63
AT5G66570	*PSBO1*	5.4	0.0E+00	0.0E+00	8.05	7.06	1.63	0	8.05	1.63
AT5G66650	AT5G66650	2.9	0.0E+00	0.0E+00	14.03	1.01	14.03	1.01	1.54	0
AT5G67070	*RALFL34*	4.3	1.3E-10	1.9E-09	8.05	0	3.6	0	8.05	1.63
AT5G67260	*CYCD3;2*	3.3	1.4E-03	6.7E-03	9.2	9.2	0	8.83	1.49	1.49
AT5G67310	*CYP81G1*	-2.7	4.1E-08	4.4E-07	9.03	0	2.12	1.63	6.57	9.03
AT5G67360	*ARA12*	5.7	2.0E-13	3.6E-12	7.55	1.14	1.14	1.14	7.55	3.11
AT5G67370	*AT5G67370*	6.3	7.8E-09	9.2E-08	7	5.9	4.43	2.22	5.16	7
AT5G67470	*FH6*	2.9	6.4E-04	3.3E-03	11.4	2.22	7.77	11.4	2.59	1.86

Table 11: List of genes from the overlap of ChIP-seq with *pGNL:GNL:HA gnc gnl* and the RNA-seq with *35S:GNL:YFP:HA:GR gnc gnl* for 3 h Dex and CHX (filtered with fold change threshold/F.C. 1.2 and FDR < 0.1).

Locus	Gene name	Fold change	P-value	FDR	Protein description	Max score	Up-stream 3 kb	Up-stream 2 kb	Up-stream 1 kb	Intragenic	Down-stream 1 kb
AT1G03870	*FLA9*	1.6	1.2E-09	4.3E-06	FASCICLIN-like arabinoogalactan 9	11.58	0.00	1.12	1.12	0.00	11.58
AT1G10170	*NFXL1*	1.2	3.6E-06	2.5E-03	Homologue of the putative human transcription repressor NF-X1	7.06	7.06	1.63	0.00	3.11	2.62
AT1G21910	*AT1G21910*	1.4	3.0E-07	3.4E-04	Integrase-type DNA-binding superfamily protein	7.73	7.73	3.69	3.69	0.00	1.12
AT1G32350	*AOX1D*	-1.4	1.0E-06	9.5E-04	Alternative oxidase 1D,oxidation reduction, response to cyclopentenone	8.85	1.12	0.00	2.94	2.03	8.85
AT1G37130	*NIA2*	1.3	1.7E-12	1.7E-08	Nitrate reductase 2	11.50	0.00	0.00	0.00	11.50	1.14
AT1G72150	*PATL1*	1.3	5.9E-05	2.7E-02	PATELLIN 1, involved in membrane trafficking	7.00	1.12	0.00	2.22	7.00	5.16
AT2G01021	*AT2G01021*	1.3	6.7E-07	6.4E-04	Unknown protein	12.12	4.19	2.77	12.12	0.00	6.30
AT2G36800	*DOGT1*	1.3	2.9E-04	9.7E-02	Don-glucosyltransferase 1	9.57	0.00	1.86	0.00	2.59	9.57
AT3G62150	*PGP21*	1.3	1.4E-07	2.0E-04	P-glycoprotein 21	8.05	4.59	8.05	3.11	2.12	0.00
AT5G02500	*HSC70-1*	1.3	2.0E-06	1.6E-03	Heat shock cognate protein 70-1	8.05	3.11	0.00	0.00	8.05	2.12
AT5G13630	*GUN5*	1.4	1.4E-04	5.6E-02	Magnesium-chelatase subunit chlH, chloroplast localized	9.03	2.62	4.59	0.00	9.03	0.00
AT5G17000	*AT5G17000*	-1.2	9.2E-05	3.9E-02	Zinc-binding dehydrogenase family protein	7.06	7.06	0.00	2.12	0.00	1.14
AT5G17920	*ATMS1*	1.3	2.6E-04	9.0E-02	Cobalamin-independent synthase family protein	7.06	1.57	0.00	1.63	7.06	2.12

Table 12: List of genes from the overlap between the common genes from the ChIP-seq with *pGNL:GNL:HA gnc gnl* and the RNA-seq with *35S:GNC:YFP:HA gnc gnl* with a list of genes with a role in chlorophyll biosynthesis.

			RNA-seq: *35S:GNC:YFP:HA:GR gnc gnl* 3 h CHX / Dex + CHX			ChIP-seq: *pGNL:GNL:HA gnc gnl*					
Locus	**Gene name**	**Protein description**	**Fold change (F.C.)**	**P-value**	**FDR**	**Max score**	**Up-stream 3Kb**	**Up-stream 2Kb**	**Up-stream 1Kb**	**Intragenic**	**Down-stream 1Kb**
AT4G25080	*CHLM*	magnesium-protoporphyrin IX methyltransferase	4.7	0	0	7.04	5.22	2.94	2.03	7.04	1.12
AT2G40490	*HEME2*	Uroporphyrinogen decarboxylase	3.4	7E-11	1E-09	7.89	7.89	1.01	1.54	5.77	0
AT1G08520	*ALB1*	ALBINA 1	2.5	4E-09	5E-08	11.06	3.13	0	0	11.06	2.07
AT1G09530	*PIF3*	phytochrome interacting factor 3	2.5	4E-04	2E-03	9.76	1.12	2.49	0	1.12	9.76
AT1G04620	AT1G04620	coenzyme F420 hydrogenase family / dehydrogenase	2.5	1E-03	7E-03	8.83	8.83	1.49	3.33	6.38	1.49
AT5G13630	*GUN5*	magnesium-chelatase subunit chlH, chloroplast, putative / Mg-protoporphyrin IX	2.5	1E-13	2E-12	9.03	2.62	4.59	0	9.03	0

Table 13: List of genes with overlap between the common genes from the ChIP-seq with *pGNL:GNL:HA gnc gnl* and the RNA-seq with *35S:GNL:YFP:HA gnc gnl* with a list of genes with a role in chlorophyll biosynthesis.

			RNA-seq: *35S:GNC:YFP:HA:GR gnc gnl* 3 h CHX / Dex + CHX			ChIP-seq: *pGNL:GNL:HA gnc gnl*					
Locus	**Gene name**	**Protein description**	**Fold change (F.C.)**	**P-value**	**FDR**	**Max score**	**Up-stream 3 kb**	**Up-stream 2 kb**	**Up-stream 1 kb**	**Intragenic**	**Down-stream 1 kb**
AT5G13630	*GUN5*	CHLH subunit of the Mg-chelatase enzyme	1.4	1.44E-04	6E-02	9.03	2.62	4.59	0.00	9.03	0.00